Designing Molecularly Imprinted Polymers for the Analysis of the Components of Complex Matrices

John O' Mahony

School of Chemical Sciences,
Dublin City University

A thesis submitted for the degree
of
Doctor of Philosophy

June 2004

Supervised By:
Prof. Malcolm R. Smyth
Dr. Kieran Nolan

Declaration

I hereby certify that this material, which I now submit for assessment on the programme of study leading to the award of Doctor of Philosophy is entirely my own work and has not been taken from the work of others, save and to the extent that such work has been cited and acknowledged within the text of my work.

Signed: John O'Mahony I.D. No: 96326026

John O'Mahony

Date: 15th September 2004

"Science may set limits to knowledge, but should not set limits to imagination"
-Bertrand Russell

"Nothing shocks me I'm a scientist"
-Indiana Jones

Acknowledgments

Thanks to all the following people

- Thanks to my supervisors Prof Malcolm R Smyth and Dr Kieran Nolan for their support & guidance over the past four years, thanks especially to Kieran for all his input, ideas, questions and healthy scepticism
- Special thanks to Dr Boris Mizaikoff at GeorgiaTech, Atlanta, for his support and endless enthusiasm, and for the opportunity to work with the ASL team
- Dr Frances Weldon, who initiated this project
- Dr Michael Jakusch, for the opportunity to work at the Austrian Research Centre at Seibersdorf
- Dr Les Gelbaum (GeorgiaTech) and Dr Dermot Brougham (DCU) for providing the answers to many questions on NMR
- Dr Joe Cochrane (School of Matenal Sciences & Engineering, Georgia Institute of Technology) for use of surface area analysis equipment.
- Dr Kim Lau, for help with the microscopy
- The technical staff at DCU
- Members of the M R Smyth group and the K Nolan group
- Thanks also to all the members (past and present) of the ASL team at GeorgiaTech, especially the ice-cold Dr Markus Janotta, who allowed me sleep on his sofa for a month when I was in Vienna, and introduced me to the pinnacle of Austrian cuisine, the kasekrainer
- Thanks to Alex Molinelli, for her HPLC expertise (Chapters 3 &4), for her boundless patience and for being a great colleague in general
- Noel Brennan for the supply of Bob Dylan CDs which got me through the writing stage, and Shane O'Malley and Jonathon Rochford, for being on hand for the thousands of coffee breaks
- My parents, Patrick and Mary, without whose support I wouldn't have been able to pursue this work, and to my siblings, Claire, Alison and Brendan
- And thanks to Christy, for putting up with me

Glossary of Abbreviations

ACM	Acrylamide
AIBN	2,2-Azobisisobutyronitrile
BET	Brunauer-Emmet-Teller adsorption isotherm method
CS	Computer Simulation
CSP	Chiral Stationary Phase
CZE	Capillary Zone Electrophoresis
DVB	Divinyl Benzene
EGDMA	Ethylene glycol Dimethacrylate
fs	Femtosecond ($1x10^{-15}s$)
GA	Gentisic Acid
GC	Gas Chromatography
HEM	Hydroxyethyl Methacrylate
HF	Hydrofluonc Acid
HPLC	High Performance Liquid Chromatography
MAA	Methacrylic Acid
MC	Monte Carlo simulation method
MD	Molecular Dynamics simulation method
MIP	Molecularly Imprinted Polymers
MISPE	Molecularly Imprinted Solid Phase Extraction
NMR	Nuclear Magnetic Resonance
ns	Nanosecond ($1x10^{-9}s$)
PPC	Pre-Polymensation Complex
ps	Picosecond ($1x10^{-12}s$)
QCM	Quartz Crystal Microbalance
QM	Quantum Mechanics
SPE	Solid Phase Extraction
SA	Salicylic Acid

TFAA	Trifluoroacetic Acid
TLC	Thin Layer Chromatography
UV	Ultra-Violet
4-VP	4-Vinylpyndine

Table of Contents

Abstract

Molecular imprinting technology is a field of analytical chemistry of ever-increasing importance, offering an effective and economic means of producing molecule-specific synthetic materials, with potential application in separation, sensing and catalytic technologies This thesis describes a detailed investigation of the method and examines how it may be incorporated into a typical analytical application (solid phase extraction of the active ingredient in a pharmaceutical preparation), and investigates some of the practical considerations of such an approach – choice of appropriate functional monomer, the possibility of swelling effects affecting recognition properties of the polymers, and the use of pH control to adjust selectivity when recognition is based on ionic interactions The performance of the MIPs presented in the second chapter is then used as a platform for probing more fundamental aspects of MIP behaviour Properties of pre-polymerisation mixtures which have consequences for final MIP recognition behaviour are examined in detail in Chapters three and four, with NMR spectroscopy (coupled with subsequent HPLC evaluation of the MIP recognition capabilities) playing an important role The impact of more subtle effects, such as π–π stacking and phase partition, is of particular note Chapter five shows how spectroscopic data, as acquired in Chapter 4, can be used to refine simulated models of pre-polymerisation complexes, which may be of significant benefit in predicting MIP properties and ultimately in creating a step-by-step protocol for designing efficient MIPs

Chapter One

The Importance of Making a Good Impression – Current Research in the field of Molecular Imprinting Technology.

1.1. Introduction to Molecular Imprinting

As research in this area has progressed during the past decade, molecular imprinting has become a valuable tool in the field of analytical chemistry, offering a cheap, facile means of creating a polymer matrix with specific recognition properties that can be used for a broad range of applications from purification of racemic mixtures[1], to chemical sensing[2], to catalytic control of difficult chemical reactions[3]. The exponential growth in publications (Fig. 1.1) on the topic reflects the attention the area has received by many research groups[4].

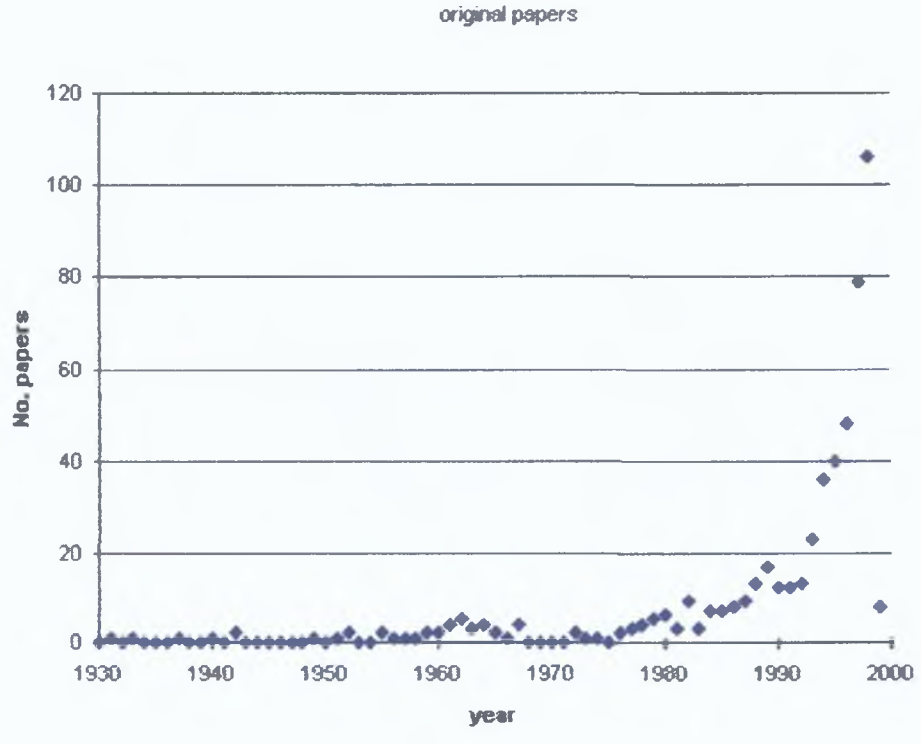

Fig. 1.1 – Literature published on molecular imprinting

The wealth of literature available on the subject frequently underlines the 'biomimetic' properties exhibited by these imprinted polymers, the substrate-

selective effect displayed being analogous to that of natural entities such as antibodies and enzymes The concepts underpinning molecular imprinting theory are perhaps best exemplified by the lock-and-key mechanism postulated by the Nobel laureate Emil Fischer to explain enzyme-substrate interactions[5] According to Fischer, enzymes possess a unique structure that is complementary in nature to the corresponding substrate This was later refuted by x-ray diffraction studies which showed that enzymes have a rather more flexible sub-structure than that indicated by the lock-and-key principle, however, the idea of a matrix designed to recognise a particular substrate remains the cornerstone of molecular imprinting theory and has been the primary goal of research since the resurgence in interest in the field in the 1970's

For a non-covalent approach to creating an imprint, the procedure begins with the self-assembly of functional monomers around the imprint molecule of choice, the bonding between the imprint molecule and the functional monomer(s) can be either covalent or non-covalent, as required For the majority of imprints, however, the non-covalent approach is preferable since the extraction process is simpler (as explained in the next section) The entire process may be represented graphically as

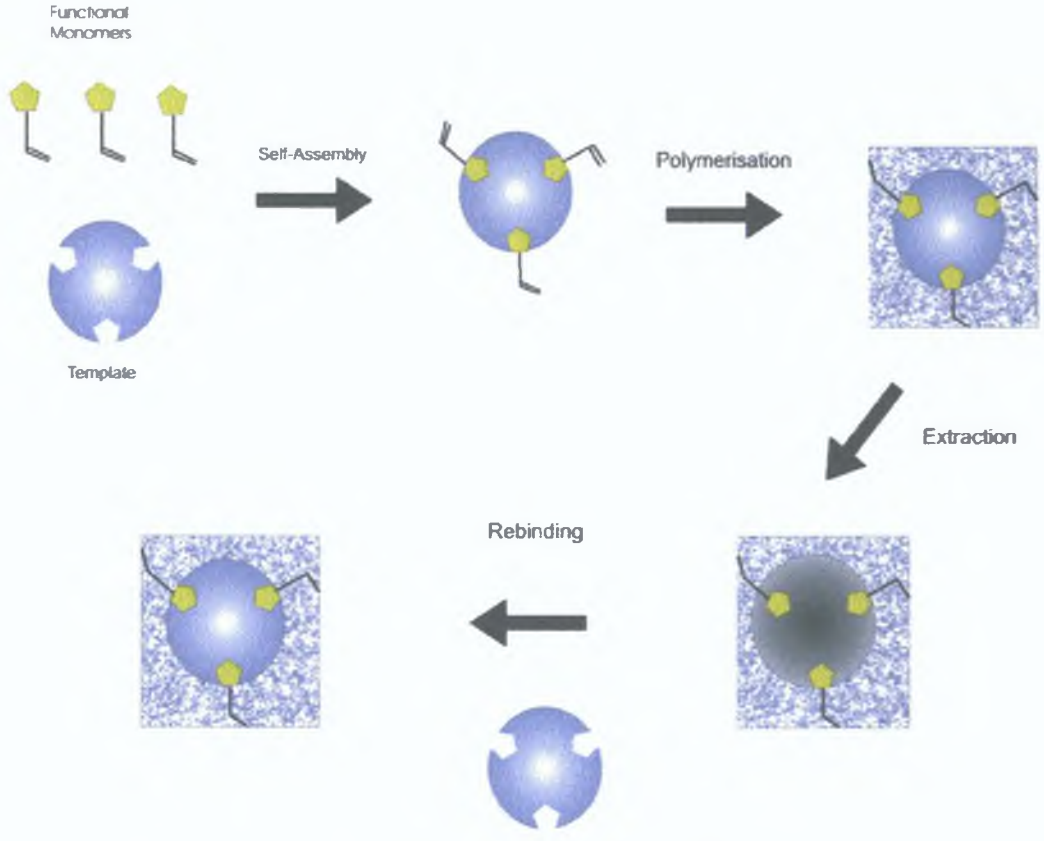

Fig. 1.2 – Molecular Imprinting via self-assembly – the non-covalent approach

Although such schematics are useful for explaining the various stages involved in preparing an imprinted polymer, their simplicity does not adequately represent the sometimes complex interactions which dictate the success of an imprinting protocol. Synthesis of an optimised imprinted polymer requires careful consideration of various factors such as polymer composition, choice of solvent, extraction procedure, degree of crosslinking and polymerisation conditions. Such considerations are examined in detailed in Section 1.11. An extended treatment of these topics, including the use of the alternative covalent imprinting technique, may be found in Sellergren's comprehensive volume published in 2001[6].

However, despite over a decade of intensive work in the area, MIPs are still the focus of much academic research and understanding of the technology continues to evolve This literature survey will first discuss the origins of molecular imprinting (and how these origins still have ramifications for contemporary research) The properties of these polymeric materials – stability, adaptability to various applications, monomer and template considerations – are described to highlight design considerations before applying MIPs to a particular analytical problem The application of MIPs to practical analytical problems will be discussed, underlining the commercial potential of the field Solid-phase extraction, the most widely-used and easily-adaptable application of the technology, will also be examined in detail Finally, the rational design of imprinted materials, which holds the most potential for the advancement of the field, will be discussed at length

1 2 Evolution of the concept. Specific Cavities or Nucleation Cluster?

"Footprints" in silica Dickey's precursor to modern MIPs

Working under the eminent chemist Linus Pauling, Dickey managed to 'imprint' silica gels with alkyl orange dyes, with the resultant silica gel possessing a definite affinity for the dye with which it was imprinted Dickey's explanation was the formation of cavities that were complementary in chemical nature to the imprint molecule[7] This theory was disputed by Morrison *et al*[8] who conducted independent research into the same experimental area They concluded that any observed retention was due not to molecules occupying specific cavities, but a self-association mechanism whereby template molecules, trapped after the synthesis step, act as nucleation centres, interacting with similar molecules when re-exposed

The association mechanism was later refuted by Beckett and Youssef[9], citing several reasons precluding an association mechanism, such as the fact that an inverse relation was seen between the amount of trapped template and amount of analyte retained A nucleation mechanism should promote greater retention when a larger amount of template remains in the polymer network Also, an association mechanism would cause an enantiomer (as trapped template), if it forms a racemic compound with its opposite enantiomer, to yield a more stable complex with this opposite enantiomer and thus selectively retain it, however, it

was observed that the reverse is true – matrixes imprinted with enantiomers will show selectivity for that enantiomer Although silica-imprinted chemistry was not pursued on the same scale that imprinted polymers currently experience, the relevance of the arguments and theories used to explain and describe the field continue to be cited in explanations of MIP behaviour

It is perhaps salient to note at this point that although the 'specific cavity' theory is the most widely accepted explanation of the recognition properties of MIPs, the actual mechanism continues to be debated Recent work by Baggiani *et al* [10] has demonstrated that for a typical 4-vinylpyridine/ ethylene glycol dimethacrylate co-polymer imprinted with 2,4,5-trichlorophenoxyacetic acid (2,4,5-T), a self-association mechanism appears to dominate Using a Freundlich-Langmuir adsorption isotherm binding model, it was found that a polymer imprinted with, as template, a mixture of ⅓ 2,4,5-T and ⅔ a polymerisable derivative of 2,4,5-T, displayed a higher affinity than a polymer imprinted purely with 2,4,5-T They concluded that the covalently bound template acted as a nucleation point for the formation of template molecule 'clusters', and binding sites created in a MIP are actually created by these aggregated clusters rather than individual template molecules However, the work does not identify whether this effect requires template molecules to remain trapped in the matrix to create nucleation points, or if it can occur as a cooperative effect between template molecules upon rebinding

The Nicholls research group have also tackled this issue, anomalous results from a chromatographic study on a MIP for nicotine, where higher sample loads resulted in higher retention and selectivity, suggested the presence of binding sites specific for template-template complexes[11] A ^{1}H-NMR study of the pre-polymerisation mixture[12] indicated that nicotine-nicotine complexes were in fact stabilised by the presence of acetic acid (as analogue of methacrylic acid monomer), with the maximum for a Job's plot analysis of nicotine-acetic acid titration occurring at 1 5 1, suggesting the formation of template-template complexes Further work in this area is evidently required to assess the contribution of self-association mechanisms to the creation of an imprinting effect

Although the concept of imprinting had been proposed in the late 1940's by F H Dickey, the principles of synthesis and application of the imprinted polymer were established in the mid 1970's, with interest in the area growing heavily throughout the 1990's The adoption of imprinting as a valuable tool in separation chemistry has been a gradual process, however, an important publication in the proliferation of the technique was that of Klaus Mosbach and Lars Andersson (University of Lund, Sweden) in 1990[13] Although the work was essentially a continuation of earlier work on the separation of amino acid conformers[14], its importance lies in the broadening of the scope of molecular imprinting It identifies the limitations of the covalent approach (e g very few reversible covalent bonds that are suitable for use) and points to the possibilities offered by

hydrogen bonding, using a carboxylic acid This was the first time that such a weak bond type had been exploited for an imprinting application, and it opened the floodgates for the vast amounts of research based around non-covalent imprinting that have been carried out since then This paper, then, probably represents the transition of molecular imprinting from being an interesting phenomenon to being a practical, easily adaptable analytical tool

An article published by Piletsky, Alcock and Turner[15], more than a decade after Mosbach and Andersson's paper, demonstrated the resultant broad diversification of MIP applications These range from more conventional uses (e g enantiomeric resolution, purification and preconcentration of samples), to more unorthodox ones, such as detection of chemical and biological warfare agents under battlefield conditions and development of electronic 'noses' to test wine quality[16] However, the cornerstone of MIP technology in commercial applications remains solid-phase extraction of samples for the pharmaceutical industry Indeed, this has proven to be the first commercially viable application of MIPs[17]

1 3 MIPs in the Marketplace – a Viable Commercial Venture?

Future research into the field of molecular imprinting will depend to a large extent on how successful the technology is when it competes in the marketplace against conventional solid-phase extraction sorbents, LC column packings, sensor recognition elements, etc The overview written by Piletsky *et al* [15] at the end of 2000 details the potential of MIPs According to this article, the projected US market for separation techniques will be approximately US$1 19 billion MIP materials could claim a share of 1-3% of this, particularly in the chromatography column sector, which is valued at US$500 million per annum The ability of imprinted polymenc matenals to resolve racemic mixtures could prove especially lucrative in the pharmaceutical industry, where as much as 68% of drugs currently in development are chiral This corresponds to a market for chiral compounds of US$120 billion (figures for 2000) This paper covers a broad selection of MIP applications, from separations and assays and sensors, to catalysis More advanced uses, such as detection of gases in space exploration and drug-release matnces, are also briefly referred to However, the main prospects for impnnting technology lie in the contract manufacturing of MIP materials, valued at US$100m-US$300m, based on demand for SPE sorbents and enantioselective materials by the pharmaceutical industry Other analysts have pointed to the potentially huge market for tailor-made sensing devices for testing the quality of consumer goods, worth up to US$4 billion[16], to which MIPs would be particularly suited

However, reviewing the work of Wulff, Mosbach, Andersson and others, it becomes apparent that it is not possible to develop a general protocol for synthesis of an effective MIP for any given analyte, rather, it is necessary to examine in detail the chemical nature of the analyte and then tailor the polymer according to this For this reason, it is indispensable to investigate the analyte-polymer interaction in as much detail as possible, with a view to understanding and optimising the MIP performance in applications This type of 'rational design' research, described in Section 1 11, is still progressing, and this may in part account for the failure of MIPs to be commercially exploited to a significant extent so far

1 4 Preparing the Polymer

For these "plastic antibodies" to be successfully employed as an analytical tool, Wulff proposed[63] several criteria that the synthesised polymer should satisfy These are

a) Stiffness of the polymer structure – to retain cavity shape and the spatial relationships of functional groups
b) Good accessibility of as many cavities as possible, to maximise capacity
c) Mechanical stability – since the polymer may be exposed to extreme conditions, such as HPLC, or in a stirred reactor as a catalyst
d) High flexibility of the polymer structure, essential for the rebinding kinetics, to give rapid equilibration with the substrate to be embedded
e) Thermal stability, since higher temperatures may offer more favourable equilibration kinetics

An adequate comprise between these criteria is required and can be tailored according to the application that the polymer is destined for

1 5 Chemical & Thermal Stability

Much MIP-related literature makes reference to 'stability' as a criterion for choosing MIP technology in preference to conventional biological-based immunoassays[18], which are notonously sensitive to extremes of heat and pH However, in order to gauge just how resistant MIPs are to extreme conditions, Svenson and Nicholls performed a conclusive study[19] using a theophylline-imprinted polymer system that has already been otherwise thoroughly researched by Vlatikis *et al*[20] Chemical stability studies demonstrated that the polymers kept over 95% of their affinity for the imprinted molecule, even after 24 hours of exposure to autoclaving treatment, triethylamine, 10M HCl acid and 25% NH_3 Heat treatment showed the polymers to be as resilient thermally as they are chemically – no affinity for the imprint molecule was lost at temperatures of up to 150°C Decarboxylation follows at higher temperatures, causing loss of MIP specificity Also of note from this work, polymers synthesised eight years prior to the study were also analysed and found to have retained their affinity for the template

This stability opens up avenues of research, such as pH optimisation, to improve recovery in SPE work (reviewed later) and optimising column temperature in LC to improve mass-transfer kinetics The latter was explored by Chen *et al*[21] in 1999 Although in this work, the thermal annealing process proved to be detrimental to the polymer selectivity (inhibiting chiral resolution of D,L-

phenylalanine anilide), it was found to improve polymer capacity This was assumed to be due to the decrease in swelling caused by the heat treatment and subsequent increase in density, resulting in an increase in the density of the remaining binding sites (both selective and non-selective) The researchers also found that thermal treatment had the additional benefit of markedly improving the long-term thermal stability of the polymer, with less baseline drift when working at temperatures of 50°C and over

1 6 Size Limitations· Difficulties in Imprinting against Large Molecules

Despite the broad range of compounds that have been successfully imprinted against – drug molecules, insecticides, nicotine, steroids, amino acids – one attribute shared by all these templates is that they all have a relatively low molecular weight Two main reasons for this is that most larger templates are less rigid and thus do not successfully create well-defined cavities during the imprinting process Large biomolecules such as proteins may lose their secondary and tertiary structures when exposed to the thermal or photolytic treatment involved in the synthesis step of imprinting Also, rebinding is more difficult, since large molecules such as peptides and proteins cannot easily slip into the polymer network and reoccupy specific cavities

In keeping with the biomimetic nature of imprinted polymers, Rachkov & Minoura[22] used a method of circumnavigating this steric problem that is analogous to biological systems In recognising an antigen, an antibody

recognises not the entire molecule, but a small characteristic site on it, known as an epitope The corresponding technique, when this approach is applied to molecular imprinting, is to imprint against a short peptide that is characteristic of the protein to be retained on the polymer Their work was based around the hormone oxytocin, in this case, the structure of the hormone receptor remains only partially characterised, and the hormone-receptor interaction is poorly understood[23] Enzymatic studies have revealed the importance of the 3-amino-acid C-terminus in intermolecular interactions, making this a suitable part of the molecule to imprint against Using a combination of MAA and EGDMA (optimum ratio ~1 20), a polymer imprinted with a tetrapeptide residue was created and successfully retained the oxytocin hormone (although exhibiting a preference for the original tetrapeptide template) This work offers a means of creating effective synthetic adsorbents for peptides and proteins, while avoiding the typical limitations involved in manipulation of biological receptors

1 7 Adaptability

The vast majority of papers on the subject use essentially the same technique to obtain the requisite imprinted material – bulk polymerisation, followed by the breaking up of the resultant monolithic structure, grinding and sieving This whole procedure can leave much to be desired – it is tedious, time-consuming and ultimately very inefficient – grinding creates irregular particles, which can cause flow problems when packed into a column, and fines, which are lost during the sieving process The consequence of synthesising and processing imprinted polymers in this way is that typically less than 50% of the synthesised polymer will be usable for chromatographic purposes[24] This renders the technique unattractive to industry, being both wasteful and problematic for scale-up Alternative means of creating imprinted surfaces have, for these reasons, been explored in recent years As a separation technique, MIPs have mostly been exploited as either the main component of solid-phase extraction cartridges, or as a packing for LC columns A major consideration of employing the polymers as a stationary phase for an LC column is that typically, MIPs that have been ground and sieved are irregular in shape, and have a range of sizes, thus resulting in columns that frequently perform unpredictably, due to the effect of this shape irregularity on diffusion processes within the column Mass transfer effects also have a bearing, as observed in studies on enantiomeric resolution of D,L-dansyl-phenylalanine[25] This points to a need to develop MIPs of uniform

shape and size, which would be better suited to use in chromatographic applications

Mayes and Mosbach broached this topic in their 1996 article[24] and came up with the elegant solution of using a liquid perfluorocarbon as the dispersing phase in a suspension polymerisation, yielding sphencal polymer beads An acrylate polymer was used in the method to stabilise the emulsion of (initiator/ crosslinker/ imprint molecule/ porogen) and by varying the amount of stabilising polymer added, the size of the beads obtained could be vaned, between 5 and 50 μm Small bead packings offer low back-pressure and rapid diffusion in LC, giving good separations even at flow rates of up to 5 ml/min On the other hand, although recyclable, the necessary perfluorocarbon solvents are quite expensive, negating the usual low-price advantage associated with MIPs

A relatively simple means of examining the effects of a particular imprinting technique is to look at the volume occupied by the pores embedded in the polymer structure size and compare it against the surface area of a control polymer, generally, it has been found that the impnnted polymer has a much greater internal porous surface area than the non-imprinted control polymer created under identical conditions The analysis is usually performed via the BET technique, work performed by Bruggemann[26] showed that the impnnted polymer may have a surface area up to six times greater than the equivalent control polymer (6 02 m^2/g for the imprinted one vs 1 05 m^2/g for the control) However,

as noted here, this is still a relatively small surface area for a porous polymer structure – mesoporous materials may have a surface size of up to 1000 m^2/g Hosaya *et al*[27] came up with an alternative to the conventional method of synthesis in 1994 This involved a two-step swelling followed by polymerisation in aqueous media The technique yielded particles of good size monodispersity, which were suitable for use in a chromatographic column

The scientific community at large has also seen the potential of molecular imprinting for the development of chemosensor recognition elements, and this has lead to further innovation with the technique Mirsky *et al*[28] described their method for creating artificial chemoreceptors, which involved the co-adsorption of a template molecule and matrix onto a gold substrate Specific binding sites were created by this, and binding events could be observed through changes in the capacitance of the gold electrode – an increase in the dielectric thickness decreases the electrode capacitance[29] The template molecule in this work was used to inhibit lateral diffusion of the monolayer on the substrate (which would cause distortion of the binding site)

The Mosbach group have also delved into the field of solid support-assisted molecular imprinting, using an aminopropyl-derivatised silica gel as a solid support[30] An 8-carboxypropyl derivative of the theophylline was immobilised onto the gel A TFAA/ DVB co-polymer was then co-polymensed together with the theophylline/ silica gel Subsequent to the polymerisation, the silica gel was

removed by a wash with HF acid, the polymer was then ready for application The advantages offered by this technique are multiple, perhaps the most significant is that the imprinting of insoluble templates becomes possible Also of note is that the danger of self-aggregation of templates in the pre-polymerisation mixture is avoided Apart from being an excellent example of how imprinting procedures can be quickly adapted to suit a particular application or requirement, solid support-assisted imprinting demonstrates a practical means of overcoming one of the more typical limitations associated with imprinting, that of low yield It can be expected that such an approach to impnnting will be exploited in the years to come

Silica has also been used by the Mosbach group, in spherical bead form, to create MIP beads of consistent size[31] The beads produced by the method are all regular spherical particles of approximately 13 μm in diameter, suitable for use in LC columns The method involves infusing porous silica beads (porous volume of 0 7 ml/g) with a MIP solution and then a thermal polymerisation, followed by removal of the silica from the resultant composite by washing with HF acid These MIP beads are also extremely porous, up to 55% more so than beads obtained through other methods, and consequently display greater chromatographic performance

MIPs prepared via some of the above techniques are suitable for chromatographic applications such as liquid chromatography and solid-phase extraction, however, for quick evaluation of the performance of a MIP, thin-layer chromatography offers a means of rapidly assessing how well a MIP retains analyte This also has the advantage that the polymer requires no special processing or filtering, just simple grinding The technique was explored by Suedee *et al*[32] to create a TLC stationary phase selective towards various adrenergic drugs such as ephedrine, pseudoephedrine and isoproterenol Creating the TLC plates for the study was achieved by coating glass slides (76mm x 26 mm) with a slurry of calcium sulphate and imprinted polymer (50/50 mixture)

1 8 Combining Different Monomers to Improve Selectivity

Despite the versatility of molecular imprinting as a useful analytical tool, there remain several challenges in modifying the technique to suit more awkward template systems An example of this is the work performed by Zhang *et al*[33] where they explored the possibility of imprinting against three structurally-similar organic compounds - gentisic acid (GA), 4-hydroxybenzoic acid (HBA) and salicylic acid (SA) The group selected acrylamide as functional monomer, which is a strongly hydrogen-bonding compound[34], but despite this, they experienced difficulty in successfully imprinting the compounds salicylic acid and gentisic acid, due to the strong intramolecular hydrogen bonding which occurs in these molecules (Fig 1 3)

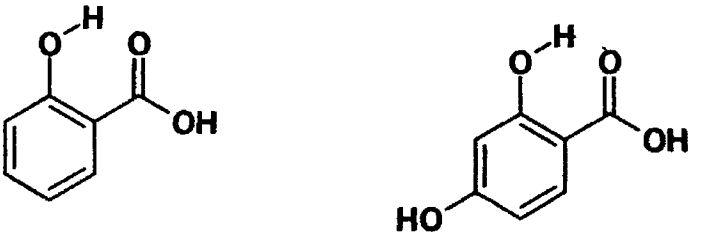

SA **GA**

Fig 1 3 – Intramolecular hydrogen bonding in salicylic and gentisic acid

Amides as functional monomers were first described by Yu and Mosbach in 1997[34] and were noted for their ability to form strongly hydrogen-bonded complexes with the amino acid templates investigated It was determined that imprinting with an amide monomer gave higher polymer capacities and greater specificity in the final MIP than using a carboxylate-based monomer This was

due to the reduction in the number of charged groups on the polymer (since the amide promotes hydrogen bonding only) and the consequent elimination of non-specific ionic interactions between the polymer and various analytes, as well as the elimination of swelling associated with having a polymer containing many charged groups – swelling which could cause distortion of binding sites and thus affect polymer specificity and capacity

However, amide groups may not improve selectivity in systems that are driven by hydrophobic interactions This was examined by Zheng *et al*[35] in their investigation into the effects of combining monomers to design to more specific imprinted polymers The templates being used here were sulfamethoxazole (SMO) and sulfamethazine (SMZ), which resemble each other structurally (Fig 1 4), but differ in terms of hydrophobicity due to an ether linkage found in SMO, but not in SMZ

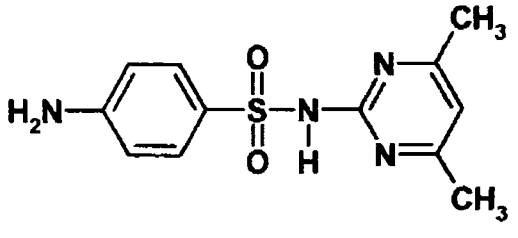

SMZ

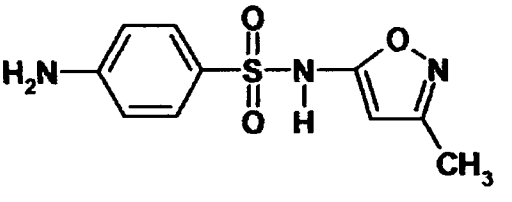

SMO

Fig 1 4 – Structures of Sulfamethazine (SMZ) and Sulfamethoxazole (SMO)

1 9 Molecularly Imprinted Materials and Sensor Technology

The stability of MIPs, as detailed above, points to their potential in the field of sensor technology, given that biological components used in contemporary biosensors are sensitive to extremes of heat, pH and use in organic solvents, as well as frequently having a short lifetime Many groups involved in detailed MIP research have, at one stage or another, explored the possibility of integrating imprinted materials into sensing devices as the recognition element As Wulff emphasises in his comprehensive 1995 review of the field[63], the formation of a complex between functional monomer and template introduces recognition properties into the polymer network Receptor-mimicking sites on the polymer therefore possess the potential to be exploited in sensing devices, if coupled to an appropriate transducing element. This has proven to be a stumbling block to developing MIP-based sensors to date – the polymer/ analyte binding event rarely creates an easily transduced signal Fluorescent compounds offer a simple means of creating a detectable binding event, for this purpose, groups such as Zhang *et al*[36] have developed fluorescent monomer species Fluorescent tagging is also a reasonably simple means of achieving a detectable binding event, as demonstrated by the tagging of homocysteine with the fluorescent N-(1-pyreneyl) maleimide – this also possesses the advantage that the MIP created acts as a catalyst in the derivatisation of the homocysteine to its fluorescent derivative[37]

Subrahmanyam *et al*[38] tackled the problem by using a 'bite-and-switch' approach, which is defined in terms of the polymer's ability to bind the analyte ('bite') and immediately generate the signal ('switch') The chemistry of the binding/ fluorescence is quite simple, their analytes of choice were the nutritional supplements creatine and creatinine Both compounds are primary amines (fig 1 5)

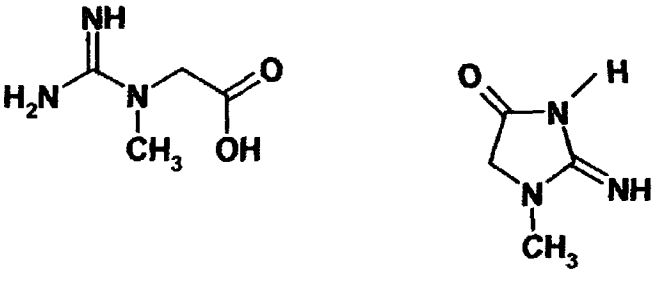

Creatine **Creatinine**

Fig. 1 5 – Structures of Creatine and Creatinine

Interactions between primary amines and thioacetals lead to formation of a fluorescent isoindole complex Thus, the group constructed a MIP using EGDMA as crosslinker, methylated creatine and creatinine as the template molecules (it must be methylated – isoindole complex cannot be hydrolysed back to thioacetal for rebinding), a mixture of allyl mercaptan and o-phthalic dialdehyde (to construct the thioacetal), and one further monomer to induce selectivity Based on computer simulations using the SYBYL-6 molecular modelling package, urocanic acid methyl ester was chosen as the additional functional monomer The net result is that the polymers generate a fluorescent signal upon recognition of the analyte in question that is proportional to the analyte concentration It is

upon this basis that the system was suggested as a potential sensor recognition element

Another system based on competitive binding, used to measure morphine concentration on a μg /l scale, was scrutinised by Kriz and Mosbach[39] in 1995 They coated a platinum wire with agarose-immobilised MIP particles (which were imprinted against morphine) For a reference polymer, the team used an L-phenylaniline anilide-imprinted polymer Using a typical 3-electrode system, the morphine solution being analysed was added and the current was allowed to equilibrate At this stage, a solution of 10 mg/ml codeine was added to competitively bind to the MIP-coated electrode After 20 minutes, the current peak was recorded This was proportional to the morphine concentration A potential of +500 mV was chosen, since current due to the oxidation of codeine is negligible at this potential Codeine is less susceptible to oxidation than morphine due to the absence of the phenol substituent in codeine (Fig 1 6)

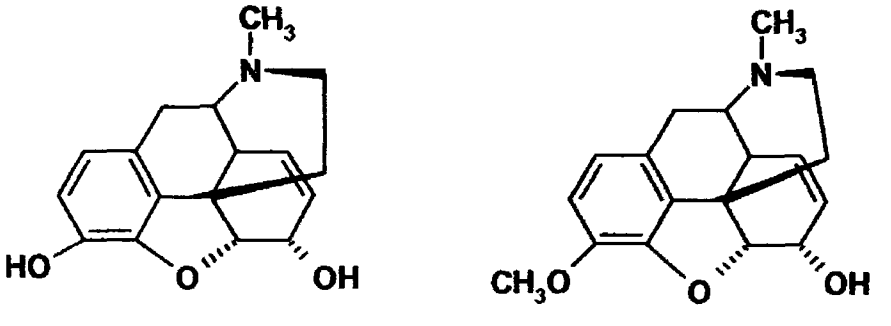

Morphine **Codeine**

Fig 1 6 – Structure of Morphine and Codeine

The MIPs used in this study were stringently examined for stability by exposure to heat, acidic and basic conditions, organic solvents and heavy metals, without any notable decrease in sensor response (94%-100% sensitivity retained) Also, the sensors were stored in water for 4 weeks and no decrease in response was observed

More recent developments in the integration of MIPs into sensor technology have been aimed at more precise quantification of analyte, and miniaturisation of the final sensor product To this end, work has been performed using the methods of quartz crystal microbalance[40] (QCM) and thickness shear mode (TSM) acoustic sensing[41] In a typical MIP/ QCM-based sensor, a polymer film is electrochemically synthesised onto the surface of one of the platinum electrodes of the QCM device Polymer film growth is controlled by the amount of charge passed during the electropolymensation Slight differences in the mass of the electrode, caused by rebinding of molecules to the specific cavities of the imprinted polymer film, correspond to a change in the frequency of the quartz crystal resonance and thus a measurable signal Work recently published by Hirayama *et al*[42] has shown the immense potential possessed by this approach, developing a QCM-based sensor for an environmental application (monitoring of acetaldehyde levels), the group constructed a sensor capable of sensing acetaldehyde levels as low as 0 015 mmol/l Also of note is that the sensor also displayed enhanced selectivity towards acetaldehyde in the gas phase, retaining

up to seven times more acetaldehyde than other gaseous small organic molecules

Alternatively, covalent-based imprinting techniques have also been employed to produce QCM-MIP sensors, as shown by Percival *et al*[43] in their work on a nandrolone sensor In this instance, the MIP was first synthesised by polymerising a vinylphenylcarbonate derivative of the template nandrolone, and then a suspension of this MIP (finely ground), together with some PVC to improve adhesiveness, was spin-coated onto a QCM electrode to form a very thin film This sensor again showed remarkable sensitivity when exposed to the imprint molecule, with no detectable decrease in frequency of the coated quartz crystal upon exposure to compounds such as testosterone and epitestosterone, despite the obvious structural similarities to the template (Fig 1 7)

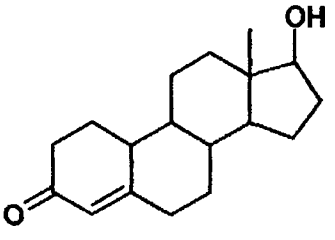

Nandrolone

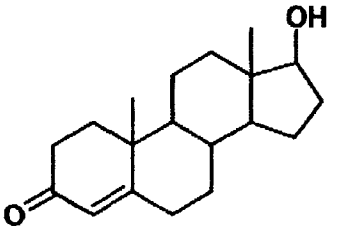

Testosterone

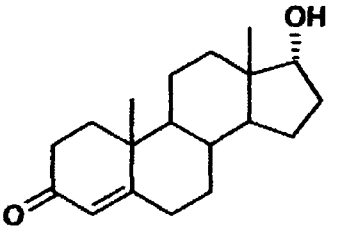

Epitestosterone

Fig 1 7 – Structures of Nandrolone, Testosterone and Epitestosterone

1 10 Solid-phase Extraction with Molecularly Imprinted Materials

The evolution of molecular imprinting from a technique primarily of interest for its theoretical implications, to a genuinely useful tool in analytical chemistry is perhaps most evident in the exploitation of molecularly-imprinted solid-phase extraction Borje Sellergren[44] published a groundbreaking paper in 1994 that paved the way for intensive research in the field of solid-phase extraction (SPE) The analytical community at large recognised the potential advantages of the technique compared to conventional solid-phase extraction sorbents These include greater reproducibility, and a rapid, easy, cost-effective synthesis This represents an attractive alternative to standard C18 phases, where the presence of residual silanol groups on reverse-phase materials leads to more than one retention mechanism affecting results and consequently greater vulnerability to variations between batches[45]

In most analytical procedures, the step that will have the most significant impact on final yield is the sample pre-treatment stage In conventional liquid-liquid extractions, sample components can be lost during the evaporation step (if they're volatile) or if emulsions form, meaning SPE can often be a preferable alternative Solid-phase extraction offers several advantages over liquid-liquid extraction (LLE), primarily the reduced cost (because of lower consumption of organic solvents) and the broader range of extraction mechanisms that can be exploited (H-bonding, ion-exchange, hydrophobicity) Currently, the more popular

SPE sorbents are silica-bonded phases (octyl C8 and octadecyl C18) and ion-exchange phases The potential of MIPs for this type of application, as specified in Sellergren's paper, has been thoroughly investigated[46], culminating in the commercial vending of MIP-based SPE cartridges by companies such as Jones Chromatography (USA) and MIP Technologies (Sweden)

April 2002 saw the release of a clenbuterol MIP[17] by MIP Technologies Clenbuterol is a potent respiratory stimulant in both human and animal medicines, however, it is also illegally used as a growth promoter in cattle and thus meat products contaminated with the drug poses a threat to consumers with cardiac deficiencies or in the later stages of pregnancy[47 48] Clenbuterol may thus be identified by preconcentration of liver extracts via SPE and subsequent HPLC analysis Masci, Casati and Crescenzi[49] have in the past researched and designed MIPs for this purpose MIP Technologies have marketed their particular product on the strengths of MISPE compared with typical SPE procedures, namely improved sensitivity (down to 0 5 ng/ml) and the use of more robust HPLC methods To evade any template bleeding problems, the polymer was imprinted with bromobuterol – this is then easily identified in chromatograms, eluting as the final peak 6 minutes after clenbuterol Emphasised heavily is the efficiency of the MIP phase in cleaning up the sample compared to C4, C8 and C18 bonded silica phases Entering the competitive marketplace represents a significant advancement of the technology, and the scale of research in this

branch of analytical chemistry in the years to come will most likely be a reflection of the success (or failure) of MIPs as a commercial venture

The sensitivity factor and the associated benefit of cleaner samples that are inherent in sample pre-treatment via MIPSE should also intrigue the environmental chemist, there is already a wealth of literature detailing MIP development towards the triazine herbicide atrazine, including application in sensor technology[50] The design of a MISPE for clean-up of chlorinated phenoxyacids from environmental water samples by Baggiani *et al*[51] is a good example of how MIPs can be employed to resolve analysis problems Chlorinated phenoxyacids are highly toxic herbicides with a long persistence in the environment, and cannot be detected (or quantified) at trace levels by GC, HPLC or CZE, necessitating a preconcentration step The difficulty of separating compounds of similar hydrophobicity/ hydrophilicity, associated with conventional C18 SPE is effectively dealt with, since imprinted polymers are reported to distinguish between subtle differences in hydrophobicity Adjusting aqueous content of the mobile phase permits complete optimisation of these types of extractions

An application with enormous potential that involves off-line SPE and offers scope for development and extensive use in industry (particularly pharmaceuticals) is combinatonal chemistry, which is further discussed in Section 1 11 2 The technique has successfully been employed to screen a small

steroid library by Ramstrom *et al*[52] The use of molecularly imprinting-based combinatorial chemistry may prove valuable in drug discovery where natural receptors for the given drug molecule are difficult to purify, costly or poorly characterised

Although most approaches to MISPE detailed in the current literature describe off-line procedures, MISPE has also been incorporated into on-line preconcentration methods One such example is that described by Mena *et al*[53] for the preconcentration of the insecticide pirimicarb on-line, which allowed selective determination of the analyte at low concentration levels (~4 1μg/l) in various environmental samples, in less than fifteen minutes This offers a sensitivity improvement of one order of magnitude for the same analysis without using a MIP pre-column

Future work in MISPE will most likely be directed at refining on-line procedures of MISPE coupled with HPLC[54] One such example is the application of MIP-coated fibres in solid-phase microextraction (SPME) Crescenzi *et al*[55] investigated the coating of a silica fibre with a clenbuterol MIP and used it for the SPME of clenbuterol and some of its structural analogues in human urine samples

1 10 1 MISPE under Aqueous Conditions

An important consideration when modifying a MIP-based SPE to enhance selectivity and overall performance is the influence of pH on the retention mechanism The influence can be attributed to its effect on both system components – the imprinted polymer network and the analytes being loaded When the functional monomer(s) used for synthesis of the impnnted polymer have a marked acidic or basic character, the resultant stationary phase frequently display good chromatographic performance and selectivity in aqueous mobile phases, where the retention mechanism is dnven by ion exchange Sellergren and Shea[56] proposed the simple cation-exchange model as a means of explaining solute retention originally in 1993 LC and potentiometric pH titration data was collated and compared to simulated data obtained using a weak cation-exchange model The close correlation between the two, as well as the fact that maximum retention was observed at an apparent pH (of the mobile phase) which corresponds to the apparent pK_a of the analyte of interest (L-phenylalanine anilide), suggested that the retention on these MIPs was controlled by a simple ion-exchange process The influence of pH on the chromatographic performance may be explained (and predicted) by considering the protonation state of the analyte and its consequent affinity for the polymer binding sites at a particular pH Thus, at lower pH the protonated analyte molecules have a strong affinity for the specific binding sites that can accommodate them sterically and that have a chemical complementanty imparted at the imprinting stage Increasing pH means that less analyte is protonated, while more non-selective sites are becoming

deprotonated, resulting in less selectivity, but a higher capacity This work was corroborated by further research by Chen *et al* [57] in 2001 into chiral resolution of D,L-phenylanilline anilide on a molecularly imprinted CSP By application of different isotherm models (Langmuir, bi-Langmuir & Jovanovic-Freundlich), the behaviour of the MIP at varying pH conditions was investigated The results support the binding site model of MIP performance, wherein there exists two types of binding site – specific and non-specific Again, once the pH of the mobile phase exceeded the pK_a of the analytes, selectivity was lost This was attributed to the number of non-selective sites increasing, with increasing pH, slightly faster than the selective sites, suggesting different pK_a ranges for the two types of site Also, the binding energy and the homogeneity of the selective sites decreased with increasing pH, supporting the binding site model involving more than one carboxylic acid functional group, providing charge complementarity and hydrogen bond donors for the L-PA analyte

Although pH can in this way control selectivity, it is worth noting that hydrophobic interactions (due to aqueous conditioning) can also adversely affect retention and selectivity as observed by Molinelli *et al*[58] In this example, in order to distinguish between two molecules containing only minor differences in polarity (quercetin and 2-carbethoxy-5, 7-dihydroxy-4-methoxy-isoflavone), it was necessary to load the SPE cartridge using acetonitrile This allowed the stationary phase to recognise subtle differences between the polar functionalities of these two analyte molecules This demonstrates the necessity of identifying hydrophobic

parts of template molecules and thus to what extent hydrophobic interactions will affect polymer performance at the SPE stage Also among these considerations when modifying pH in order to adjust MIP selectivity, is the possibility that protonation (or deprotonation) of analyte molecules may lead to a distortion of its overall structure, lowering its affinity for binding sites created through imprinting Mena *et al*[53] found a lowered response with their pirimicarb-imprinted polymer at pH 2 0, which indicated analyte breakthrough during the loading stage They hypothesised that this was due to the protonated, charged analyte molecules being unable to "fit" the binding sites and consequently not being adsorbed by the uncharged polymer

As noted earlier, it is usually necessary to add a certain quantity of acid to the eluent when obtaining the elution fraction, although this may affect selectivity, it is often necessary to yield a quick and quantitative elution[59] This is particularly so when the polymer is acid based (e g methacrylic acid), to rupture the interactions between the carboxylic acid residues of the polymer and the corresponding functionality of the analyte molecule, acetic acid is frequently used, as it can successfully compete for the bound analyte However, the acidity of the monomer used cannot be excessive – using very acidic monomers such as trifluoromethacrylic acid[60] has been found to lead to a higher degree of ionisation, regardless of the pH at which the polymer is studied This leads to lower overall specificity – although the polymer network displays a strong affinity for positively charged species, where selectivity is hydrogen-bonding driven the specific retention will be reduced

1.11 Assembling the ideal MIP Rational Design in Molecular Imprinting

1 11 1 The Study of The Mechanisms of Molecular Imprinting

The phenomenon of imprinting and subsequent recognition properties of the imprinted media has been observed and reported in detail, however, the mechanisms of recognition are, as of yet, not entirely understood and this inhibits the optimisation of the process Despite the wealth of literature on the subject that has been published across the past decade, much remains to be discovered This becomes apparent in articles such as that published in 2001 by P D Martin *et al* [61] It was found that, after imprinting a polymer against the drug tamoxifen for solid-phase extraction, a control polymer imprinted against propanolol exhibited greater affinity for tamoxifen than the tamoxifen-imprinted polymer, despite the obvious differences in the structures of the two molecules (Fig 1 8)

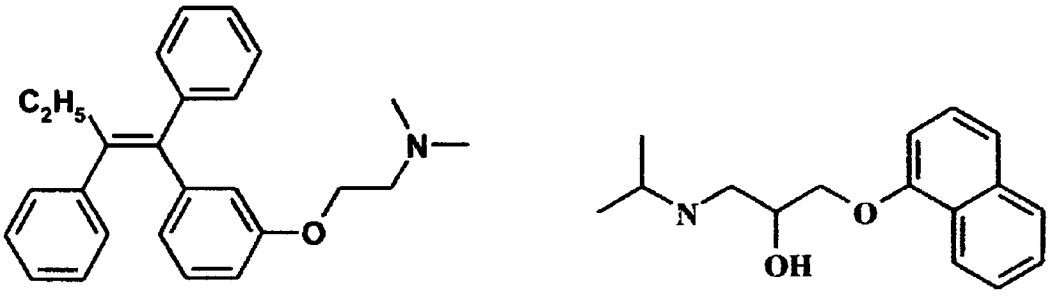

Tamoxifen **Propanolol**

Fig. 1.8 – Comparing structures of tamoxifen and propanolol

Of further concern in the field of molecular imprinting is the application of MIPs to advanced techniques in analytical chemistry – as exemplified by the work of Dickert *et al*[62], wherein imprinting against highly complex analytes such as yeasts and micro-organisms is discussed In particular, the described molecular imprinting of caffeine to produce a specific coating for a QCM sensor suggests further scrutiny is required to ascertain the mode of recognition Comprehensive understanding of the concerted interactions involved in achieving a strong imprinting effect is a prerequisite of exploiting imprinting in advanced techniques, to ensure that observed selectivity is indeed due to creation of cavities specific to these analytes, and to facilitate optimisation of these polymers For the sake of clarity, 'imprinting' as discussed here refers to creation of specific cavities which are not only complementary in size and shape to the template molecule, but also in chemical nature Thus, 'stamping' protocols as outlined by Dickert, where a physical imprint of a larger biomolecule is created in a polymer, are not included in this discussion of MIPs

Irregularities and increasing analyte complexity, as outlined above, necessitate detailed and stringent study of MIP systems before they can be widely accepted as a facile analytical chemistry technique In his 1995 review[63], Wulff observed that for a non-covalent interaction-based polymer, only 15% of cavities formed will be reoccupied upon rebinding of template If the structural criteria (as outlined in section 1 4) have been satisfied, then the only avenue left for exploration and optimisation is the chemical complementarity of the pre-polymerisation

monomer/template complex As will be discussed, the caveat that the stronger the interaction between monomer and template, the higher the specificity of the polymer, generally holds true for non-covalent molecular imprinting procedures This brings us to the topic of 'rational approaches to molecular imprinting', whereby extensive trial-and-error approaches to imprinting are discarded in favour of a more systematic approach that takes into consideration aspects of the process such as the nature of monomer-template interactions in the pre-polymerisation complex (PPC), the effect of crosslinker, stability of PPC during polymerisation and physical characteristics of the polymer formed by a given protocol The identification of vanables to be examined and quantification of their contribution/ effect on an impnnting procedure is currently an extensive area of research in molecular imprinting It offers a logical and methodical way of both improving the efficiency of molecular imprinting, and of bringing MIP research away from being purely a technique employed by analytical chemists, and more in line with contemporary supramolecular synthetic receptor research

Rational design of MIPs for optimum performance in chromatographic applications is an excellent starting point for such investigation Recent work by Davies *et al* [64] has broached this topic, having found only limited success with the standard template monomer crosslinker ratios used in the literature, the team performed a chemometric study to identify the optimum ratio for their sulphonamide templates This required a series of 13 polymers to be created and characterised via HPLC Statistical analysis of the data indicated that the most

suitable ratio of template to monomer (MAA in this case) for their sulfamethazine template was in fact 1:10, well above the typical values found in the literature. This underlines two fundamental considerations in the logical design of MIPS:

(1) It is not possible to apply a generalised imprinting protocol to any given analyte, but rather it is necessary to 'tune' conditions and components depending on the chemical nature of the template.

(2) A methodical imprinting protocol also needs to evade the time-consuming approach of testing many different polymers, in order to be efficient and broadly applicable.

1.11.2. Optimisation via Post-polymerisation Characterisation

Combinatorial chemistry is one means of rational design that has been explored[65]. In work performed by Takeuchi, Fukuma and Matsui (Hiroshima City University), 49 polymers were synthesised simultaneously, altering functional monomer and quantity thereof, and then analysed *in situ* via HPLC. A preliminary investigation, involving incubating the MIPs (without any washing step) with acetonitrile and quantifying the amount of released template, to determine polymer affinity for the template, permitted rough selection of the polymers with higher affinity for the analyte. These MIPs were then more rigorously analysed via regular screening, with exhaustive washing and a comparative incubation with a template analogue (atrazine) and not simply the template (ametryn). The process was almost entirely automated from start to finish; only the UV

polymerisation step was carried out manually The procedure offers the advantage of allowing the many different polymers to be tested quickly, using only a small amount of reagent Such a system whereby high-throughput is enabled satisfies the second criterion stipulated above, since a large volume of data can be yielded relatively quickly The efficiency of the technique can be improved even further via introduction of fluorescence- or chromophore-labelled template analogues These can be analysed without interference from impurities, a drawback of the HPLC analysis described The small scale on which the MIPs are produced in this approach also means that consumption of chemicals is minimised But the single greatest advantage of implementing such a method is the reduced time (and labour) required to synthesise, analyse and determine which MIP is most suitable for the given analyte There is no laborious polymer processing, and automation of much of the procedure reduces the room for human error to affect results Despite the obvious potential offered by such an approach, Takeuchi's work is one of the few examples of combinatorial chemistry applied to molecular imprinting, though doubtlessly further exploitation of the technique will occur in future years

Another approach to characterising the analyte-MIP interaction with a view to understanding the recognition mechanism is the work performed by Chen *et al* [66] Changes in enthalpy, traced via isothermal titration microcalorimetry, were used to probe rebinding of the 2,4-dichlorophenoxyacetic acid (2,4-D) template to the

imprinted 4-VP/EGDMA co-polymer This research presented excellent insight into the nature of the binding processes as 2,4-D occupied specific cavities in the MIP, as well as clarifying the mechanisms by which a strong imprinting effect can be achieved in an aqueous environment This is useful in that most non-covalent imprinting protocols, a non-polar solvent is chosen as it will typically interfere least with monomer-template interactions and thus improve the quality of the imprint[67] However, this means that hydrophobic forces, which are an important energetic consideration in analogous biological recognition systems[68], may not be exploited By studying the rebinding properties of the polymer at pHs of 3,6 and 9, the authors were able to establish the net contribution of electrostatic attraction/ repulsion and π–π stacking effects to overall system entropy and enthalpy It was observed that highest overall capacity was observed when both types of interaction participated (at pH=6) These findings are in concurrence with experimental findings for the pre-polymerisation mixture of this system, as described in Chapter 4 of this thesis This is of note particularly for the corroboration of pre-polymensation events with the recognition properties of the MIP formed, which aids in the elucidation of the nature of molecular-level events and the fate of PPCs during the polymerisation process This remains one of the biggest challenges in analysing imprinting events – determining what exactly occurs at this stage Although the chemical nature of binding sites can be effectively studied using such techniques as described by Chen and co-workers, the physical nature of the nano-cavities produced during imprinting must also be considered in deriving any theory on selectivity and recognition effects Work

performed by Spivak and co-workers[69] has demonstrated the significance of template shape and thus the importance of considering the structure of a template molecule when designing an optimised imprinting protocol for the given template Branched structures were observed to be better templates than straight-chain hydrocarbons in imparting selectivity, due to the uniqueness of the branched structure

Using spectroscopy to investigate molecular-level events in a MIP is rendered difficult by the high degree of crosslinking which makes the polymer network insoluble in all solvents, eliminating the possibility of using liquid-phase spectroscopic techniques Analysis of binding of a substrate via x-ray crystallography is also excluded here since isolation of a single crystal from an amorphous polymer network is impossible Shea and Sasaki[70] at the University of California have employed the solid-state techniques of FT-IR and ^{13}C CP/MAS NMR analysis to this end, with intriguing results that shed light on the nature of analyte-MIP binding events The crosslinker used here was DVB, which permits observation of changes in the FT-IR carbonyl band at 1690cm^{-1} to examine template (a diketone) binding events This precludes use of the carbonyl-rich EGDMA as crosslinker In the ^{13}C-NMR spectrum, similarly, the ketone carbon absorption at δ198ppm is observed, while the formation of the ketal carbon absorption due to binding at δ100ppm is also closely monitored A significant finding of the study was the timescale upon which rebinding events take place – it was observed to be much slower than in analogous protein-substrate events –

although one-point binding was initially observed to be the major binding event, reorganisation to two-point binding occurs slowly and is the rate-limiting step here This is attributed to slow polymer chain motion The two techniques are in general agreement as to the quantity of 2-point rebinding 55% for FT-IR and 64% for NMR Although this approach offered excellent insight into molecular level events, it has not been pursued much further in current MIP literature Application of spectroscopic techniques to monitoring events in the pre-polymerisation mixture is more commonly found in the literature, and this is detailed in Section 1 11 3

1 11 3 Optimisation via pre-polymerisation mixture characterisation

The creation of recognition sites in a molecularly imprinted matrix is a direct consequence of the formation of self-assembled non-covalent complexes in the pre-polymerisation mixture, as identified by Andersson and Nicholls[71] Thus it follows that procedures wherein the researcher can evaluate the strength of interaction between monomer and template, and compare it to other systems with other templates (or monomers) will be of benefit in optimising the composition of a MIP mixture (and the quantities of its components) Analysis of molecular-level events in the pre-polymerisation mixture has been the source of much new information on understanding MIP behaviour and the processes which dictate recognition effects

A simple, effective way of evaluating bonding between monomer and template is via proton NMR studies Lancelot[72] suggested a NMR titration experiment in the analysis of the complexation of nucleic acid bases with carboxylic acids Here, shifts in a proton signal (relative to a reference peak) as a mixture component is gradually added to the other one, are presented as evidence of complex formation This theory has been applied to pre-polymerisation complexes, such as 17α-ethynlestradiol/ methacrylic acid system[73] In this paper, analysis of the signal shifts in different complexes are compared and used in the selection of the most appropriate monomer for the given template The work, performed by Idziak, Benrebouh and Deschamps, used radioassay techniques to evaluate

binding capacity of the polymers synthesised As they point out, observations made during the process of polymer synthesis can give indications of the suitability of a monomer for a given template The example they cite is that ethynylestradiol (their chosen template) was insoluble in the solvent toluene, but solubilised upon addition of either vinylpyridine or methacrylic acid, suggesting formation of a hydrogen-bonded complex The ethynylestradiol template is suitable for this kind of study for two reasons Firstly, the four fused rings that form the molecule's skeletal structure endow it with rigidity Secondly, there are only two sites capable of hydrogen bonding, meaning spectral shifts due to hydrogen binding will be immediately identifiable (Fig 1 9)

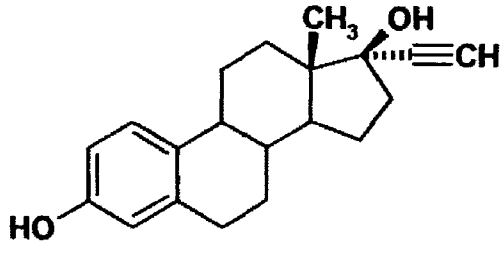

Fig.1.9 - Structure of 17α-Ethynylestradiol

This kind of study has also been used by the Mosbach group[74] to study phenylalanine/ methacrylic acid complexes This particular study indicated a link between extent of complex formation at the pre-polymerisation stage and observed polymer selectivity Other factors influencing selectivity were shape and rigidity of the template molecule, and self-association of the template molecule, as discussed in section 1 2 Quantification of the interaction is generally achieved

by performing a titration of the monomer and template constituents, a Job's plot analysis yields complex stoichiometry data, while a non-linear regression analysis of the titration data points (i e observed proton shift vs quantity of monomer added to mixture) can be used to determine the association constant of the complex Work by Hall *et al* [75] offers an excellent example of the utility of this technique With a view to creating MIPs selective for larger molecules (which contained the glutamate structure, such as the anti-cancer drug methotrexate), the group synthesised some larger functional monomers and then gauged the strength of interaction of the synthetic bis-urea receptor-containing monomer with a glutarate derivative via ^{1}H-NMR titrations The study yielded an association constant of 790M^{-1}, suggesting a strong interaction This type of study has also been used to identify monomers which can engage in stoichiometric non-covalent interactions with monomers, producing MIPs of exceptional recognition properties Wulff[76] has identified a particular benzamidine derivative which has displayed an association constant of 3.4×10^{6} M^{-1} in complexation with a carboxylic acid, with a 99 9% degree of complexation in chloroform

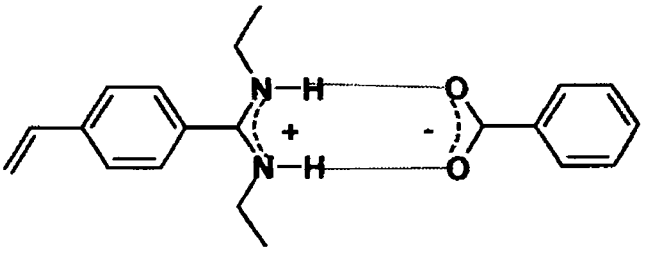

Fig 1 10 - Stoichiometric interaction between carboxylic acid and benzamidine monomer

The utility of spectroscopy in this type of application is not limited to ^{1}H-NMR, UV titration studies have also proved invaluable [71 77] Andersson and Nicholls' work focussed on methacrylic acid monomer complexing with N-acetyl-L-phenylalaninyl-L-tryptophanyl methyl ester, yohimbine and cinchonidine A similar titration approach to the NMR work described above was used in the study The experimental data indicated that addition of crosslinker to the monomer-template solution did not significantly decrease the stability of the complexes – a loss of stability of approximately 0 3 KJ mol^{-1} was observed upon addition of EGDMA This allowed the authors to exclude the effect of crosslinker on complex stability for the remainder of the study Of significant interest was the low degree of complexation observed in this study – only between 0 3% and 0 6% of template participated in adduct formation This serves to underline the importance of optimising the monomer-template ratio prior to commencing an imprinting procedure – with such a low extent of complex formation, slight improvements in complex stability should result in considerable improvements in the recognition properties of the MIP formed This is confirmed by authors highlighting that literature has indicated that only 0 5-1% of obtained binding sites can be classed as high affinity – which correlates to the degree of complexation

Another factor which may play a significant role in determining the success of an imprint is the polarity (and miscibility) of the polymer constituents Work by Katz and Davis[78] at the California Institute of Technology has clearly demonstrated that phase separation can occur during an imprinting procedure By using

chlorophenol red dye, the authors were able to visually observe the macroscopic phase separation of the monomer-template portion from the ethylene glycol dimethacrylate phase, a clear indication that the formed polymers were not homogeneous in nature (phase separation remained during the polymerisation, eventually yielding a MIP with two separate bands – one coloured by the chlorophenol dye) They suggested that the selectivity observed in the system originally introduced by Mosbach and *colleagues*[74] (where template was L-phenylalanine anilide and monomer was methacrylic acid) was more likely due to a self-association mechanism than to the creation of specific cavities This hypothesis was further supported by ^{1}H-NMR and FT-IR analysis which indicated the formation of simple 1 1 complexes – and according to the dictates for creation of a selective matrix laid down by Wulff[63], at least two points of interaction between monomer and template are required to induce selectivity The authors conclude that recognition is in fact due to the clustering/ nucleation mechanism described in section 1 2, which accounts for the observed selectivity despite the one-point interaction between template and monomer, and also for binding site heterogeneity Although this work was more of an investigation of the mechanisms governing the recognition properties of MIPs than an application of rational design to imprinting, the ramifications for any imprinting procedure are evident

Nicholls *et al.*[79] have also described a method for a thermodynamic analysis of monomer-template interactions to predict ligand-receptor binding constants:

$$\Delta G_{BIND} = \Delta G_{t+r} + \Delta G_r + \Delta G_h + \Delta G_{vib} + \Sigma \Delta G_p + \Delta G_{conf} + \Delta G_{vdw}$$

Where:

ΔG_{BIND}= complex formation energy

ΔG_{t+r} = translational and rotational energy

ΔG_r = restriction of rotors upon complexation

ΔG_h= hydrophobic interactions

ΔG_{vib}= residual soft vibrational modes

$\Sigma \Delta G_p$ = sum of interacting polar group contributions

ΔG_{conf} = adverse conformational changes

ΔG_{vdw} = unfavourable van der Waals interactions

This equation offers a rational description of the molecular level events prior to polymerisation – the concept of imprinting is simple, but the interactions are subject to many different influences, and their relative contributions to the interactions. The use of thermodynamic control has already been used for MIP design[80], employing computer simulations to test the validity of the hypotheses postulated. Thermodynamic control is a particularly important tool in the control of MIP performance; although a stable monomer-template complex may be achievable prior to polymerisation, the actual conditions of elevated temperature or of UV radiation may significantly alter the nature of this complex. This was observed in a comparative study of two L-Phenylalanine imprinted polymers,

prepared at two different temperatures[81] Improved performance was observed at elevated column temperature, most likely due to improved mass-transfer kinetics Whitcombe, Martin & Vulfson wrote an extensive article[82] in 1998 describing assessment of template-monomer complex equilibrium concentration as a function of the association constant of the functional groups involved in the interaction, which was then used to predict the selectivity of polymers prepared under different conditions The model was also tested against experimentally determined K values

A thermodynamic treatment of energy contributions dictating polymer properties necessarily requires the use of computational methods to perform the extensive calculations, however, molecular modelling has proven the most important application of computational science to MIP technology, as demonstrated by the work of Piletsky *et al*[83] This research was based on the premise that a strong interaction between a modelled monomer/template complex will correspond to a strongly specific polymer One template (ephedrine) was used and 20 monomers were modelled with it (the modelling package used was SYBYL 6 7) This approach may not always be suitable, since it does not take account of effects such as disruption of monomer/ template complexes by crosslinker, reactivity of monomers as they become incorporated into the growing polymer chain, or solvent influence However, in the cited examples of this text, it accurately predicted selectivity with only one exception The exception was the functional monomer hydroxyethyl methacrylate, HEM (Fig 1 11)

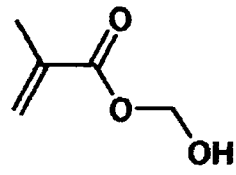

Fig 1 11– Structure of 2-Hydroxyethyl Methacrylate

This highlights the drawbacks inherent in such an approach to predicting polymer selectivity via computer simulation – effects such as hydrophobicity (the most likely explanation for the discrepancy between predicted binding strength and observed binding strength) are difficult to adequately incorporate into the simulated system in a manner which will accurately reflect the actual interaction Despite this, molecular modelling represents a means of avoiding the testing of large numbers of polymers and thus narrowing the number of MIPs to synthesise in a study, however, the accuracy of the simulated results will very much depend on the quality and capabilities of the software used Research in the area has continued, and it is expected that improvements in software capabilities and processor power will eventually render simulations closer to the reality of complicated polymer/ analyte interactions Indeed, work published recently by Wu *et al* [84] has again shown that interaction energy (ΔE) for a pre-polymensation system

$$\Delta E = E_{\text{template- monomer complex}} - \Sigma E_{\text{template}} - \Sigma E_{\text{monomer(s)}}$$

can be closely correlated to the capacity factor of a MIP column for the impnnt molecule This topic holds much potential for advancing rational design of MIP technology, as well as advancing understanding of molecular-level interactions

as models are refined and developed to more accurately describe MIP behaviour

Bibliography

[1] B Sellergren, *J Chromatogr A*, 906 (2001), 227

[2] R Suedee, T Snchana, C Sangpagai, C Tunthana & V Chapichanichat, *Anal Chim Acta*, 504 (2004), 89

[3] O Bruggemann, *Biomol Eng* , 18 (2001), 1

[4] http //www smi tu-berlin de/

[5] E Fischer, *Ber Dtsch Chem Ges* , 27 (1894), 2985

[6] B Sellergren (Ed), *Molecularly Imprinted Polymers – Man-made Mimics of Antibodies and Their Application in Analytical Chemistry* (2001), 1st Ed , Elsevier (Amsterdam)

[7] F H Dickey, *Proc Natl Acad Sci USA*, 35 (1949), 227

[8] J L Mornson, M Worsley, D R Shaw & G W Hodgson, *Can J Chem* , 37 (1959), 1986

[9] A H Beckett & H Z Yousseff, *J Pharm Pharmacol*, 15 (1963), 253T

[10] C Baggiani, G Giraudi, C Giovannoli, C Tozzi & L Anfossi, *Anal Chim Acta*, 504 (2004), 43

[11] H S Andersson, J G Karlsson, S Piletsky, A-C Koch-Schmidt, K Mosbach & I A Nicholls, *J Chromatogr A*, 848 (1999), 39

[12] J Svenson, J G Karlsson & I A Nicholls, *J Chromatogr A*, 1024 (2004), 39

[13] L I Andersson & K Mosbach, *J Chromatogr A*, 516 (1990), 313

[14] L I Andersson, B Sellergren & K Mosbach, *Tetrahedron Lett*, 25 (1984), 5211

[15] S A Piletsky, S Alcock & A P F Turner, *TRENDS in Biotechnology*, 19 (2001), 9

[16] Anonymous, *The Economist (London)*, 348 (1998), 78

[17] www.miptechnologies.se

[18] N Lavignac, C J Allender & K R Brain, *Anal Chim Acta*, (2004), *in press*

[19] J Svenson & I A Nicholls, *Anal Chim Acta*, 435 (2001), 19

[20] G Vlatakis, L I Andersson, R Muller & K Mosbach, *Nature*, 361 (1993), 645

[21] Y Chen, M Kele, P Sajonz, B Sellergren & G Guiochon, *Anal Chem*, 71 (1999), 928

[22] A Rachkov & N Minoura, *Biochimica & Biophysica Acta*, 1544 (2001), 255

[23] C Barberis, B Mouillac & T Durroux, *J Endocrinol*, 156 (1998), 223

[24] A G Mayes & K Mosbach, *Anal Chem*, 68 (1996), 3769

[25] T P O' Brien, N H Snow, N Grinberg & L Crocker, *J Liq Chromatogr & Rel Technol*, 22 (1999), 183

[26] O Bruggemann, *Anal Chim Acta*, 435 (2001), 197

[27] Hosoya, K, Yoshizako, K, Tanaka, N, Kimata, K, Araki & T Haginaka, J *Chem Lett*, 1994, 1437

[28] V M Mirsky, T Hirsch, S A Piletski & O S Wolfbeiss, *Angew Chem Int Ed*, 38 (1999), 1108

[29] V M Mirsky, M Riepl & O S Wolfbeis, *Biosens Bioelectron*, 12 (1997), 977

[30] E Yilmaz, K Mosbach & K Haupt, *Angew Chem Int Ed*, 39 (2000), 2115

[31] E. Yilmaz, O. Ramstrom, P. Moller, D. Sanchez & K. Mosbach, *J. Mater. Chem.*, 12 (2002), 1577.

[32] R.Suedee, T. Srichana, J. Saelim & T.Thavornpibulbut, *Analyst*, 124 (1999), 1003.

[33] T. Zhang, F. Liu, W. Chen, J. Wang & K. Li, *Anal. Chim. Acta*, 450 (2001), 53.

[34] C.Yu & K. Mosbach, *J. Org. Chem.*, 62 (1997) 4057.

[35] N. Zheng, Y.Z. Li, W.B. Chang, Z.M. Wang & T.J. Li, *Anal. Chim. Acta.*, 452 (2002) 277.

[36] H. Zhang, W. Verboom & D.N. Reinhoudt, *Tetrahedron. Lett.*, 42 (2001), 4413.

[37] C.F. Chow, M.H.W. Lam & M.K.P. Leung, *Anal. Chim. Acta,* 466 (2002), 17.

[38] S. Subrahmanyam, S.A. Piletsky, E.V. Piletska, B. Chen, K. Karim & A.P.F. Turner, *Biosensors & Bioelectronics,* 16 (2001), 631.

[39] D. Kriz & K. Mosbach, *Anal. Chim. Acta.*, 300 (1995) 71.

[40] C. Malitesta, I. Losito & P.G. Zambonin, *Anal. Chem.*, 71 (1999), 1366.

[41] H. Peng, Y. Zhang, J. Zhang, Q. Xie, L. Nie & S. Yao, *Analyst*, 126 (2001), 189.

[42] K. Hirayama, Y. Sakai, K. Kameoka, K. Noda & R. Naganawa, *Sensors & Actuators B*, 86 (2002), 20.

[43] C.J. Percival, S. Stanley, A. Braithwaite, M.I. Newton & G. McHale, *Analyst*, 127 (2002), 1024.

[44] B. Sellergren, *Anal. Chem.*, 66 (1994), 1578.

[45] D. Stevenson, *TRAC*, 18 (1999), 154.

[46] R. Smith, *J. Chromatogr. A*, 1000 (2003), 3 *and references therein.*

[47] L A Hılakıvı, T Taıra, I Hılakıvı, E MacDonald, L Tuomısto & K Hellevuo, *Psychopharmacology*, 96 (1988), 353

[48] Z Spıeser, A Shved & S Gıtter, *Psychopharmacology*, 79 (1983), 148

[49] G Masci, G Casatı & V Crescenzı, *Journal of Pharmaceutical & Biomedical Analysis*, 25 (2001), 211

[50] T A Sergeyeva, S A Pıletsky, A.A Brovko, E A Slınchenko, L M Sergeeva & A V El'skaya, *Anal Chım Acta* , 392 (1999), 105

[51] C Baggıanı, C Gıovannolı, L Anfossı & C Tozzı, *J Chromatogr A*, 938 (2001), 35

[52] O Ramstrom, *Anal Commun* , 35 (1998), 9

[53] M L Mena, P Martınez-Ruız, A J Revıejo, J M Pıngarron, *Anal Chım Acta*, 451 (2002), 297

[54] N Masqué, R M Marcé & F Borrull, *TRAC*, 20 (2001), 477

[55] C Crescenzı, W den Hoedt, E H M Koster, G J de Jong & K Ensıng, 1st International Workshop on MIPs, Cardıff (2000)

[56] B Sellergren & K J Shea, *J Chromatogr A*, 654 (1993), 17

[57] Y Chen, M Kele, I Quınones, B Sellergren & G Guıchon, *J Chromatogr A*, 927 (2001), 11

[58] A Molınellı, R Weıss & B Mızaıkoff, *J Agnc Food Chem* , 50 (2002), 1804

[59] J Matsuı & T Takeuchı, *Analytical Communications*, 34 (1997), 199

[60] A Zander, P Fındlay, T Renner, B Sellergren & A Swıetlow, *Anal Chem* , 70 (1998), 3304

[61] P D Martın, T D Wılson, I D Wılson & T R Jones, *Analyst*, 126 (2001) 757

[62] F L Dickert, O Hayden & K P Halikias, *Analyst*, 126 (2001), 766

[63] G Wulff, *Angew Chem Int Ed Engl*, 34 (1995), 1812

[64] M P Davies, V D Biasi & D Perrett, *Anal Chim Acta*, 504 (2004), 7

[65] T Takeuchi, D Fukuma & J Matsui, *Anal Chem*, 71 (1999), 285

[66] W Y Chen, C S Chen & F Y Lin, *J Chromatogr A*, 923 (2001), 1

[67] B Sellergren, C Dauwe & T Schneider, *Macromolecules*, 30 (1997), 2454

[68] C Tanford, *The Hydrophobic Effect*, (1980), 2nd Ed , Wiley (New York), 14

[69] D A Spivak, R Simon and J Campbell, *Anal Chim Acta*, 504 (2004), 23

[70] K J Shea & D Y Sasaki, *J Am Chem Soc*, 113 (1991), 4109

[71] H S Andersson & I A Nicholls, *Bioorg Chem*, 25 (1997), 203

[72] G Lancelot, *J Am Chem Soc*, 99 (1977), 7037

[73] I Idziak, A Benrebouh & F Deschamps, *Anal Chim Acta*, 435 (2001), 137

[74] B Sellegren, M Lepisto & K Mosbach, *J Am Chem Soc*, 10 (1988), 5853

[75] A J Hall, L Achilli, P Manesiotis, M Quaglia, E De Lorenzi, B Sellergren, *J Org Chem*, 68 (2003), 9132

[76] G Wulff, *Chem Rev*, 102 (2002), 2

[77] J S Svenson, H S Andersson, S A Piletsky & I.A Nicholls, *J Mol Recogn*, 11 (1998), 83

[78] A Katz & M E Davis, *Macromolecules*, 32 (1999), 4113

[79] I A Nicholls, K Adbo, H S Andersson, P O Andersson, J Ankerloo, J Hein-Dahlstrom, P Jokela, J G Karlsson, Olofsson, J Rosengren, S Shoravi, J Svenson & S Wikman, *Anal Chim Acta*, 435 (2001), 9

[80] V S Pande, A Y Grosberg, T Tanka, *Proc Natl Acad Sci U S A*, 91 (1994), 12976

[81] D J O' Shannessy, B Ekberg & K Mosbach, *Anal Biochem*, 177 (1989) 144

[82] M J Whitcombe, L Martin & E N Vulfson, *Chromatographia*, 47 (1998), 457

[83] S A Piletsky, K Karim, E V Piletska, C J Day, K W Freebairn, C Legge, A P F Turner, *Analyst*, 126 (2001), 1826

[84] L Wu, B Sun, Y Li & W Cheng, *Analyst*, 128 (2003), 944

Chapter Two

Creating Molecularly Imprinted Polymers for use in Solid-Phase Extraction of Pseudoephedrine & Analogues.

2 1 Abstract

Molecular imprinting presents a facile means of introducing molecular recognition capabilities into polymer matrices The resultant polymer can be used for a diverse range of applications, the most prominent in recently published work being chromatographic applications, as LC stationary phases or SPE sorbents The objective of this work was to develop a molecularly imprinted polymer for use in solid-phase extraction, to investigate how the imprinting technique may be best exploited and developed for this practical analytical use

The polymer matrix investigated was a conventional methacrylate polymer, with different functional monomers employed to introduce the recognition effect The process involves the polymerisation of the functional monomer, together with a crosslinking agent, in the presence of the requisite analyte, to form an imprinted monolith This bulk polymer was then ground down to a fine consistency and packed into empty syringe barrels to act as the SPE stationary phase It was then evaluated by examining the MIPs' ability to isolate the imprint molecule from a mixture and preconcentrate it prior to HPLC analysis

2 2 Introduction

The practical application of MIPs in separation technology has been demonstrated for techniques such as liquid chromatography[1], capillary electrochromatography[2], and the technique of interest in this chapter, solid-phase extraction[3 4] Chapter 1 has detailed many of the inherent advantages associated with the technique – the ease of preparation, the low cost of polymer components, the chemical, thermal and mechanical stability relative to techniques requiring the use of biological entities such as enzymes and antibodies This chapter investigates the practicality of using a MIP system to solving an analytical problem - in this case, quantifying the active ingredient content of a pharmaceutical preparation The analytes chosen for this study were the β-adrenergic agent pseudoephedrine and its structural analogues norephedrine and methylephedrine These molecules were chosen for their structural simplicity, as well as their pharmaceutical significance Previous work has been carried out by Suedee *et al*[5] on a MIP system to create a TLC stationary phase towards this family of compounds They are more usually determined by techniques such as capillary-zone electrophoresis[6] Various monomers were used to create a specific stationary phase, including methacrylic acid, 4-vinylpyridine, acrylamide and other nitrogen-containing heterocyclic monomers Following the typical schematic for a MIP procedure, Fig 2 1 shows how this polymerisation is expected to occur (using 4-Vp as monomer)

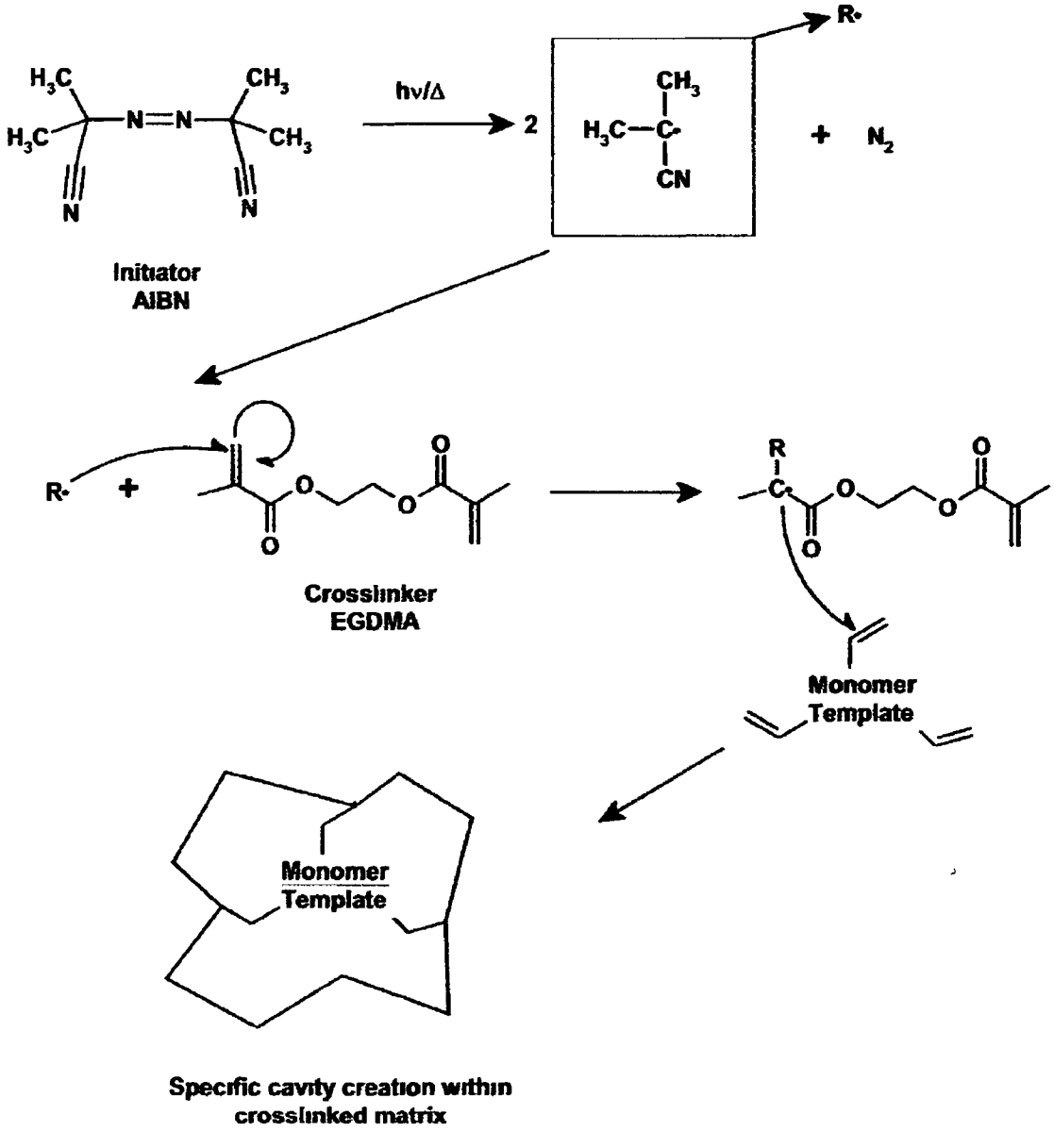

Figure 2.1: Pyridine/ methacrylate co-polymer chain growth under radical conditions, with AIBN as initiator.

2 3 Materials

Norephedrine, methylephedrine, pseudoephedrine, ethylene glycol dimethacrylate (EGDMA), 4-vinylpyridine (4-VP), acrylamide (AA), 2,2-azobisisobutyronitrile (AIBN), sodium dodecyl sulphate (SDS), methacrylic Acid (MAA), 1-vinyl-1, 2,4-triazole were supplied by Sigma-Aldrich (Dublin, Ireland) HPLC-grade acetonitrile and methanol supplied by Labscan (Stillorgan, Dublin, Ireland) Glacial acetic acid supplied by Merck, Sharp & Dohme (Clonmel, Co Tipperary, Ireland) Ethylene glycol dimethacrylate was distilled at reduced pressure 4-Vinylpyridine was distilled at reduced pressure and stored at 0°C [7] Solvents used for NMR analysis were deutenum oxide and deuterated chloroform (99 9%) and used as supplied

2 4 Experimental

All polymers prepared according to the following procedure

2 4 1 Preparation of the Imprinted Polymer

Polymerisation was based on the method reported by Suedee *et al*[8] AIBN was the chosen initiator (50 mg per polymerisation) This was dissolved in 10 cm^3 dichloromethane 4-Vinylpyridine (4-VP, 4 mmol, 0 421 g), (or acrylamide (AA, 4 mmol, 0 284 g), or methacrylic acid (MAA, 4 mmol, 0 344 g)) and the template molecule (1 mmol – norephedrine, 0 151 g, methylephedrine, 0 179 g) were stirred together for 5 minutes Ethylene glycol dimethacrylate (EGDMA, 50 mmol, 9 9 g) was then added It was necessary to have a ratio of EGDMA to functional monomer of approximately 12 1, above this, the polymer was excessively cross-linked and too tough to grind The mixture was placed in a 100 cm^3 two-necked round-bottomed flask The mixture was stirred for 10 minutes to ensure complete dissolution of mixture components The mixture was sparged with N_2 for 5 minutes and then sonicated for a further 20 minutes to degas it The mixture was then gradually heated to 60°C with refluxing, under nitrogen, for 16 hours A gelatinous formation was observed after 4 hours, before solidifying to form the polymer monolith Following this, the polymer mass was fragmented with a spatula and removed from the round-bottomed flask, before being ground to a fine consistency using an electric grinder (Braun coffee grinder model 4041) (A

disadvantage of using this monolith-synthesis approach is that much of the material was lost at the grinding stage)

To remove the template trapped within the polymer matrix, 5g of polymer was placed in a soxhlet extraction thimble and extracted over 12 hours with a mixture of methanol and acetic acid (10%) The extracted particles were then washed with methanol to remove residual acetic acid before being oven-dried for 6 hours (70 °C) The following table (Table 2 1) details the polymers created in this study, with monomer system, template used and the solvent system

MIP No	Monomer	Template	Template: Monomer: Crosslinker	Solvent System
1	MAA	(+)-Norephedrine	1 4 52	40 cm^3 DCM
2	MAA	(+)-Methylephedrine	1 4 52	10 cm^3 DCM
3	4-Vinylpyridine	"	1 4 52	13 cm^3 DCM
4	4-VP+ACM	(+)-Methylephedrine	1 4 4 52	10 cm^3 MECN
5	4-VP+ACM	(+)-Norephedrine	1 4 4 52	10 cm^3 MECN
6	1-Vinyl-1,2,4-triazole + ACM	(+)-Norephedrine	1 4 4 52	10 cm^3 MeCN
7	MAA	(+) - Norephedrine	1 4 52	20 cm^3 DCM
13	"	"	1 4 52	20 cm^3 MECN
14	"	"	1 4 52	20 cm^3 DCM

15	"	"	1: 4: 52	20 cm^3 Toluene
16	"	Phenylethylamine	1: 4: 52	20 cm^3 DCM
17	"	(+)-Norephedrine	1: 4: 26	20 cm^3 Chloroform
18	"	(-)-Norephedrine	1: 4: 26	20 cm^3 Chloroform
19	"	Cyclohexylethylamine	1: 4: 52	20 cm^3 DCM
20	"	(+)-Norephedrine	1: 4: 104	40 cm^3 DCM
21	"	(+)-Norephedrine	1: 10: 40	8 cm^3 DCM
22	MAA	"	1: 4: 52	10 cm^3 $CHCl_3$
24	MAA	"	1: 4: 104	"
26	"	(+)-Ephedrine	1: 4: 52	13 cm^3 DCM
27	MAA	(+)-Ephedrine	1: 4: 52	10 cm^3 $CHCl_3$
29	4-VP	(+)-Norephedrine	1: 4: 52	13 cm^3 DCM
30	HEMA	(+)-Norephedrine	1: 4: 52	13 cm^3 DCM
31	4-VP	(+)-Methylephedrine	1: 4: 52	13 cm^3 DCM
32	4-VP&ACM	(+)-Methylephedrine	1: 4: 4: 52	13 cm^3 MeCN
33	4-VP	(+)-Methylephedrine	1: 4: 52	13 cm^3 DCM
34	4-VP&ACM	(+)-Methylephedrine	1: 4: 4: 52	13 cm^3 DCM
35	4-VP	(+)-Methylephedrine	1: 4: 52	13 cm^3 DCM
36	4-VP&ACM	(+)-Methylephedrine	1: 4: 4: 52	13 cm^3 MeCN
37	Itaconic Acid	(+)-Methylephedrine	1: 4: 52	10 cm^3 DCM
38	Itaconic Acid	(+)-Norephedrine	1: 4: 52	10 cm^3 DCM
41	4-VP	Carbinoxamine	1: 4: 52	10 cm^3 DCM
42	4-VP	Carbinoxamine	1: 4: 52	10 cm^3 MeCN

43	4-VP + ACM	(-)-Pseudoephedrine	1 4 4 52	10 cm^3 MeCN
44	1-Vinylimidazole + ACM	(+)-Norephedrine	1 4 4 52	10 cm^3 MeCN

Table 2.1 - Polymers synthesised for this study

2 4 2 Polymer Composition (#1-6):

All polymers in Table 2 1 were prepared, polymers 1 to 6 were examined in detail, since these MIPs were observed to have superior retention capabilities compared to the others in Table 2 1 Some MIPs in the series, such as 16, 19 ,41 & 42, were unusable as template solubility was an issue, even upon addition of monomer This contrasts with the reported work of Idziak and colleagues[9], where it was indicated that addition of monomer, and subsequent monomer-template complex formation, leads to increased solubility of template molecules Other members in the series (e g nos 13, 15, 17, 20 & 21) were used to determine which solvent system acted as the most appropriate porogen – i e produced a suitably brittle polymer monolith for the purpose of grinding and packing into SPE cartridges This series thus represents a preliminary examination of experimental conditions which resulted in imprinted material most suited for analysis The first six MIPs listed in the series were the most suitable and their characterisation is described

MIP#1 Polymethacrylate-based

The monomer (methacrylic acid, 0 344 g) and template (norephedrine, 0 151 g) were dissolved in 10 cm^3 of porogenic solvent (dichloromethane) Following stirring, the crosslinker (ethylene glycol dimethacrylate, 9 9 g) and initiator (2,2'-azobisobutyronitrile, 0 05 g) were added The pre-polymerisation mixture was then stirred, sparged, sonicated and then polymensed

MIP#2. Polymethacrylate-based

The monomer (methacrylic acid, 0 344 g) and template (methylephedrine, 0 179 g) were dissolved in 10 cm^3 dichloromethane Following stirring, the crosslinker (ethylene glycol dimethacrylate, 9 9 g) and initiator (2,2'-azobisobutyronitrile, 0 05 g) were added The mixture was then stirred, sparged, sonicated and then polymerised

MIP#3 Polyvinylpyridine-based

The monomer (4-vinylpyridine, 0 421 g) and template (norephedrine, 0 151 g) were dissolved in 10 cm^3 of dichloromethane Following stirring, the crosslinker (ethylene glycol dimethacrylate, 9 9 g) and initiator (2,2'-azobisobutyronitrile, 0 05g) were added, prior to further stirring, sparging, sonicating and then polymerisation

MIP#4 Poly(vinylpyridine/ acrylamide)-based

In this procedure, a mixture of monomers was used 4-vinylpyridine (0 421 g) and acrylamide (0 284 g), together with the template (methylephedrine, 0 179 g), were dissolved in 10 cm^3 of porogenic solvent, acetonitrile Following stirring, the crosslinker (ethylene glycol dimethacrylate, 9 9 g) and initiator (2,2'-azobisobutyronitrile, 0 05 g) were added The mixture was then stirred, sparged, sonicated and then polymensed

MIP#5 Poly(vinylpyridine/ acrylamide)-based

Again, a mixture of monomers was used 4-vinylpyridine (0 421 g) and acrylamide (0 284 g), together with template (norephedrine, 0 151 g), were dissolved in 10 cm^3 acetonitrile Following stirring, the crosslinker (ethylene glycol dimethacrylate, 9 9 g) and initiator (2,2'-azobisobutyronitrile, 0 05 g) were added The mixture was then stirred, sparged, sonicated and then polymensed

MIP#6 Poly(vinyltriazole/ acrylamide)

A mixture of monomers was used in this procedure 1-Vinyl-1,2,4-triazole (0 38 g) and acrylamide (0 284 g), together with template (norephednne, 0 151 g), were dissolved in 10 cm^3 of porogenic solvent (acetonitrile) Following stirring, the crosslinker (ethylene glycol dimethacrylate, 9 9 g) and initiator (2,2'-azobisobutyronitrile, 0 05 g) were added The mixture was then stirred, sparged, sonicated and then polymensed

2 4 3 Microscopy

All images were recorded on a Nikon Eclipse E800 microscope, using Panss© imaging software Magnification was kept at x400 for all measurements

2 4 4 HPLC Determination

The analysis of MIPSE fractions was carried out via HPLC (Beckman Coulter, System Gold) Injection volume was 20 μl for all analyses Separations were carried out an *ACE* C-18 column (25cm x 4 6 mm, particle size 5 μm) The mobile phase was a 65 35 0 4 mixture of acetonitrile, water and sodium dodecyl sulphate Separations were performed at 25°C (isocratic elution) The UV lamp was set at 254 nm [10]

2 4 5 MISPE (molecularly-imprinted solid-phase extraction)

Polypropylene syringes (5 cm^3 capacity) were used as the SPE cartridges in this study The plunger was removed from the barrel, and the barrel was washed with methanol and air-dried Two filter papers were placed inside the syringe barrel as the lower frit, and 500 mg of extracted polymer (in methanol) was slurry-packed on top of this Three more filter papers were then used as the upper frit, and the column was then washed extensively with methanol to remove any residual air bubbles that may affect solvent flow The SPE cartridge was first washed with 5

cm^3 of methanol-acetic acid (5%), which was tested via HPLC to ensure that extraction had been successful The cartridge was then rinsed again with 10 cm^3 of methanol prior to loading The extraction of analytes was investigated by loading the cartridge with 300 $\mu g/ cm^3$ of analyte (or mixture of analytes, according to the experiment) Following loading, the cartridge was washed with 3 x 5 cm^3 of dichloromethane to remove anything that was non-specifically bound Elution of bound substrate was performed using 5 cm^3 of methanol-acetic acid (5%) The loading and elution fractions were allowed to evaporate to dryness and then reconstituted with mobile phase, before being analysed via HPLC The amount of analyte recovered was quantified using calibration curves

2 4 6 Real Samples

A tablet of Sudafed© (*Warner-Lambert Healthcare*), a commercially available pseudoephedrine-based decongestant/ cough treatment, was ground finely, dissolved in 100 cm^3 of methanol and filtered to remove insoluble coating components The resulting solution was loaded onto the relevant imprinted SPE cartridges, as described later on Similarly, Actifed© (also from *Warner Lambert Healthcare*), a cough-treatment syrup wherein pseudoephedrine is the active ingredient, was also analysed by dissolution of 5 cm^3 in 100 cm^3 of methanol, before being filtered (Whatman no 1 filter paper) and loaded onto the MIP-SPE cartridges

2 4 7 NMR Investigation

NMR Spectra were recorded on a Bruker AVANCE 400 MHz NMR spectrometer (Bruker Biospin UK) at 25°C Chemical shifts are referenced to the solvent reference signal Deuterated chloroform was analysed via NMR prior to use to ensure the absence of water For the titration, the ratios of monomer and template are systematically varied (between 0 1 to 8 1) using equimolar solutions (0 04 M), with a constant sample volume of 0 75 cm^3

2 5 Results & Discussion

The compounds used in this study were pseudoephedrine, norephedrine and methylephedrine, as is evident, all three are very closely structurally related (Fig 2 2)

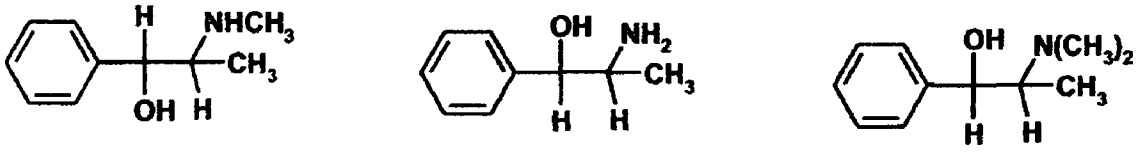

Pseudoephedrine **Norephedrine** **Methylephedrine**

Figure 2 2 - Analytes used in the study.

All three compounds have a pharmacological significance Pseudoephedrine is used as a bronchodilator and peripheral vasoconstrictor in preparations for the relief of nasal and bronchial congestion, particularly in bronchial asthma Norephedrine and methylephedrine have similar pharmaceutical applications (+)-Pseudoephedrine is also of note because of its use in the illicit production of the narcotic (+)-methamphetamine [10]

These compounds belong to a class of drug known as phenylethanolamine adrenergic agents, and possess a hydroxyl group on a chiral carbon that must be in the *R* configuration for optimal activity, which is the case in natural neurotransmitters of similar structure[11] The absolute configurations of the pharmacologically active enantiomers are shown in Fig 2 3

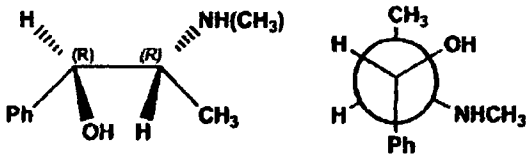

(-)-Pseudoephedrine (1R, 2R)

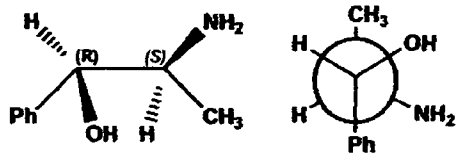

(-)-Norephedrine (1R, 2S)

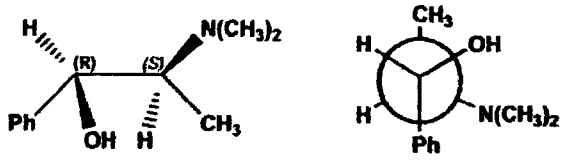

(-)-Methylephedrine (1R, 2S)

Fig.2 3 – Structures of pharmacologically active enantiomers, with Newman projections.

The following series of polymers, outlined in Table 2 2 were prepared using the above mentioned analytes as templates and investigated

Polymer No	Template Molecule	Monomer System	Crosslinker
1	(+)-Norephedrine	Methacrylic Acid	Ethylene Glycol Dimethacrylate
2	(+)-Methylephedrine	Methacrylic Acid	Ethylene Glycol Dimethacrylate
3	(+)-Norephedrine	4-Vinylpyridine	Ethylene Glycol Dimethacrylate
4	(+)-Norephedrine	4-Vinylpyridine/ Acrylamide	Ethylene Glycol Dimethacrylate
5	(+)-Methylephedrine	4-Vinylpyridine/ Acrylamide	Ethylene Glycol Dimethacrylate
6	(+)-Norephedrine	1-Vinyl- 1,2,4-triazole/ Acrylamide	Ethylene Glycol Dimethacrylate

Table 2.2 - Polymers synthesised & analysed in this study.

In order to confirm that retention of analytes by these polymers at the analysis stage was indeed due to an imprinting effect rather than non-specific binding, for each polymer synthesised, a blank polymer was also synthesised in an identical fashion, but without the inclusion of a template molecule The MIPs and blanks were stored in methanol for at least 24 hours prior to use to avoid any swelling effects occurring upon exposure to solvents at the SPE stage

2 5 1 Swelling of MIPs

The efficiency of a molecularly imprinted stationary phase, in any given chromatographic application, depends on the fidelity of the binding site to the chemical nature of the original imprint molecule – any distortion of the binding site will in theory result in a decrease in the recognition capabilities of the MIP To examine the stability of the polymer matrix when exposed to solvents for extended periods of time, imprinted polymer samples (MIP#5 (ref Table 2 2) was arbitrarily chosen) were tested for swelling/ shrinking To quantify the swelling, the procedure was as follows A photograph of a MIP particle (chosen arbitrarily from MIP #5, ground & processed as described in Section 2 4 1), viewed through a microscope, was taken, and the 2-dimensional surface area occupied by the crystal was calculated, by determining the space occupied in screen pixels The particle was then soaked in solvent overnight, and the area occupied by the particle subsequent to this was then measured and compared In the following example, methanol was the solvent used

Fig. 2.4 – Swelling of a MIP particle upon exposure to methanol overnight.

Table 2.3 below describes the relative changes in the observed surface area of MIP crystals subjected to overnight exposure to different solvents, which are commonly used in either the preparation or analysis stages of imprinting.

SOLVENT	% Change in surface area
Chloroform	-9 (±2)
Dichloromethane	+13 (±3)
Methanol	-21 (±3)
Water	+5.5%(±4.5)

Table 2.3 - Polymer swelling in solvents used during analysis (n=2).

This evidence of shrinkage and swelling means that distortion of binding sites is likely, and so prior to use in chromatography, the MIPs were stored overnight in methanol (the solvent used for conditioning the MISPE cartridges, and for loading and elution) to minimise effect on retention.

2.5.2 Using the MIPs

The imprinted polymers were synthesised and processed as described in the experimental (Section 2.4), and incorporated into SPE cartridges. One of the most common problems encountered in molecular imprinting is the phenomenon of template leeching (or bleeding). This phenomenon is a result of template that remains trapped inside the polymer matrix following the extraction step and can 'bleed' out during the elution step, giving a false positive result. With a view to designing a pseudoephedrine-selective SPE sorbent material, norephedrine was used as the template instead of pseudoephedrine. This was done to avoid any difficulties with bleeding effects. This method of circumnavigating leeching via imprinting with a structural analogue of the analyte of interest was first used by Andersson *et al.*[12] in their work with sameridine. Figure 2.5 shows bleeding occurring with polymer no.3 (ref. Table 2.2) during analysis.

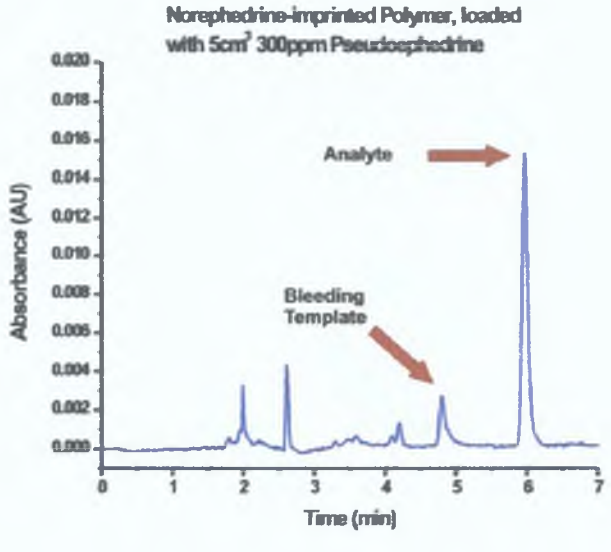

Figure 2.5 – Elution profile showing norephedrine bleeding from polymer #4.

The norephedrine imprinted polymer demonstrated a lack of specificity for the target analyte This lack of specificity suggested a poor imprinting effect, and was attributed to the influence of intramolecular hydrogen bonding NMR data suggested that the amino protons were undergoing hydrogen bonding with the hydroxyl substituent of this molecule, indicated by a broad peak that integrates to three protons

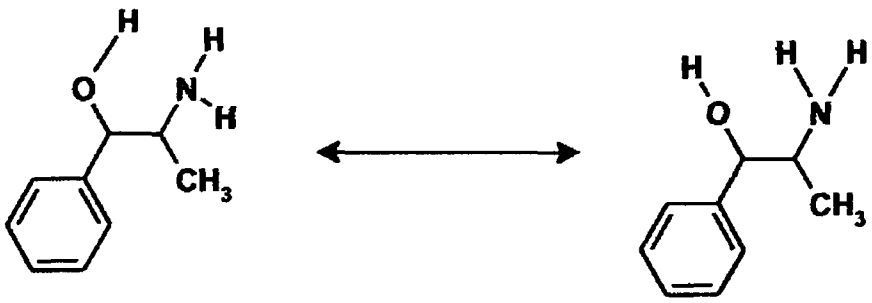

Figure 2.6 - Intramolecular hydrogen bonding in Norephedrine.

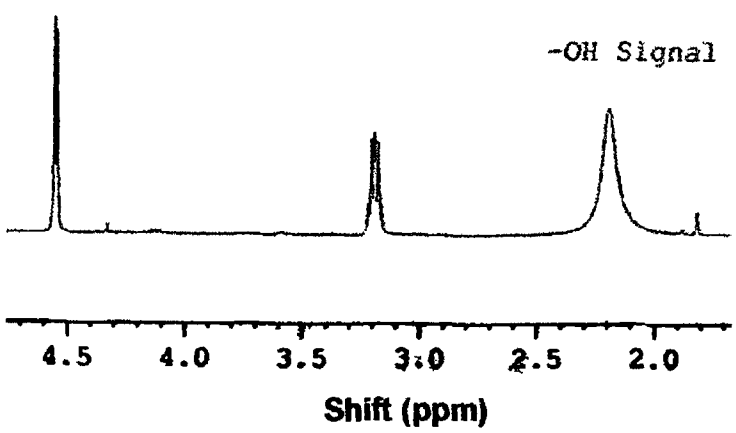

Figure 2.7 - Characteristic broad signal of hydrogen-bonded protons in norephedrine.

In order to confirm the identity of this peak, some D_2O was added to the norephedrine sample, causing this broad signal to disappear This confirmed the assignment as a hydroxy proton

It has already been demonstrated by Zhang and colleagues[13] that such intramolecular H-bonding can inhibit or even entirely prevent a successful imprinting procedure, due to a reduced interaction between functional monomer and template in the pre-polymerisation mixture This explanation for the poor specificity of the norephedrine-imprinted methacrylic acid polymer (P(MAA)) is further reinforced by the improved retention displayed by MIP#2 (also containing methacrylic acid as functional monomer), which is identical in composition, but is imprinted with methylephedrine (which is not subject to intramolecular hydrogen bonding) However, this study revealed that PMAA polymers (MIP nos 7-27) do not exhibit high selectivity even when the intramolecular H-bonding adversity is avoided, retaining a high amount of analyte on the blank polymer (see Table 2 4) This table indicates that although the imprinted polymer exhibited a higher affinity for norephedrine than the corresponding blank polymer, the difference was negligible, suggesting that methacrylic acid, and the non-specific binding it induces, is unsuitable for these analytes

POLYMER	% Recovery of loaded norephedrine on elution
Imprinted P(MAA) – MIP #1	46 9 (S D =4 8)
Blank P(MAA)	41 1

Table 2.4 - Imprinted & blank methacrylate polymers loaded with 300ppm Norephedrine in MeOH (n=3).

This may be best explained by the possibility of the methacrylic acid carboxylate groups on the polymer surface interacting electrostatically (and thus with less specificity than hydrogen-bonding based interactions) with these mildly basic compounds (polymers #7-24) For this reason, itaconic acid (Fig 2 8) was also deemed an unsuitable monomer for these compounds (polymers 37 & 38), as it too will simply form acid-base ion pairs with the basic analytes without any specificity

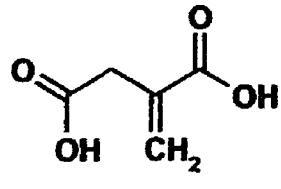

Fig. 2 8 - Structure of Itaconic Acid

To evade this eventuality, a basic monomer (4-vinylpyridine) was employed in place of methacrylic acid, to increase the likelihood of hydrogen bonding between monomer and template at the pre-polymensation stage The aromatic vinylpyridine compound also offers scope for π–π stacking interactions with the aryl substituent of the template molecule The resulting polymer offered improved performance over the P(MAA)-based polymers It selectively retained

norephedrine from a norephedrine/ methylephedrine mixture, albeit with a low capacity As is evident in the table below (Table 2 5), the imprinted polymer was still lower-performance relative to its non-imprinted counterpart in terms of retention

POLYMER	% Recovery of loaded norephedrine on elution
Imprinted P(Vpy) (MIP #3)	14 (S D =2 3)
Blank P(Vpy)	18 3

Table 2.5 - Pyridinyl polymer loaded with 300ppm Norephedrine in MeOH (n=3).

The MIPs' performance is still hampered by the effect of acidic conditioning After soxhlet extraction of the polymer with methanol and 10% acetic acid, the polymer was washed with methanol This is because any acetic acid remaining on the polymer beyond this stage will compete for binding sites with analyte loaded at a later stage, or in this case, result in protonation of basic analytes and foster ionic interactions between analyte and functional groups of the polymer chain This was confirmed as when the polymer was used without first washing thoroughly with methanol, virtually no retention was observed

To overcome the ionisation problem, a further modification of the monomer-template system was investigated by Zheng *et al* [14] The addition of acrylamide to the pre-polymerisation mixture (in quantities equal to the 4-vinylpyridine content) creates a co-functional monomer system that is even less conducive to ionisation than the simple 4-vinylpyridine/ template complex, since the amide group is not

ionisable[15] An added benefit of using this system is that with ionisation problems effectively removed, the polymer is then suitable for use in analysing aqueous samples Acrylamide is poorly soluble in dichloromethane, and this necessitated the use of acetonitnle to facilitate dissolution of monomer species This did not appear to have a significant bearing on subsequent recognition properties Using this combination of monomers resulted in polymers that gave the highest performance of the entire series (Table 2 6)

Polymer	% Recovery of loaded norephedrine on elution	%Recovery of loaded methylephedrine on elution
Imprinted P(Vpy/ACM) (MIP #4)	13 6 (S D = 2)	0 00
Blank P(Vpy/ACM)	6 6	4 6

Table 2.6 - Polymers loaded with 2 5 cm^3 300ppm Norephedrine, 2.5 cm^3 300ppm Methylephedrine (n=3).

Given that the chosen porogen for this synthesis was acetonitrile, the solid-phase extraction was repeated using acetonitrile in place of methanol for loading and elution purposes This was anticipated to give an improved response, since use of acetonitrile should minimise solvent swelling effects that may occur on exposure to a solvent that is different to the original porogen However, as is evident above, although selectivity was maintained, the polymer did not exhibit improved performance – in fact, a slightly lower recovery was observed This was attributed to the strong eluting power of acetonitnle, making it unsuitable for use at the loading stage, although the slightly higher polarity of acetonitnle (compared to chloroform or dichloromethane) may also be a factor

Evaluation of pseudoephedrine content was then investigated using two pseudoephedrine-based medicines, containing different quantities of the compound (Table 2 7) For analysis of the medicines, the samples were first prepared as described in Section 2 4 6 For the syrup-based medicine (Actifed®), the MISPE (Table 2 2 MIP #4) allowed facile clean-up and quantification of pseudoephedrine content – Figure 2 9 shows the relatively clean chromatogram obtained after extraction For "Sudafed", the tablet-based preparation, the quantification was less accurate and suggests further optimisation is required before this approach can be considered suitable

Product	Declared Pseudoephedrine Quantity	Observed potency as determined by MISPE	% Difference
ACTIFED	30 mg/5 cm^3 syrup	31 8 mg/5 cm^3 (±0 7mg)	6%
SUDAFED	60 mg/tablet	45 mg/tablet (±2 6mg)	25%

Table 2 7 - Pseudoephedrine content in over-the-counter pharmaceutical products, as determined by HPLC (n=3)

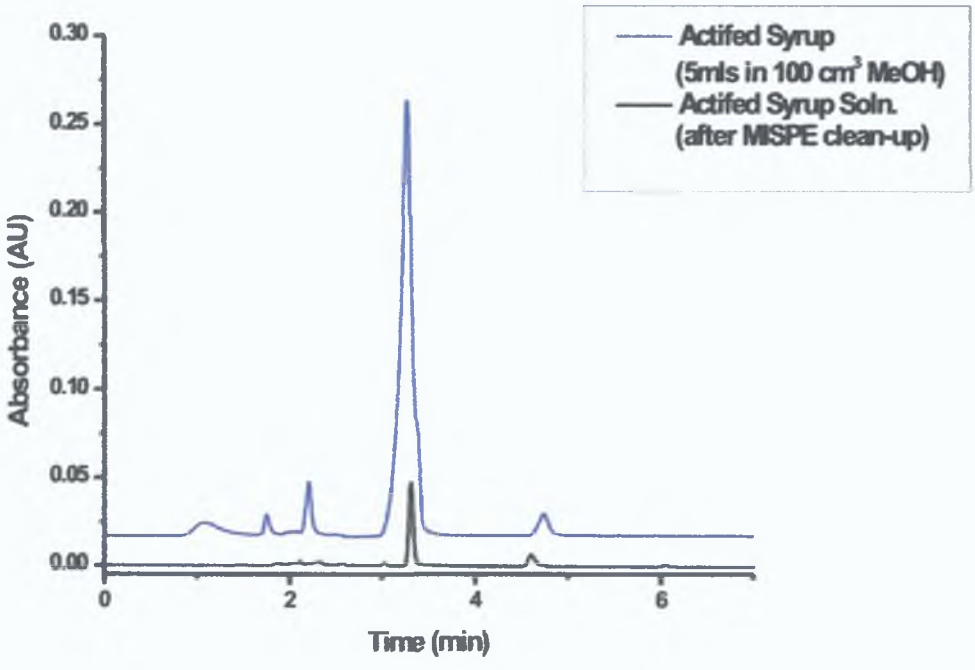

Figure 2.9 - Pseudoephedrine isolated from Actifed sample (Pseudoephedrine retention time=3.27mins).

2 5 3 Alternative Monomers

The acrylamide/ 4-vinylpyridine monomer combination resulted in a successful imprint, and other monomers were investigated to examine the potential for improving on this performance 1-Vinylimidazole (Vim) and 1-vinyl-1,2,4-triazole (Vtri) (Fig 2 10) were chosen for this purpose, since both these compounds are easily polymerised and are basic nitrogen-containing heterocycles

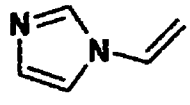

1-Vinylimidazole

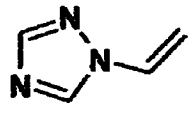

1-Vinyl-1,2,4-triazole

Fig 2.10 - Structures of 1-Vinylimidazole and 1-Vinyl-1,2,4-triazole.

It was anticipated that the increased electron density of the aromatic parts of these molecules would facilitate non-covalent interactions with the template molecule However, vinylimidazole-based polymers displayed little or no recognition properties, as predicted by the molecular modelling study carried out by Piletsky[16] on ephedrine Conversely, a 1-vinyl-1,2,4-triazole/ acrylamide norephedrine-imprinted polymer did show encouraging results when tested with a norephedrine loading, suggesting that it may represent a useful alternative to 4-vinylpyridine As shown in Table 2 8, it also exhibited a substantial capacity for non-specific binding and would require further modification of the loading and washing stages of SPE to restrict this effect

POLYMER	% Recovery of loaded norephedrine on elution
Impnnted P(Vtn/ACM) (MIP #6)	44 3 (S D =2 2)
Blank P(Vtn/ACM)	19 9

Table 2.8 - Mixed-monomer polymer loaded with 300 ppm Norephedrine in MeOH (n=3)

An important consideration when modifying a MIP-based SPE to enhance selectivity and overall performance is the influence of pH on the retention mechanism This topic has been researched in some detail by Sellergren and Shea[17] Their work pointed to a weak cation-exchange model as being the best method for describing how changes in pH alter retention in an imprinted-polymer based system The influence of pH on the chromatographic performance may be explained (and predicted) by considering the protonation state of the analyte and its consequent affinity for the polymer binding sites at a particular pH Thus, at a lower pH the protonated analyte molecules have a strong affinity for the specific binding sites that can accommodate them sterically and that have a chemical complementanty imparted at the imprinting stage Increasing pH means that less analyte is protonated, while more non-selective sites are becoming deprotonated, resulting in less selectivity, but a higher capacity This is confirmed by the findings of a study of aqueous loading of polymer no 5, which was imprinted with methylephedrine This polymer selectively retained norephednne from a norephednne/ methylephedrine mixture, following acidic conditioning of the SPE cartridge This was presumed to be due to protonation of the norephednne, causing it to have a greater affinity for the basic functionalities of the polymer

network If this is the case, it should be found that increasing the pH gradually will alter the selectivity in favour of the impnnt molecule, methylephedrine, since this is less subject to protonation and will replace norephednne as the selectively retained analyte, once ionic interactions are no longer the dominant retention mechanism

The chromatographic data obtained in this investigation supports this theory - norephednne being the analyte to elute first in both chromatograms (Fig 2 11) At pH=9, methylephedrine is the selectively retained analyte The effect of pH on retention time is also evident in these chromatograms, since acidified analytes have a stronger affinity for the stationary phase of the column and thus have longer retention times This necessitates spiking of fractions to positively identify peaks However, the study revealed that pH control is a useful tool in controlling selectivity at the solid-phase extraction stage

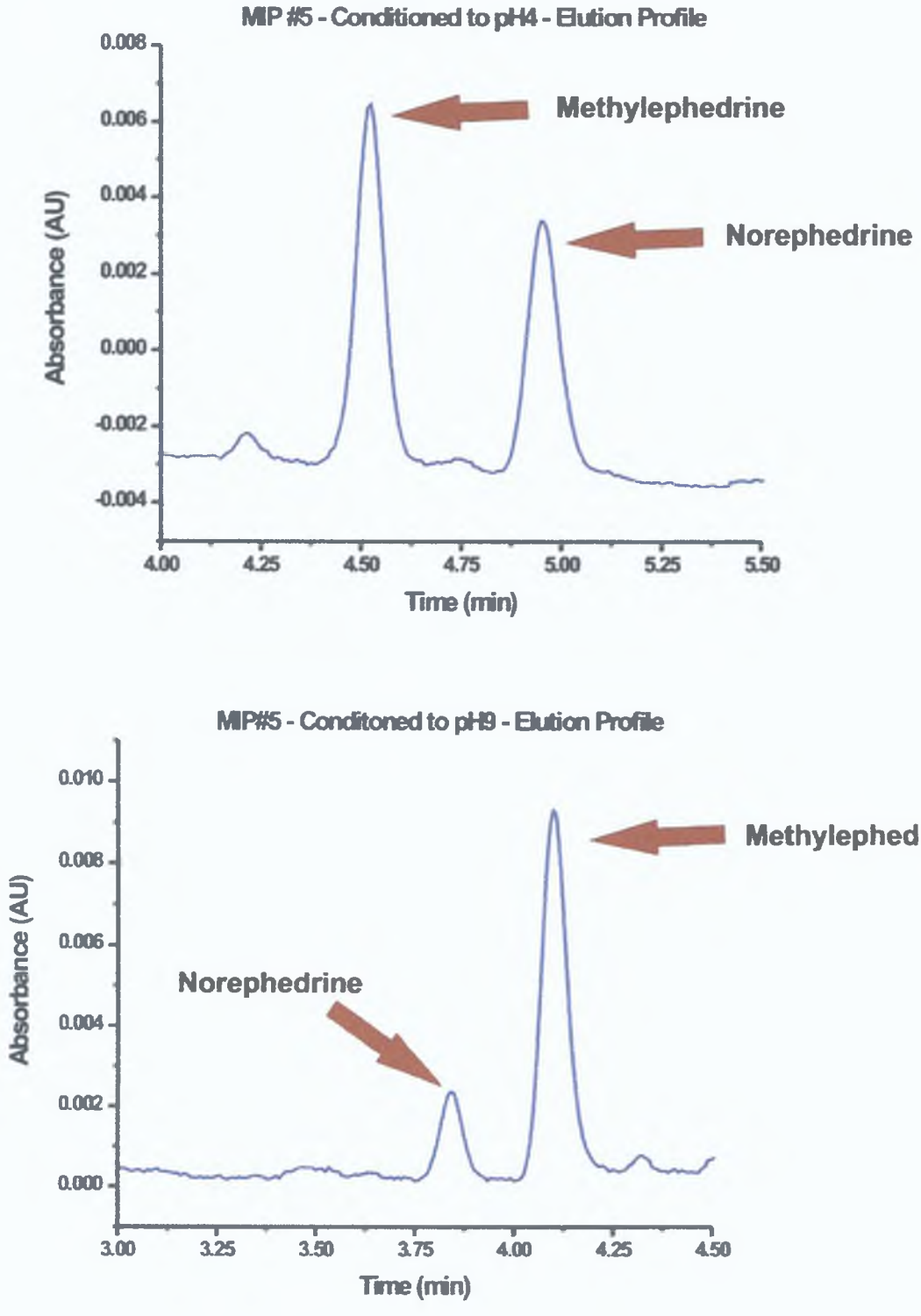

Figure 2.11 - pH control of elution on MISPE columns.

2.5.4 Examining the Pre-polymerisation Mixture: NMR Titration Experiment

The system with norephedrine (template) and MAA (monomer) presented significant difficulties in imprinting, providing MIPs of low specificity. NMR titration data demonstrated that the only major interaction occurring in the pre-polymerisation solution of this system is an electrostatic interaction between the $-NH_2$/-OH group of the norephedrine and the acid carboxylate functionality of MAA (see Fig.2.12 & 2.13).

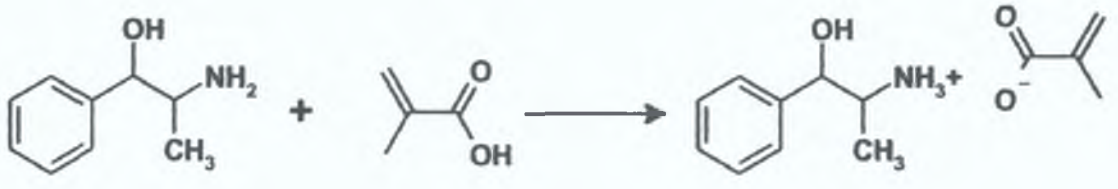

Fig. 2.12 – Formation of Norephedrine/ MAA ion pair; for ^{1}H-NMR titration, chemical shift of $-NH_2$ protons followed.

No other signal shifts were observed. This most likely indicates a 1:1 complex, which would support the theory proposed by Wulff[18], who observed that a simple one-point binding is insufficient to induce selectivity in a MIP.

Similar research on an ephedrine/methacrylic acid system by Dong *et al.*[19] suggests that both electrostatic and hydrogen bonding stabilises the pre-polymerisation complex. In the present study only the ionic interaction could be observed without any evidence of additional complex stabilisation by hydrogen bonding. This concurs with observations of MIP performance in SPE analysis,

wherein the tendency of the imprinted polymer to interact with charged analytes prevented any selectivity

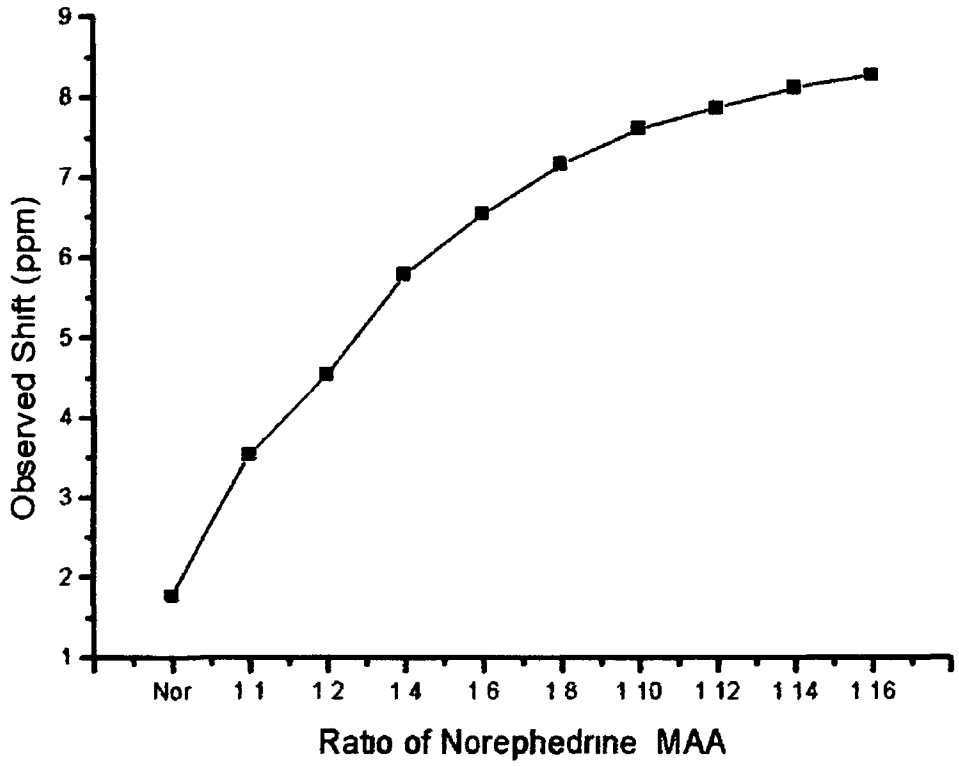

Fig 2.13 – Titration of Norephedrine with methacrylic acid in $CDCl_3$, (^{1}H-NMR, 16 scans).

2 6 Conclusion

A MIP against norephedrine was successfully synthesised and tested for separation of norephedrine from a mixture of similar compounds, cross-reactivity towards structural analogues was also investigated by testing the polymers' ability to retain pseudoephednne from a complex sample matrix (that of a commercially available cough medicine) The efficiency of imprinted polymers created from a combination of monomers, that of 4-vinylpyridine and acrylamide, suggests that this type of co-functional monomer system warrants further investigation This study indicates that by carefully selecting monomer systems and solid-phase extraction conditions, an efficient selective SPE sorbent can be prepared conveniently and at low cost, side-stepping the need for lengthy liquid-liquid extractions that require larger quantities of organic solvent (and thus are more expensive)

The capacity of these MIPs is disappointing, however – even with the most selective MIP (no 4), a mere 14% of the loaded analyte was recovered This is in strong contrast to high-performance MISPE, such as the quercetin polymer examined in the next chapter, which can offer recoveries of over 98% Although analysis conditions (such as conditioning the surface pH of the MIPs) can be tuned to improve this, it is evident that the creation of specific binding sites via imprinting needs a more rational approach than the trial-and-error method demonstrated here Development of MIP materials for analytical applications is

evidently a useful technique, but future research should focus on establishing and understanding which experimental variables have greatest the influence on the imprinting process This could be achieved by using a simple NMR titration experiment as described in this work

Bibliography

[1] B Sellergren, *J Chromatogr A*, 906 (2001), 227

[2] L Schweitz, L I Andersson & S Nilsson, *Analyst*, 127 (2002), 22

[3] B Sellergren, *Anal Chem* , 66 (1994), 1578

[4] C Baggiani, *J Chromatogr A*, 938 (2001), 35

[5] R Suedee, C Songkram, A Petmoreekul, S Sangkunakup, S Sankasa, N Kongyarit, *J Pharm & Biomedical Analysis,* 19 (1999), 519

[6] R M Iwanicki, K Maier, J A Zlotnick, R H Liu, T L Kuo, F Tagliaro, *J Forensic Sciences*, 44 (1999), 47

[7] D D Perrin & W L F Armarego, "Purification of Laboratory Chemicals", (1980), 2nd Ed , Pergamon Press (Oxford)

[8] R Suedee, T Srichana, J Saelim & T Thavornpibulbut, *Analyst*, 124 (1999), 1003

[9] I Idziak, A Benrebouh & F Deschamps, *Anal Chim Acta* , 435 (2001), 137

[10] R M Iwanicki, K Maier, J A Zlotnick, R H Liu, T L Kuo & F Tagliaro, *J Forensic Sciences*, 44 (1999), 47

[11] R Suedee, C Songkram, A Petmoreekul, S Sangkunakup, S Sankasa & N Kongyarit, *J Pharm & Biomedical Analysis*, 19 (1999), 519

[12] L I Andersson, A Paprica & T Arvidsson, *Chromatographia*, 46 (1997), 57

[13] T Zhang, F Liu, W Chen, J Wang & K Li, *Anal Chim Acta*, 450 (2001), 53

[14] N Zheng, Y Z Li, W B Chang, Z M Wang & T J Li, *Anal Chim Acta* , 452 (2002) 277

[15] C Yu & K Mosbach, *J Org Chem* , 62 (1997) 4057

[16] S Piletsky, K Karim, E V Piletska, C J Day, K W Freebairn, C Legge, A P F Turner, *Analyst*, 126 (2001), 1826

[17] B Sellergren & K J Shea, *J Chromatogr A*, 654 (1993), 17

[18] G Wulff, *Angew Chem Int Ed Engl*, 34 (1995), 1812

[19] X Dong, H Sun, X Lu, H Wang, S Liu & N Wang, *Analyst*, 127 (2002), 1427-1432

Chapter Three

Rationalised Development of Quercetin-Imprinted Polymers.

3 1 Abstract

Work described in Chapter 2 has demonstrated the feasibility of utilising imprinting to resolve analytical problems However, much trial-and-error work suggests that refinement of the current technique of MIP development is required to make the technology more efficient and practical This necessitates a retrospective look at a successful molecular imprint, the efficiency of which permits investigation of precisely how an effective MIP can be rationally designed A quercetin MIP system was deemed suitable for this purpose Polymers of varying composition were synthesized and characterized chromatographically to examine the effects of monomer template ratios ^{1}H-NMR and ^{13}C-NMR analysis of the pre-polymerisation mixture yielded further information on the nature of the complexes formed prior to the polymerization step A direct correlation between the optimal ratio of monomer-template in the chromatographic study, and the ratio of fastest molecular tumbling rate, as observed via ^{1}H-NMR T_1 relaxation time measurements, suggest the formation of particularly stable microenvironments which preserve the complexes during the polymerisation step Physical aspects of the polymensation, such as surface area and macroscopic phase partition of the mixture during polymerisation, are also examined The observed effects thus offer an insight into the mechanisms at molecular-level which govern MIP selectivity, and are discussed

3 2 Introduction

Contemporary research in molecular imprinting technology has been somewhat restricted in the past number of years by the lack of a rational approach to designing effective molecularly imprinted materials Successful imprints can usually be obtained through preparing a bulk polymer using one of the more conventional choices of functional monomer (such as 4-vinylpyridine, methacrylic acid or acrylamide), however, this leaves much of the underlying processes that control the phenomenon of imprinting unexplained and hinders advancement in the design of more effective MIP materials More systematic methods of optimising MIPs have been applied, such as combinatorial chemistry, molecular modelling and thermodynamic analysis, as described in Chapter 1, Section 1 11 The following work, used in the analysis of quercetin-imprinted polymers, is in a similar vein Building on research already carried out on this system, optimisation of this MIP was investigated using two systematic approaches variation of the functional monomer content of the polymer, and NMR titration experiments to observe monomer-template complex formation in the pre-polymerisation mixture This MIP system achieved recovery rates, in SPE trials, of 98 2%[1] This performance marks it as one of the most efficient MIPs described in the current literature, (similar work[2] using an acrylamide monomer achieved only 90% recovery) and thus an ideal candidate for this type of investigation

3 3 Materials

3,3',4',5,7-Pentahydroxyflavone (quercetin), morin, rutin, 2-carbethoxy-5,7-dihydroxy-4-methoxyisoflavone (C-fla), azobisisobutyronitrile (AIBN), 4-vinylpyridine (4-VP), acrylamide (AA), methacrylic acid (MAA), ethylene glycol dimethacrylate (EGDMA), acetone-d_6, pyridine-d_5 were obtained from Sigma-Aldrich (Milwaukee, WI, USA and Dublin, Ireland) 4-vinylpyridine was distilled under vacuum prior to use, all other chemicals were used as supplied Solvents used (excluding deuterated solvents, and technical grade acetone for sedimentation) were of HPLC grade and obtained from Burdick & Jackson (Muskegon, MI, USA)

3 4 Experimental

3 4 1 MIP Preparation

All polymers were prepared via thermally-initiated polymerization (60°C in a water bath), using AIBN as initiator (0 05 g) and ethylene glycol dimethacrylate as crosslinking agent (according to polymer composition described in tables in results and discussion section), in glass vials For all MIPs prepared, a corresponding control polymer was synthesised using identical composition and conditions, but with the exclusion of template from the polymensation mixture The MIPs were synthesized using 15 cm^3 of acetone as solvent The pre-polymerisation mixture was cooled in an ice bath and sparged with nitrogen for 5 minutes pnor to polymerisation Polymerisation was carried out overnight

3 4 2 MIP Processing

The polymer monolith obtained was then broken down into smaller particles and ground in a mechanical mortar (Retsch, Haan, Germany) Wet sieving in acetone was used to eliminate particles of size >25 μm Fine polymer particles were then removed via sedimentation in acetone, giving particles of approximate size range 5-25 μm (as determined by sieving) Sedimentation required approximately 250 cm^3 of solvent, and was allowed to proceed for 1 hour Approximately 5-6 sedimentations were required to remove all fine particles Polymers were then

washed with methanol, filtered and dried in an oven at 50°C overnight For the evaluation step, approximately 3 g of polymers were packed into stainless steel HPLC columns (150 x 4 6 mm) with acetone at 200 bar, using an air-driven fluid pump (Alltech, USA)

3 4 3 MIP Characterisation

All measurements were performed on both the imprinted polymer and its corresponding blank counterpart The relative performance of the polymer was gauged by its ability to selectively retain quercetin Acetone was used as the void marker The capacity factors (k') of the MIPs were evaluated as

$$k' = \frac{t - t_{ACETONE}}{t_{ACETONE}}$$

where t is the retention time of quercetin and $t_{acetone}$ is the retention time of acetone on the column Other parameters used in the evaluation of MIP properties were separation factor (α) and retention index (RI)

- Separation factor $$\alpha = \frac{k'_{printmolecule}}{k'_{testmolecule}}$$
- Retention index $$RI = \frac{\alpha_{CTL}}{\alpha_{IMP}}$$

The HPLC analysis was performed using a Dionex HPLC (Dionex, Sunnyvale, CA, USA) with a P580 low-pressure mixing pump and an UVD-340S diode array

detector with a spectral range from 200 to 600 nm In order to extract the template molecule from the MIP polymer, the prepared column was washed on-line with methanol acetic acid mixture (7 1, v/v) at 1 ml/min until the baseline was stable After complete extraction of the quercetin template, the imprinted and the control columns were equilibrated with a mobile phase of acetonitrile/water/acetic acid (80 10 10, v/v/v) The elutions were performed at room temperature at a flow rate of 1 ml/min and monitored spectrophotometrically at 200-450 nm The injection volume was 20 µl and the preferred channel was set at 265 nm, a characteristic absorption of quercetin A selection of compounds from the flavonoid class were used in chromatographic evaluation (see Fig 3 1) These compounds were chosen because of their structural similarity, enabling facile evaluation of column efficiency

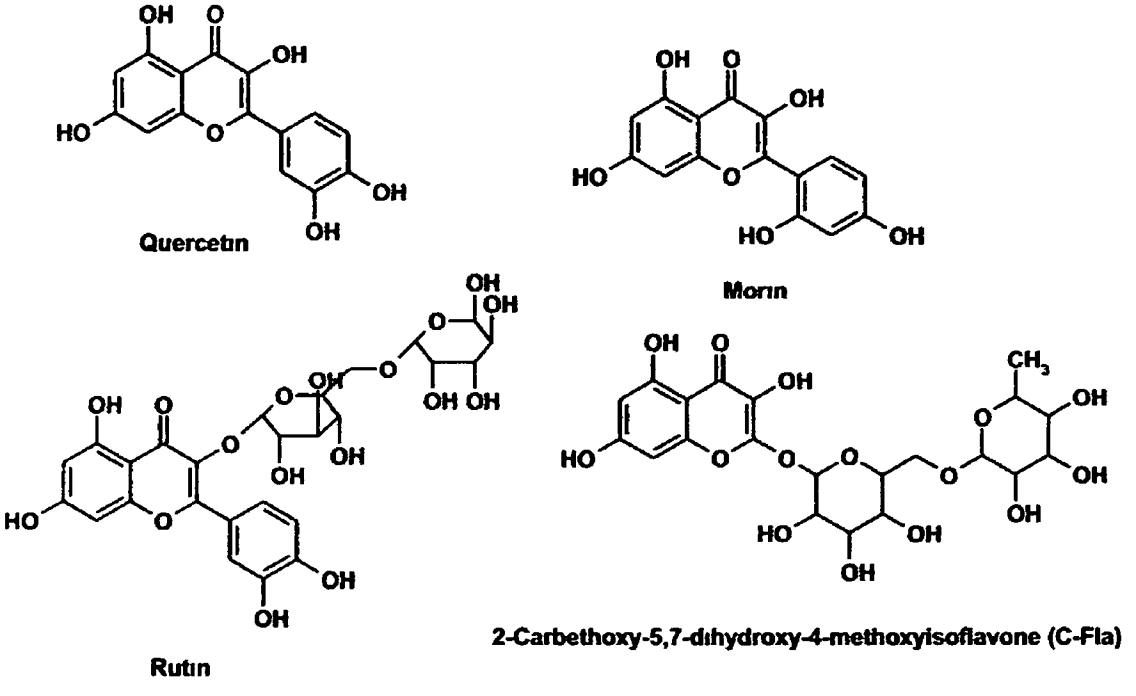

Figure 3 1 – Structures of compounds used in MIP column characterisation for this study

For each standard solution, 2 mg were dissolved in 20 cm^3 of the mobile phase (concentration of 100 mg/l) Acetone was used as void marker (stock solution 20 µl in 4 cm^3 mobile phase) A standard stock solution of quercetin, monn (140 mg/l respectively), and acetone (5 µl/cm^3) was used to determine the separation efficiency of the imprinted columns

3 4 4 NMR Analysis

All ^{1}H-NMR Spectra were recorded on a Varian Gemini 300MHz spectrometer at 20°C The poor solubility of quercetin restricted the choice of solvent for the experiments to acetone and dimethyl sulfoxide For T_1 studies, a standard inversion-recovery experiment (*'t1'*) supplied by Varian was used T_1 values were calculated using Mestre-C software Degassing was performed via sonication of samples for 30 seconds prior to measurement The concentration of the quercetin template molecule was maintained at 0 04 M in acetone-d_6, and to this the corresponding equivalents of pyridine-d_5 (also 0 04 M in acetone-d_6) were added For the titration experiments, the ratio of template to monomer was again systematically varied, using equimolar solutions of quercetin and pyridine-d_5 (0 04 M, to approximate polymensation mixture concentrations), with a constant sample volume of 0 75 cm^3

3 4 5 BET Analysis

A defined amount of MIP or control polymer (between 0 03 g - 0 05 g) was outgassed at 100°C for a period of 4 hours prior to analysis to remove adsorbed gases and moisture A Beckmann-Coulter instrument was employed (Coulter SA3100 Surface Area and Pore Size Analyzer) and polymer surface areas were determined from multi-point N_2 adsorption isotherms

3 5 Results & Discussion

3 5 1 Investigation of influence of monomer/ template ratio on quercetin imprinting effect (4-vinylpyridine/ quercetin system).

The series of polymers described in Table 3 1 was prepared and processed as described in the experimental section For each MIP created, a blank MIP (identical, but with the exclusion of template molecule) was simultaneously created to permit evaluation of non-specific binding effects The quantity of crosslinker relative to functional monomer was kept constant (at 5 1) to eliminate the possibility of polymer density/ overall morphology affecting chromatographic performance EGDMA was the crosslinker used in each case It was found that polymers with a ratio of template to monomer of less than 1 6 produced polymer structures that, upon grinding, were too fine to pack into HPLC columns An interesting observation at this point was that the control MIPs for III-1 and III-2 were less fine upon grinding, suggesting differences in the polymerisation process due to the presence of template molecule, an effect which appears to support the observations in Section 3 5 3 of PPC aggregates forming during polymerisation However, these polymers are excluded from evaluation of chromatographic performance for this reason

Polymer Ref No	Functional monomer	Template · Monomer . Crosslinker
III – 1	4-VP	1 2 10
III – 2	4-VP	1 4 20
III – 3	4-VP	1 6 30
III – 4	4-VP	1 8 40
III – 5	4-VP	1 10 50
III – 6	4-VP	1 12 60
III – 7	4-VP	1 16 60

Table 3.1 Series of MIPs prepared in this study In all cases, template molecule is quercetin and crosslinker is EGDMA.

However, the imprinted polymers with a monomer template ratio of 6 1 and higher demonstrated a strong imprinting effect, to varying degrees, as is evident from the following results

Analyte	t_{CTL} [min]	k'_{CTL}	t_{IMP} [mm]	k'_{IMP}	α_{CTL}	α_{IMP}	RI
Acetone	3,78	-	3,43	-	-	-	-
Quercetin	8,12	1,15	~37,0	9,77	1	1	1
Morin	8,68	1,30	24,35	6,09	0,88	1,60	0,55
C-fla	4,83	0,28	4,73	0,38	4,11	25,71	0,16
Rutin	4,22	0,12	4,11	0,20	9,58	48,85	0,20

Table 3 2 – Performance of MIP III-3 in chromatographic evaluation in terms of capacity factor, separation factor and retention index

One tangible difficulty associated with MIPs, which becomes quite evident in this type of chromatographic study, is the heterogeneity of binding sites. The range of affinities for the template molecule thus results in a broad retention peak for the quercetin elution. The retention times thus given for quercetin here (and in results to follow) are not precise. Nevertheless, the strong imprinting effect is easily identifiable (see Fig. 3.2), with quercetin having a retention time almost five times longer for the imprinted column, than on the blank counterpart, and thus a higher capacity factor. Morin is the only molecule to display significant binding (which may be evaluated via the retention index parameter), which may be attributed to the close structural similarity (only one hydroxyl group in difference). This points to strong specific binding sites.

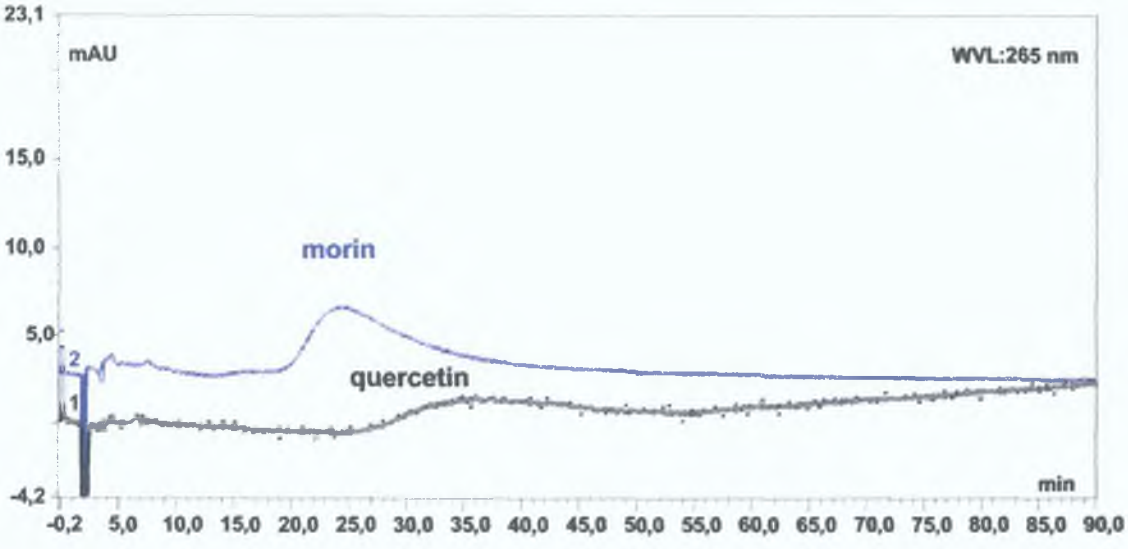

Fig. 3.2 –Retention of quercetin (1) and morin (2) on imprinted column III-3. Mobile phase of MeCN:HAc:H2O (80:10:10, v/v/v), flow rate of 1ml/min.

However, it was noted that in the case of this polymer, separation of the constituents of a quercetin/ morin mixture was not possible with these conditions, although the mixture was more strongly retained on the imprinted column than on the blank column, as displayed in Fig. 3.3.

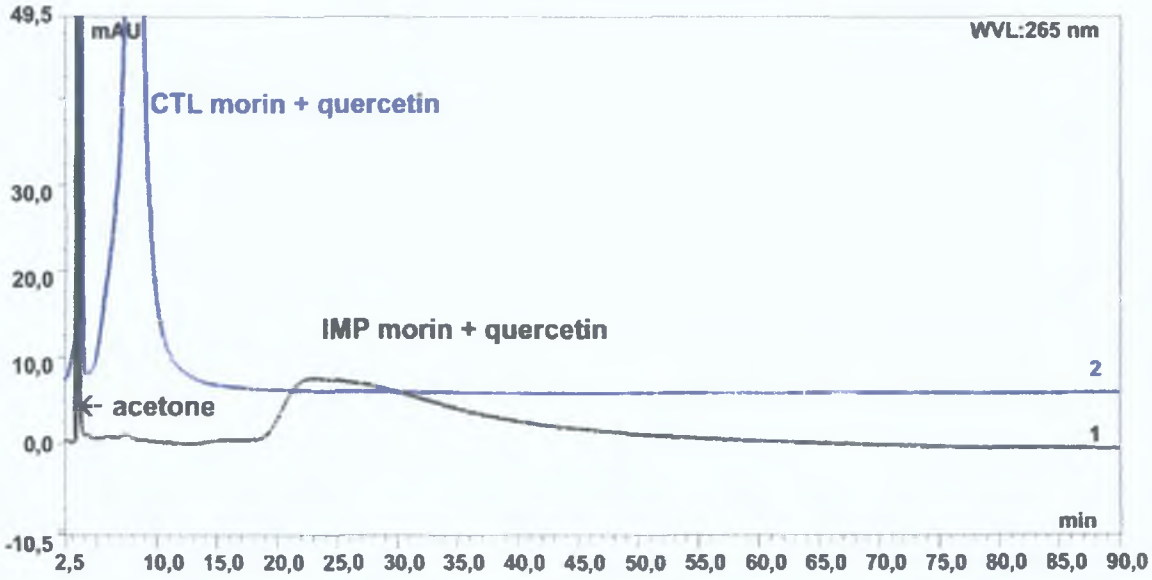

Fig.3.3 – Retention of a quercetin/ morin mixture on (1) imprinted column III-3 and (2) blank column III-3.

The requisite data for MIP III-4, having been already determined in the prior study[1], is summarised in Table 3.3:

Polymer Ref. No.	Functional Monomer	Cross-linker	Ratio	k'_{CTL} morin	k'_{IMP} morin	k'_{CTL} quercetin	k'_{IMP} quercetin	Relative Imprinting effect
III-4	4-VP	EGDMA	1: 8 :40	1,4	6,8	1,4	10,0	strong

Table 3.3 – Summary of chromatographic properties of imprinted polymer III-4.

This polymer displays improved recognition properties compared to MIP III-3, indicating that increasing the ratio of monomer to template warranted further investigation, to determine the optimum ratio. The point of this process is to establish at what point the excess of monomer to template induces maximum complex formation, before the non-specific binding of randomly distributed excess functional monomer groups on the polymer network negates the specific binding of those functional groups 'frozen' in particular configurations in binding sites. Table 3.4 describes the binding properties of the next polymer in the series, III-5.

Analyte	t_{CTL} [min]	k'_{CTL}	t_{IMP} [min]	k'_{IMP}	α_{CTL}	α_{IMP}	RI
Acetone	3,59	-	3,40	-	-	-	-
Quercetin	8,79	1,45	43,10	11,67	1	1	1
Morin	8,89	1,47	28,46	7,36	0,98	1,59	0,62
C-fla	4,75	0,32	4,66	0,37	4,53	31,54	0,14
Rutin	4,18	0,16	4,30	0,26	9,06	44,88	0,20

Table 3.4 - Performance of MIP III-5 in chromatographic evaluation, in terms of capacity factor, separation factor and retention index.

Here, the retention time of quercetin is again five times longer on the imprinted column than on the blank, the primary indicator of a strong imprinting effect; the capacity factor was even higher in this case. Cross-reactivity towards morin remains consistently high, although the other analytes, C-fla and rutin, displayed

similar retention times on the blank and imprinted columns. However, perhaps the most significant property of this MIP is its capacity to partially separate a mixture of quercetin and morin, as is displayed in Figure 3.4.

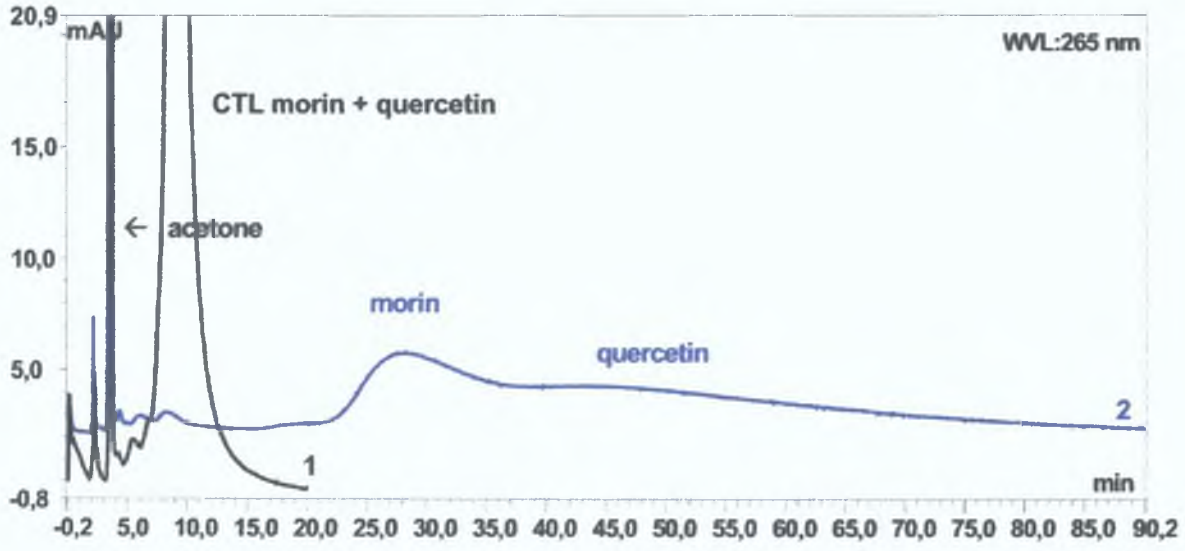

Fig. 3.4 – Separation of a mixture of quercetin and morin on (1) – control polymer and (2) imprinted polymer III-5.

This analysis demonstrates the remarkable recognition properties of this MIP – despite the difference of a single hydroxyl substituent, separation is achieved. To obtain the desirable sharp peaks and baseline resolution necessary in most analytical applications, further modification of both the mobile phase composition, and the nature of the polymer matrix to reduce binding site heterogeneity, is required. However, for the purposes of this qualitative investigation, the separation observed above is adequate for comparison with the behavioural properties of other MIPs in this series. Also of note from this MIP analysis is the greater affinity displayed by the blank polymer for morin and quercetin, compared to rutin or c-fla. These chromatograms are displayed in Fig. 3.5.

(a)

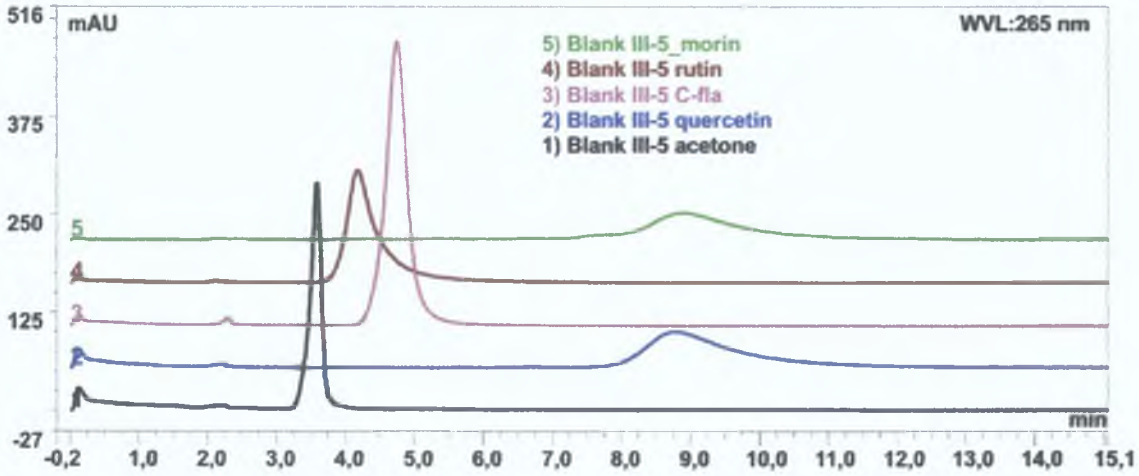

(b)

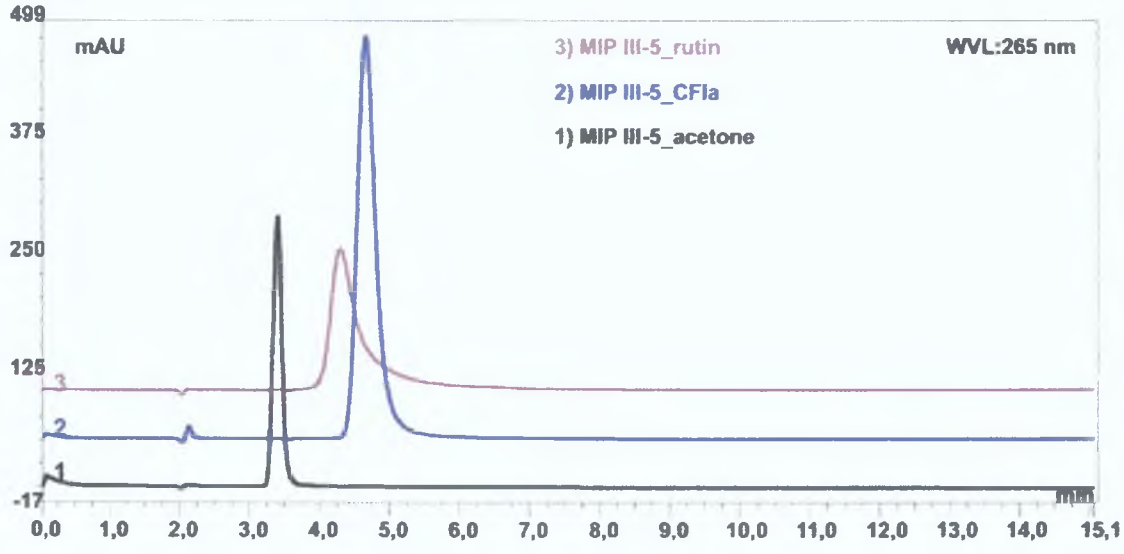

Fig. 3.5 – Chromatograms of (a) acetone, quercetin, c-fla, rutin and morin on blank polymer III-5 and (b) acetone, c-fla and rutin on imprinted polymer III-5. Analysis conditions as in Fig. 3.2.

The data for these two MIPs in this series, III-6 & III-7, display the same trends, although with a slightly lower selectivity for the template molecule. The difference in retention time between quercetin and its closest structural analogue morin increases, although this is counterbalanced by a marked increase in tailing of the quercetin peak, suggesting an even broader distribution of binding site affinities as excess monomer increases. The recognition properties of the last two polymers in the series are described in Tables 3.5 and 3.6, and little difference is evident in their properties.

Analyte	t_{CTL} [min]	k'_{CTL}	t_{IMP} [min]	k'_{IMP}	α_{CTL}	α_{IMP}	RI
Acetone	3,28	-	3,48	-	-	-	-
Quercetin	8,58	1,62	39,23	10,28	1	1	1
Morin	8,81	1,69	21,00	5,04	0,96	2,04	0,47
C-fla	4,28	0,30	4,89	0,40	5,40	25,70	0,21
Rutin	3,63	0,11	4,19	0,20	14,73	51,40	0,29

Table 3.5 - Performance of MIP III-6 in chromatographic evaluation, in terms of capacity factor, separation factor and retention index.

Analyte	t_{CTL} [min]	k'_{CTL}	t_{IMP} [min]	k'_{IMP}	α_{CTL}	α_{IMP}	RI
acetone	3,18	-	3,28	-	-	-	-
quercetin	9,25	1,91	46,24	13,09	1	1	1
morin	9,77	2,07	25,44	6,75	0,92	1,94	0,47
C-fla	3,99	0,26	4,15	0,26	7,35	50,35	0,15
rutin	3,69	0,16	4,30	0,31	11,94	42,23	0,28

Table 3.6 - Performance of MIP III-7 in chromatographic evaluation, in terms of capacity factor, separation factor and retention index.

Having thus created and characterised a series of quercetin-imprinted polymers using just 4-vinylpyridine as functional monomer, two more polymers were included to the series to investigate the possibilities offered by mixing monomers (4-vinylpyridine and acrylamide), as described in Chapter 2. Methacrylic acid, the archetypal functional monomer used in molecular imprinting protocols, was used as the second monomer. The composition is thus described in Table 3.7, and again the polymerisation was carried out using the conditions described in the experimental section (including use of ethylene glycol dimethacrylate as crosslinking agent and azobisisobutyronitrile as initiator).

Polymer Ref. No.	Functional monomer	Template : Monomer : Crosslinker
III - 8	4-VP:AA	1 : (4 : 4) : 40
III - 9	MAA	1 : 4 : 40

Table 3.7 – Composition of additional 2 quercetin-imprinted polymers included in series.

For MIP III-8, the observed retention time of quercetin was higher in the imprinted polymer, compared to the control polymer (see Table 3.8). The quercetin analogue morin again showed a relatively high cross-reactivity ; when injected as a mixture, quercetin and morin were not separated by the imprinted polymer III-8 (see Fig. 3.6), but they were retained longer versus the control polymer. The peak produced by this flavonoid mixture showed a distinctive tailing effect. This is indicative of a heterogeneous binding site distribution, which is a typical attribute of MIP stationary phases. In synopsis, the evidence points to the presence of specific binding sites, but with an excess of non-specific binding sites. Thus, this MIP exhibited a poor imprinting effect.

Analyte	t_{CTL} [min]	k'_{CTL}	t_{IMP} [min]	k'_{IMP}	α_{CTL}	α_{IMP}	RI
Acetone	3,57	-	3,56	-	-	-	-
quercetin	6,31	0,77	7,94	1,23	1	1	1
Morin	6,06	0,70	7,99	1,24	1,10	0,99	1,11
C-fla	4,30	0,20	4,37	0,23	3,85	5,35	0,72
Rutin	4,09	0,15	4,05	0,14	5,13	8,79	0,58

Table 3.8 - Performance of MIP III-8 in chromatographic evaluation, in terms of capacity factor, separation factor and retention index.

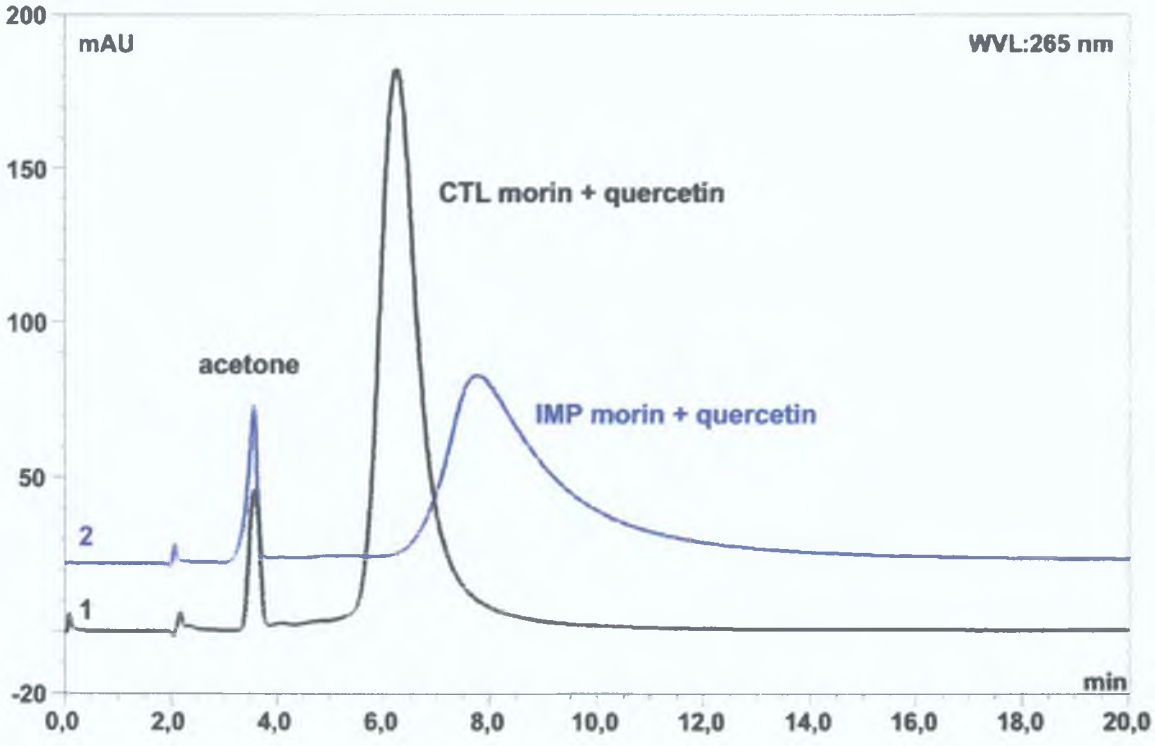

Fig. 3.6 – Separation of quercetin/ morin mixture on (1) blank polymer III-8 and (2) imprinted polymer III-8; analysis conditions as described in Fig.3.2.

The final member of the series was a quercetin-imprinted methacrylic acid/ EGDMA co-polymer, which is the most frequently used functional monomer in non-covalent imprinting found in the current literature. Although suitable for a broad range of analytes, imprinting with MAA as functional monomer was not seen to result in high specificity – indeed, morin was more strongly retained than the quercetin template, as seen in Table 3.9. As seen in earlier members of the series, rutin and c-fla were retained to the same extent by both the imprinted and control polymers. Although quercetin and morin were separated when injected as a mixture, the anomalous behaviour of this MIP meant that morin was the more

strongly retained analyte. This would seem to concur with the findings of Katz and Davis, who determined methacrylic acid to be more conducive to the formation of non-specific electrostatic interactions, rather than more subtle hydrogen bond creation, with a consequential low level of selectivity. Overall, a moderate imprinting effect is observed, as displayed in the chromatograms of Figure 3.7. One aspect of this analysis which may be significant is that negative values are observed for the retention of rutin. This may indicate that for future analyses with these MIPs, a different void marker to acetone should be used.

Analyte	t_{CTL} [min]	k'_{CTL}	t_{IMP} [min]	k'_{IMP}	α_{CTL}	α_{IMP}	RI
Acetone	3,66	-	3,62	-	-	-	-
quercetin	4,58	0,25	4,87	0,35	1	1	1
Morin	4,29	0,17	5,92	0,63	1,47	0,56	2,63
C-fla	4,22	0,15	4,28	0,18	1,67	1,94	0,86
Rutin	3,55	-0,03	3,51	-0,03	-8,33	-11,67	0,71

Table 3.9 - Performance of MIP III-9 in chromatographic evaluation, in terms of capacity factor, separation factor and retention index.

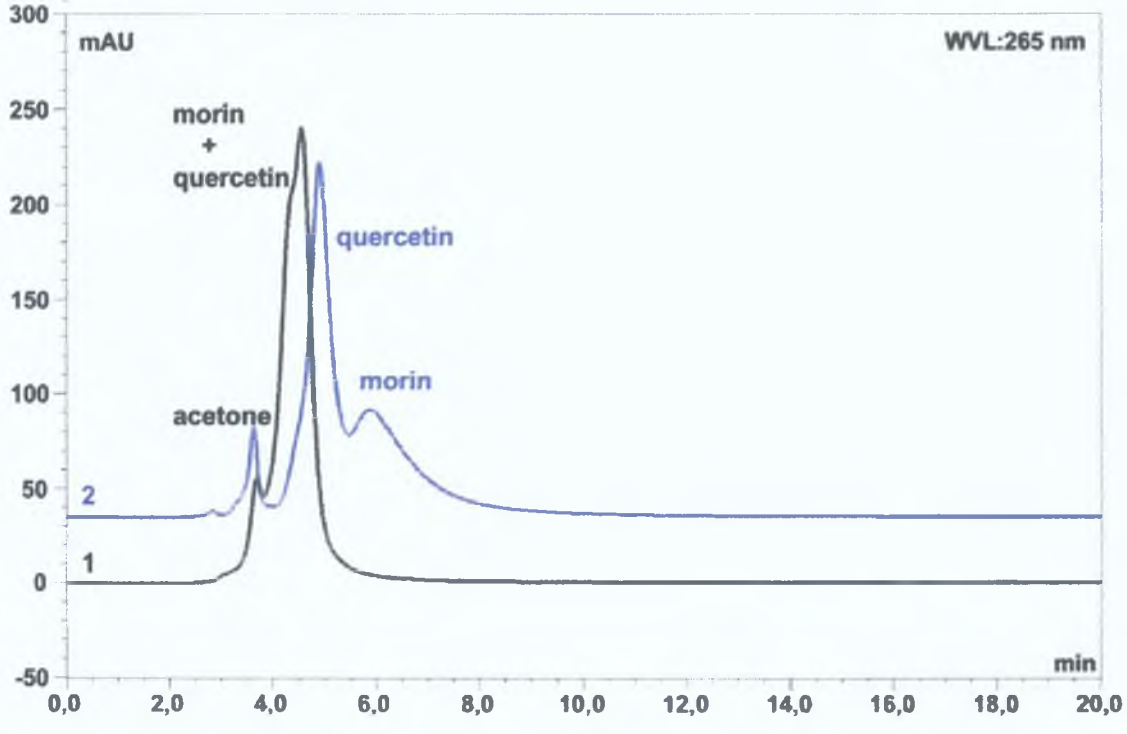

Fig. 3.7 - Separation of quercetin/ morin mixture on (1) blank polymer III-9 and (2) imprinted polymer III-9; analysis conditions as described in Fig.3.2.

This series of polymers provided a platform for investigation of to what extent monomer: template ratio, and choice of functional monomer, play a role in determining the selectivity of the MIP being investigated. To facilitate comparison, the performance of each of the members of the series is described in Table 3.10, and capacity factors are compared in Figure 3.8. This provided an excellent opportunity to concurrently apply NMR techniques to PPC analysis, and possibly correlate the findings. This is described in Section 3.5.2.

Polymer Ref. No.	Functional Monomer	Cross-linker	Ratio	k'_{CTL} morin	k'_{IMP} morin	k'_{CTL} quercetin	k'_{IMP} quercetin	Relative Imprinting effect
II-3	4-VP	EGDMA	1: 6: 30	1,3	6,1	1,2	9,8	strong
II-4	4-VP	EGDMA	1: 8 :40	1,4	6,8	1,4	10,0	strong
II-5	4-VP	EGDMA	1: 10: 50	1,5	7,4	1,5	11,7	strong
II-6	4-VP	EGDMA	1: 12: 60	1,7	5,0	1,6	10,3	strong
II-7	4-VP	EGDMA	1: 16: 60	2,1	6,75	1,9	13,09	strong
II-8	4-VP:AA	EGDMA	1:(4 : 4):40	0,7	1,2	0,8	1,2	poor
II-9	MAA	EGDMA	1: 4: 40	0,2	0,6	0,3	0,4	moderate

Table 3.10 Comparative analysis of chromatographic performance of MIPs investigated.

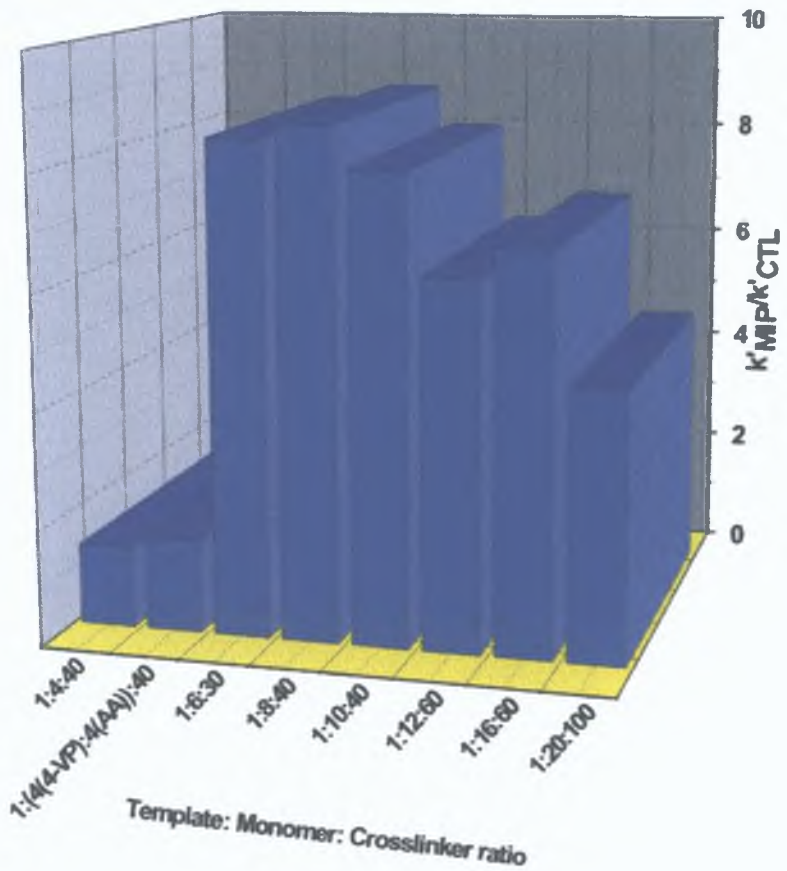

Fig. 3.8 – Graph of relative chromatographic performance of quercetin-imprinted MIPs (data for 1:20:100 ratio provided by A. Molinelli).

3.5.2 NMR Investigation of Pre-polymerisation Events

In non-covalent imprinting, the formation of hydrogen bonds (among other types of non-covalent interaction) between the template molecule and the functional monomer is crucial to the success of an imprinting protocol and thus observation of these bonds forming can be an aid in predicting the suitability of a functional monomer to a particular analyte. One means of observing these bonds forming is via NMR titration experiments. This method of studying hydrogen bonding is a well-researched field, having been used in the past for applications such as looking at bonding between nucleic acid bases and carboxylic acids[3], as well as H-bonding properties of monosaccharides[4]. Proton NMR has also recently been used as a way of showing the extent of complex formation in pre-polymerisation complexes in molecular imprinting[5], by using the chemical shift change of a proton signal due to participation in a hydrogen bond as a basis for selecting a monomer for an imprinting procedure. Complex properties such as stoichiometry and association constants can thus be derived, since the signal for the proton being observed for the interaction is a weighted average of the signals of uncomplexed protons and complexed protons.

Studies by Andersson and Nicholls[6] have shown that in typical pre-polymerisation mixtures, the number of stable complexes formed between monomer and template are quite low – usually, the template-to-functional-monomer ratios used correspond to between 0.3 and 0.6% of complex formation.

Also, literature values indicate that for all binding sites formed by an imprinting procedure, only 0.5 to 1% can be classed as medium-to-high affinity. Therefore, it is significant that the proportion of complex formed prior to polymerisation correlates with the amount of highly selective recognition sites found in the corresponding MIPs. This indicates that, since a good imprinting effect can be observed even with a relatively low number of binding sites being formed, then any stress introduced into the pre-polymerisation system that favours complex formation, will result in a significantly improved recognition effect in the resultant polymer. Again, this draws attention to the importance of identifying and optimising pre-polymerisation monomer-template complex interactions.

The quercetin system being examined here was successfully imprinted against, albeit in the polar solvent acetone. Conventional MIP technology theory states that for non-covalent interactions, polar solvents acting as porogen will inhibit complex formation and consequently, any significant imprinting effect. Examining the quercetin/ 4-vinylpyridine system via ^{1}H-NMR, it becomes apparent that the acidic nature of 4 of the 5 hydroxyl substituents (pKa ~9.5) allow them to participate in an acid /base-type equilibria with the basic 4-vinylpyridine monomer. The hydroxyl group at the 5 position undergoes intramolecular hydrogen bonding with the carbonyl functionality and does not appear to participate in any interactions[7].

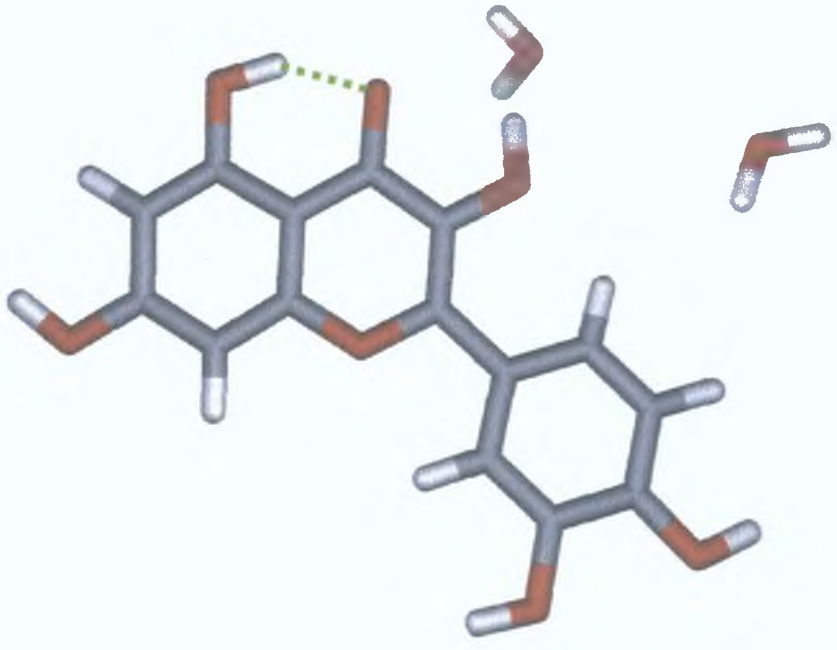

Fig. 3.9 – Crystal structure of quercetin dihydrate, showing intramolecular hydrogen bond. From reference 7.

Also of note from the crystal structure of quercetin dihydrate is that the molecule is almost planar. In this respect, quercetin is unusual: in crystal structure analysis, many flavonoid compounds of similar structure have the pendant aromatic ring at an angle of up to 30° to the main aromatic/ heterocyclic fused ring system, making π–π stacking sterically difficult. It is anticipated that for quercetin in solution, the pendant aromatic ring is free to rotate. However, if the quercetin molecule does adopt a planar conformation, such interactions should be possible, especially with the energetic incentive of reducing area of

hydrocarbon exposed to the polar acetone solvent, and this was also investigated during the titration experiments. Although addition of D_2O to a sample of 0.04M quercetin in acetone-d_6 resulted in the disappearance of all hydroxyl protons (see Fig. 3.10), addition of 4-vinylpyridine by contrast only resulted in the disappearance of 4 of the hydroxyl proton signals. This indicates that the proton at position 5 remains unaffected by 4-vinylpyridine, and the intramolecular bond indicated in Fig. 3.11 remains unperturbed (see Figure 3.11).

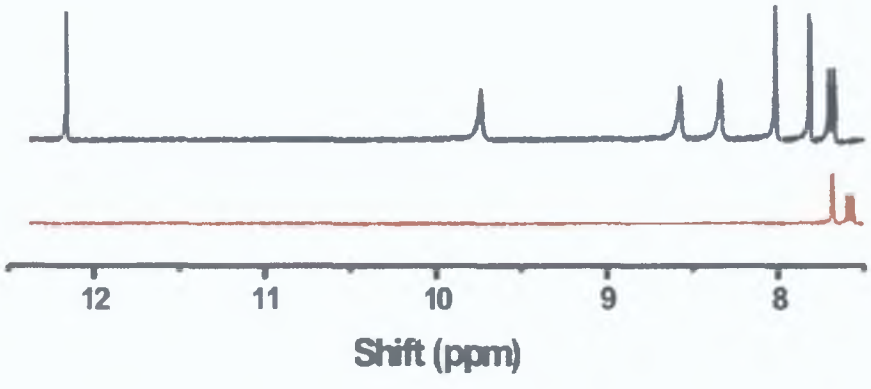

Fig.3.10 – Addition of a few drops of D_2O to a sample of quercetin (0.04M in DMSO) results in disappearance of all hydroxyl protons.

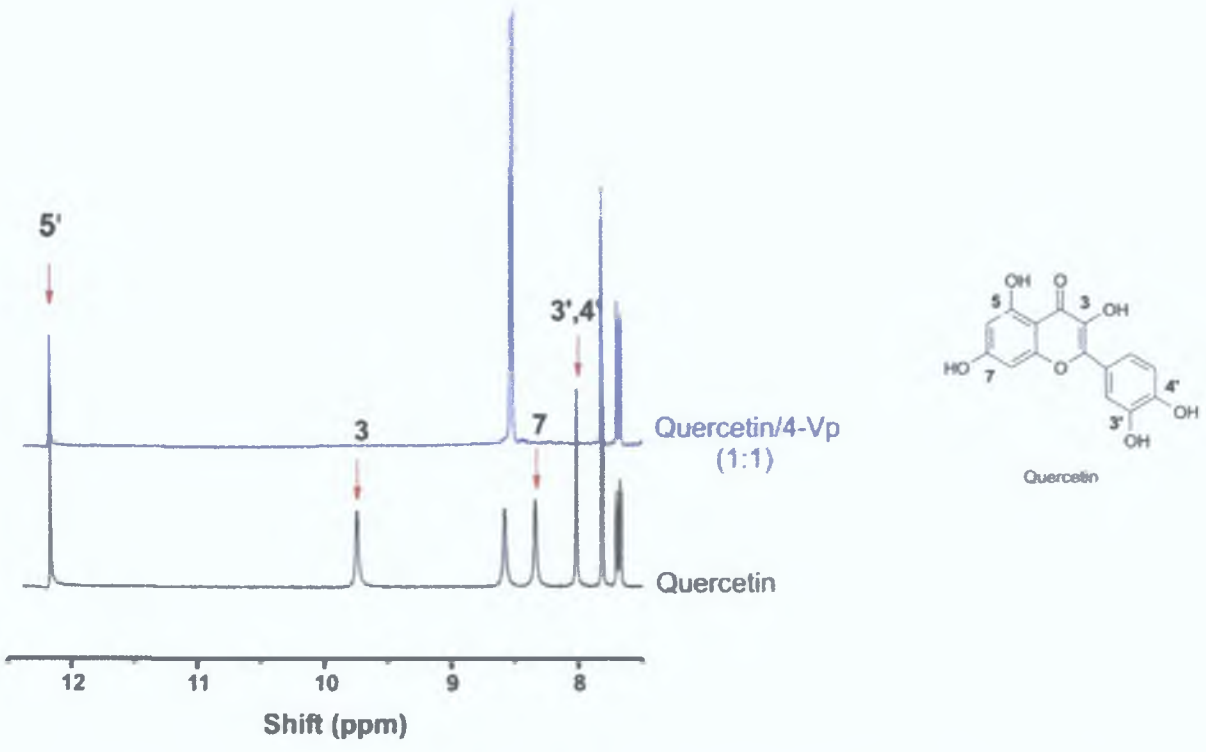

Fig. 3.11 - Effect of addition of 1 equivalent of 0.04M 4-vinylpyridine upon hydroxyl protons at positions 3,7, 3' and 4' on quercetin (0.04M in acetone-d_6) molecule (signals marked with arrow).

Titrating 4-vinylpyridine with quercetin and analysing via ^{1}H-NMR thus proved an ineffective way of tracing the formation of hydrogen bonds between the basic pyridine ring of the monomer and (acidic) phenolic hydroxyl substituents of the quercetin. The hydroxyl proton signals disappear as soon as titration commences. This is most likely due to the protons rapidly exchanging position from complexed state to free state. As explained by Hore[8], if the exchange rate is faster than the frequency difference of the proton signal's two separate states, observation of equilibrium phenomena is difficult – resulting in line-broadening, signal coalescence and signal disappearance, as may be the case with this

experiment (see Fig. 3.12). It is probable that the ion-pair formed by the acidic phenolic protons of the quercetin and the basic nitrogen atom of the pyridine moiety is subsequently exchanging with the deuterated solvent, with the consequence of the disappearance of phenolic proton signals from the NMR spectrum.

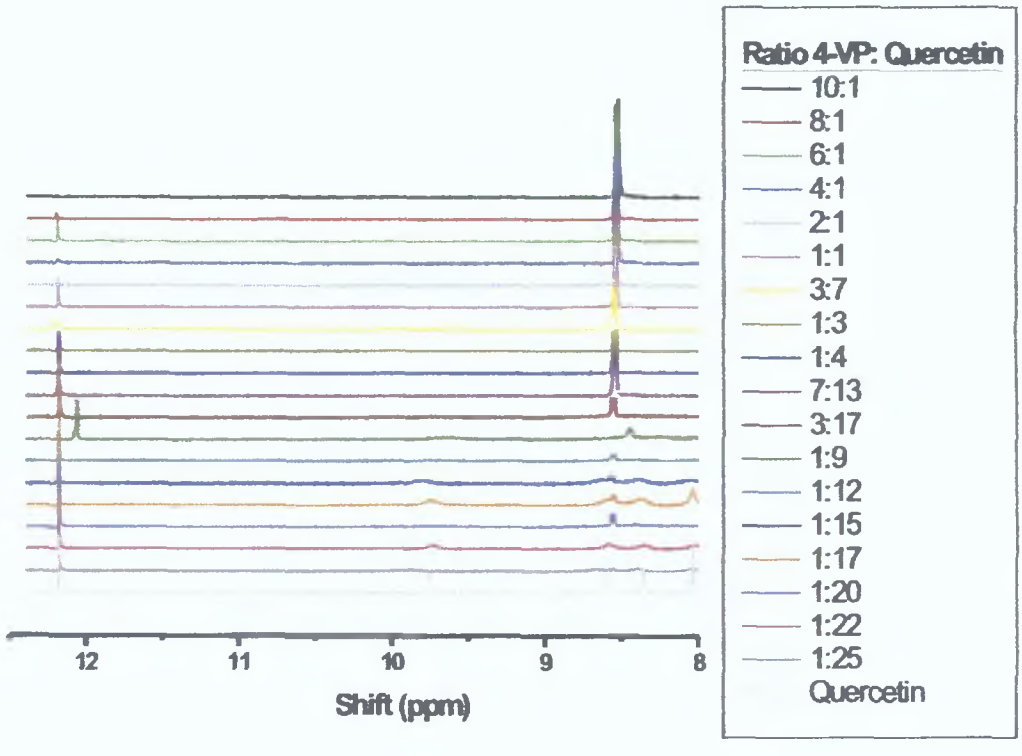

Fig. 3.12 – Titrating quercetin with 4-vinylpyridine (each at 0.04M) in acetone-d_6. ^{1}H-NMR, 16 scans/ sample.

Given the somewhat vague results seen in the ^{1}H-NMR studies, the system was next studied using ^{13}C-NMR spectroscopy. An alternative method of probing the interaction is by observing changes in the ^{13}C-NMR spectrum of 4-vinylpyridine across a range of ratios of monomer/ template. As the 4-vinylpyridine participates

to a greater extent in a hydrogen-bonding interaction, the introduction of a positive charge onto the pyridine nitrogen atom will alter the signal shifts of the carbon atoms of the molecule (see Fig. 3.13).

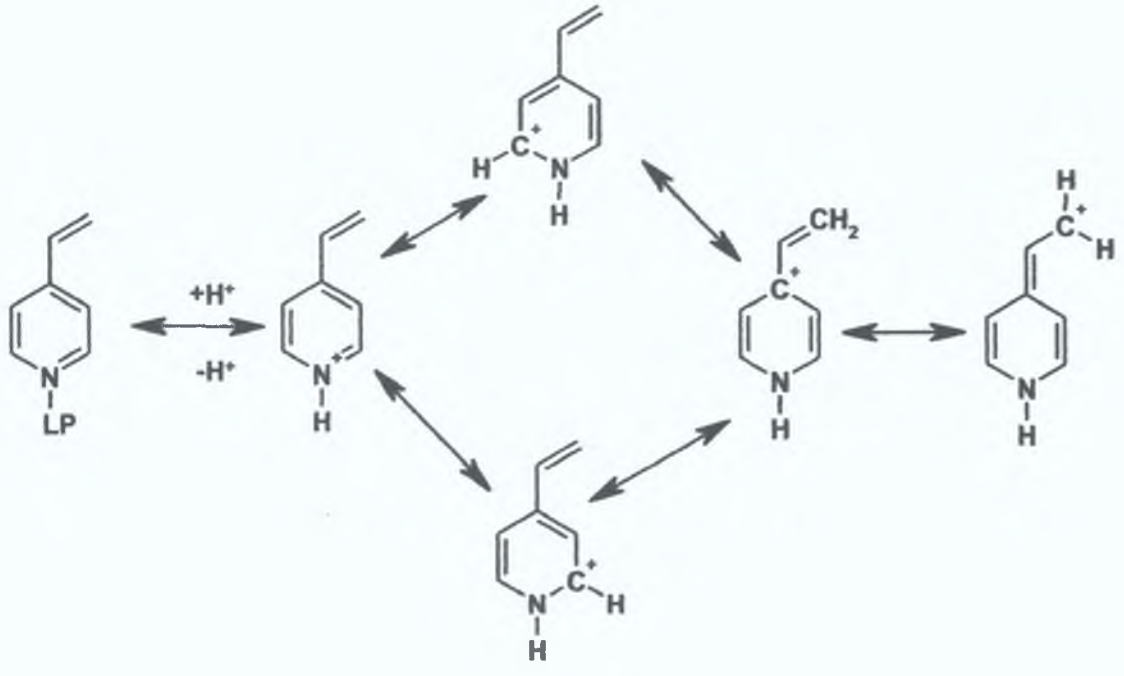

Fig. 3.13 – Proposed equilibria for protonation of 4-vinylpyridine, with canonical forms of protonated species.

This approach offered a clearer insight into the monomer-template system; firstly, the introduction of a positive charge into the molecule establishes a resonance, meaning three separate signals can be observed for changes (the vinylic carbon, the carbon at ring position no.4 and the signal for the carbons in ring positions 2 and 6). Taking the example of the vinylic carbon shift at approximately 118 ppm, a gradual shift downfield is clearly evident (refer to Fig. 3.14).

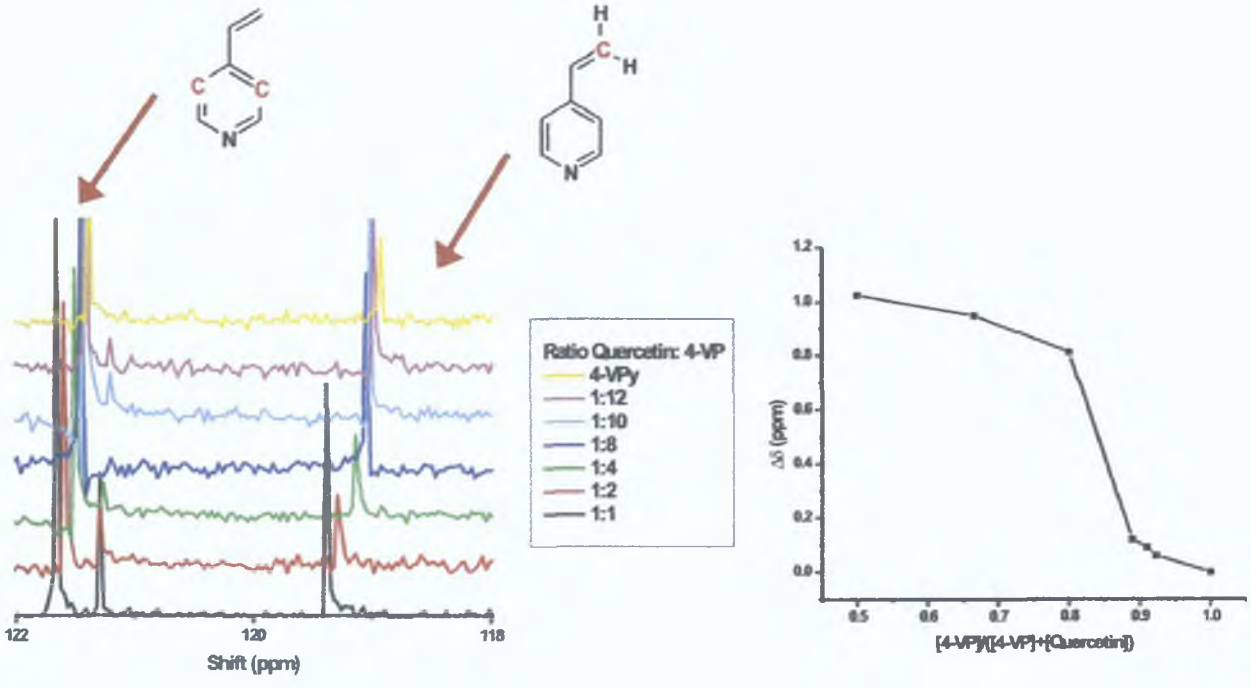

Fig. 3.14 - Titrating quercetin with 4-vinylpyridine (each at 0.04M) in acetone-d_6. ^{13}C-NMR, 256 scans/ sample.

Perhaps even more revealing in this experiment is the evidence that acetone, used as the solvent/ porogen for the quercetin MIP pre-polymerisation mixture, actively participates in hydrogen bonding in the system. The signal for the carbon belonging to the acetone's carbonyl group, found at 205 ppm, shifts as quercetin is added to the 4-vinylpyridine (ref. Fig. 3.15), as do the methyl carbon signals. The effect may be a consequence of excess base (4-VP) catalyzing the keto-enol tautomerism of the acetone solvent (see Fig. 3.16).

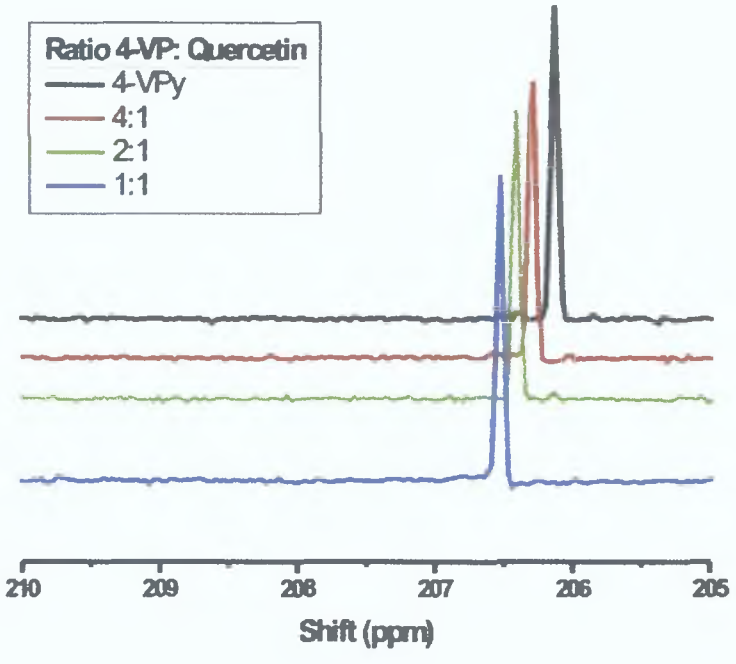

Fig. 3.15 – Observing the acetone carbonyl C signal during quercetin/ 4-Vp titration in deuterated acetone. ^{13}C-NMR, 256 Scans/ sample.

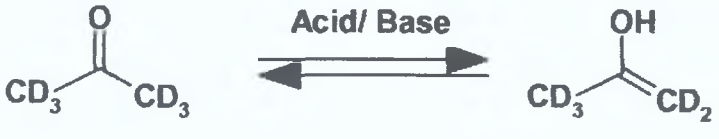

Fig. 3.16 – Proposed keto-enol tautomerisation of acetone.

A final stage in this qualitative assessment of the interactions occurring in the pre-polymerisation mixture is to replace quercetin with a molecule of similar size, but without the hydroxyl substituents, that are thought to induce selectivity. For this purpose, the relatively inert structural analogue naphthalene was chosen. Choosing the same carbon atom of the 4-vinylpyridine for observation as in the previous experiment, the carbon of the vinyl functionality, a series of titrations were run (see Fig. 3.17).

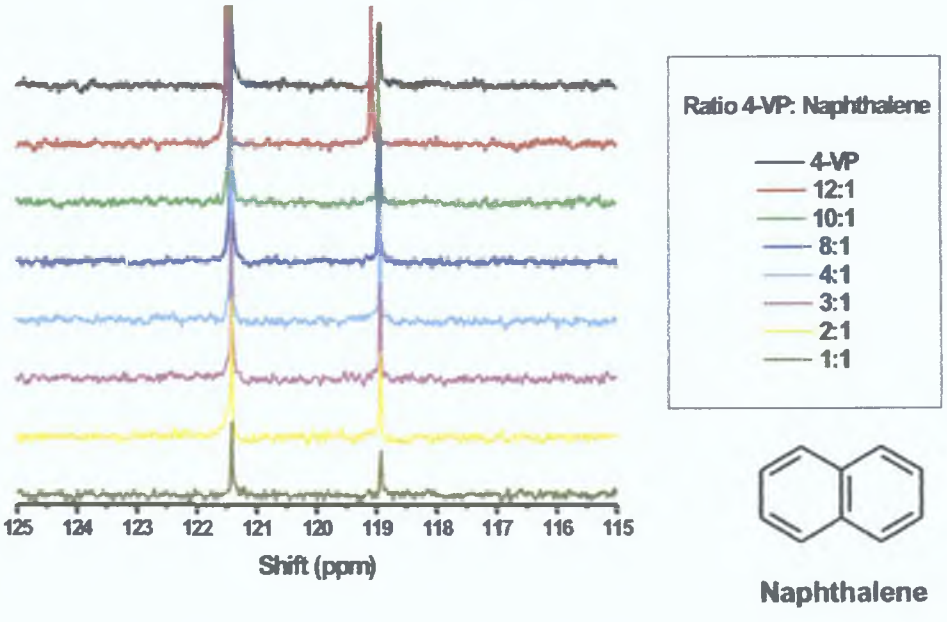

Fig. 3.17 - Titrating naphthalene with 4-vinylpyridine (each at 0.04M) in acetone-d_6. ^{13}C-NMR, 256 scans/ sample.

Due to the absence of any hydrogen bonding in this system, the resonance distribution of charge fails to occur and so no shift in this carbon's signal is observed. Also of note is that after an initial change upon addition of naphthalene, the signal shift of the carbonyl carbon of the acetone is also

unaffected, supporting the hypothesis that there is a cooperative interaction between quercetin, 4-VP and acetone together, rather than just two of the three system components (see Fig. 3.18).

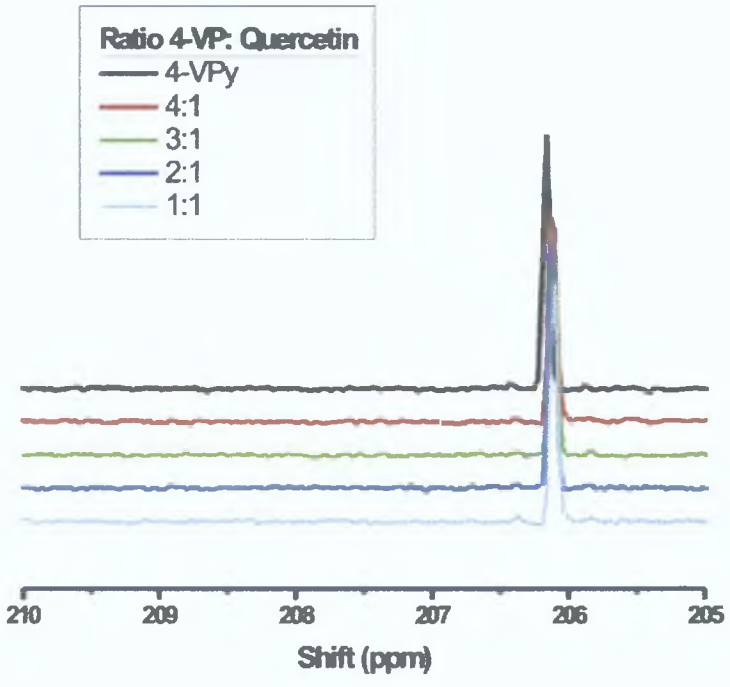

Fig. 3.18 – Observing the acetone carbonyl C signal during naphthalene/ 4-Vp titration in acetone-d_6. ^{13}C-NMR, 256 Scans/ sample.

These initial titration results support the formation of a pre-polymerisation complex, with at least 4 points of the quercetin molecule capable of participating in interactions, as indicated by the disappearance of 4 hydroxyl proton signals in the ^{1}H-NMR spectra. ^{13}C-NMR spectra also support this, with the observed changes in signals for the 4-vinylpyridine monomer molecule. However, these findings do not shed much light on the actual nature or stoichiometry of the

complexes. Titration of quercetin with pyridine-d_5 (which was used in place of 4-vinylpyridine to simplify spectra and make observations of changes in aromatic proton signals possible) revealed slight changes in the chemical shifts of the aromatic protons, which may indicate formation of aggregated oligomers in the pre-polymerisation mixture, (see Fig. 3.19). Aggregation effects may be followed by observing changes in the shifts of aromatic protons[9], and has been traced in the 2,4-D/4-VP system described in chapter 4. For a more detailed description of aggregation effects/ π–π stacking and ^{1}H-NMR, refer to Chapter 4, Section 4.2.2.

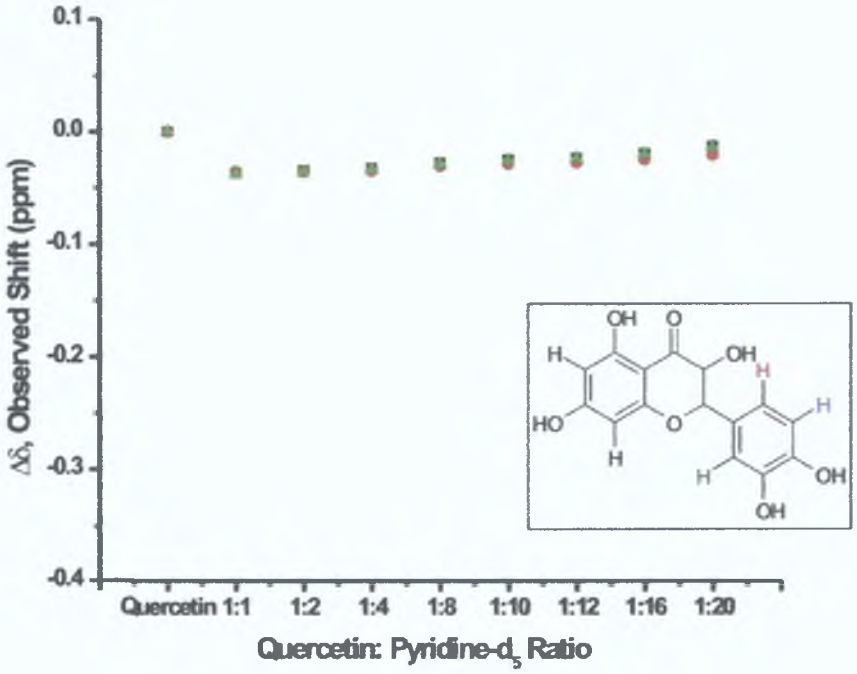

Fig. 3.19 - Titrating Quercetin with pyridine-d_5 in acetone-d_6. Observed shifts of protons on pendant aromatic ring.

Crystallographic evidence from the literature[7] indicates that the molecule is almost planar in configuration in the solid phase, and so should be capable of $\pi-\pi$ stacking effects. In the liquid phase, the free rotation of the pendant aromatic ring means that clear observation of such stacking is not facile. However, aggregation based on hydrophobicity/ $\pi-\pi$ stacking would explain the high performance of the 8:1 monomer: template ratio MIP in chromatographic analysis – formation of ion-pairs with 4 monomer units and hydrophobic association with 4 more providing a stable monomer: template complex. Another possibility currently being investigated is the self-association of the phenolic hydroxyl groups of quercetin as they participate in H-bonding interactions with the nitrogen atoms of the 4-vinylpyridine functional monomer. Such effects have been observed in the interactions between phenol and tertiary amines[10].

To use an alternative approach to determining the stoichiometry/ structure of the monomer-template complex formed, the spin-lattice (T_1) relaxation times of the quercetin molecule was measured as incremental amounts of monomer were added. This is known to be an effective method of determining stability constants[11] – to summarise, the T_1 time may be used as a measure of rate of molecular tumbling, and as equilibrium is reached, the measured T_1 time should be a weighted average of free and complexed quercetin, reaching a plateau at the ratio where formation of the quercetin/ 4-vinylpyridine complex is most favoured. The apparent optimum template: monomer ratio in this respect is again 1:8 (see Fig. 3.20).

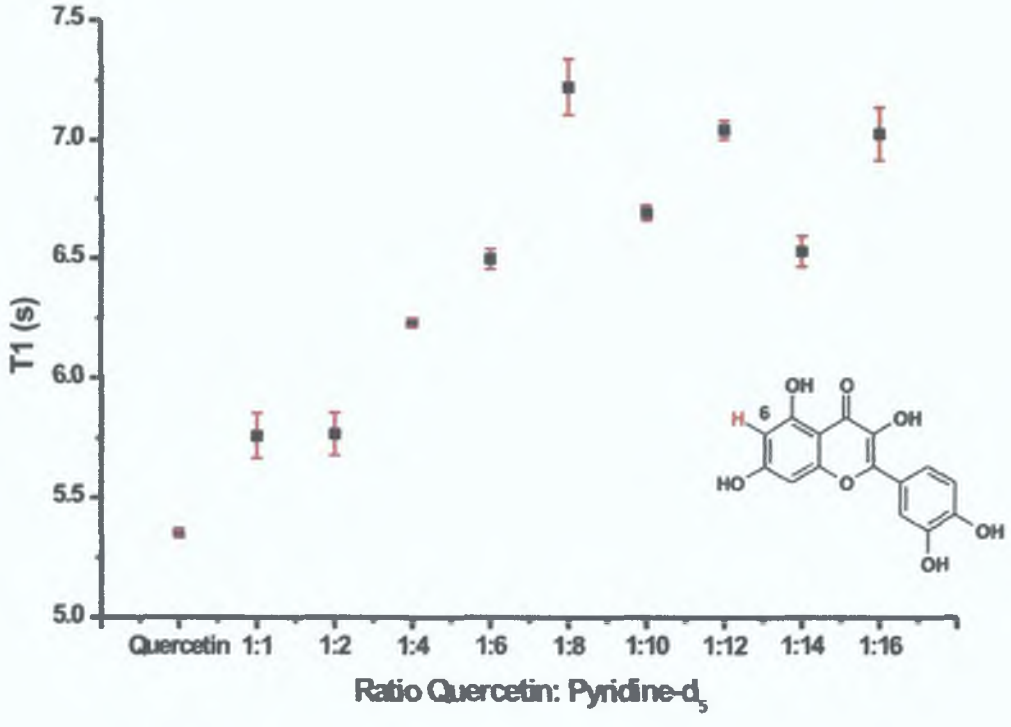

Fig. 3.20 - T_1 ^{1}H-NMR relaxation data (average of 2 separate experiments). Experiments performed in acetone-d_6 at 294K. Monitoring proton at position 6 on quercetin molecule.

The behaviour of this system as analysed by T_1 relaxation time yielded intriguing results; the data does not quite achieve a plateau. Also, T_1 increases with increasing ratio of functional monomer analogue (pyridine-d5). As the M_r of the complex increases, there ought to be a corresponding decrease in the T_1 time observed (as typically, T_1 is inversely proportional to rate of relaxation). This would appear to be a consequence of macroscopic phase partition of hydrophobic monomer/ template aggregates within the polar solvent

environment. T_1 times are a direct reflection of the mobility of these molecules, suggesting that molecular tumbling is quickening with addition of monomer. This may be due to the formation of micro-environments of lower viscosity than the solvent medium. This partition effect appears to be amplified greatest at a monomer: template ratio of 8:1, which also corresponds to the ratio of the MIP of highest chromatographic performance. Ratios above 1:8 in chromatographic evaluation result in poorer performance, which is attributed to the excess monomers participating in non-specific interactions. This NMR experiment thus permits direct correlation of pre-polymerisation complexation events with post-polymerisation chromatographic performance. Although MIP limitations (such as minimum template: monomer ratio of 1:4 to produce a polymer not too dense to be used in chromatographic analysis) prevent all ratios analysed in T_1 studies to be used in MIP preparation & chromatographic characterisation, the trend of highest performance/ shortest relaxation rate is evident (see Fig.3.21). This finding is thus important in that it may permit MIP performance to be predicted, although further research is required to substantiate this.

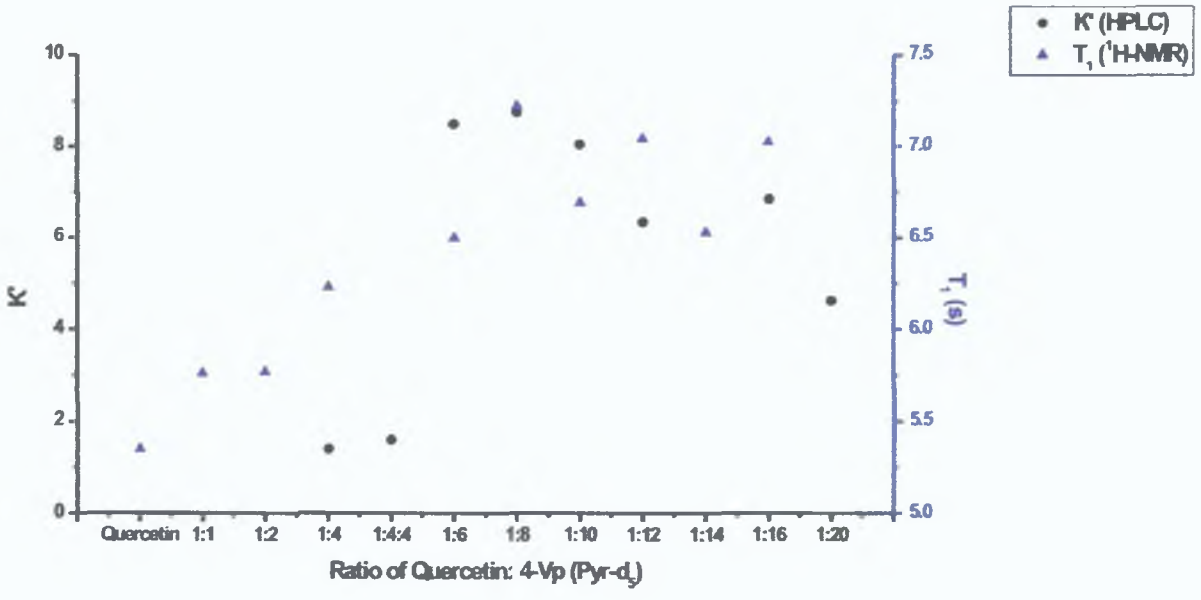

Fig.3.21 – Correlating the chromatographic performance of the MIP series with the T_1 relaxation times determined via ^{1}H-NMR.

3.5.3 Physical Characteristics of the MIP & the Polymerisation Process

The rational design of MIPs in place of typical trial-and-error approaches remains a challenging aspect of this field of analytical chemistry, given the number of parameters to be evaluated – template-monomer interactions, acidity/ basicity of functional monomer, choice of solvent, polymerisation conditions, conformational flexibility of template molecule and degree of crosslinking being some of the more important variables for consideration. To facilitate research on characteristics of this particular polymer which resulted in its high specificity, the investigations were approached not only from the perspective of molecular-level interactions in the mixture prior to polymerisation, but also in terms of physical aspects of the polymer during and after the polymerisation process. With this in mind, careful observation of the process (as detailed in Figure 3.22) revealed the formation of aggregates, which appears to be a macroscopic phase separation effect as detailed by Katz and Davis[12].

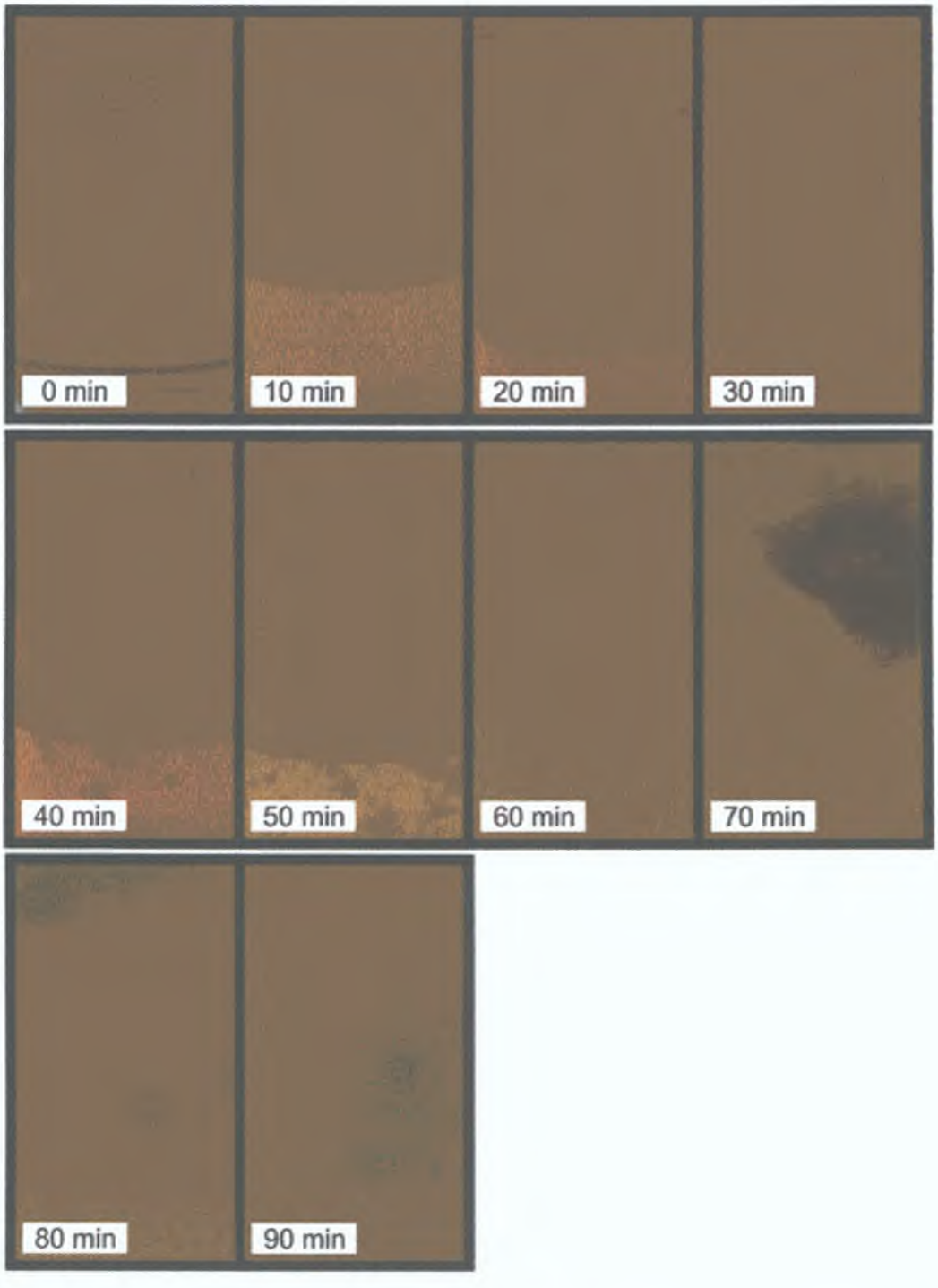

Fig.3.22 - Phase separation of quercetin MIP during processing from t=0min (prior to initiation of the polymerization) to t=90min. Initial composition: 15 cm^3 acetone, 0.05 g AIBN, 1 mM quercetin (0.338 g), 8 mM 4-vinylypyridine (0.8505 cm^3), 40 mM EGDMA (7.544 cm^3).

Small aggregates form and coagulate, frequently forming one 'cluster', as evident in Fig.3.22 (70 min.). This suggests the formation of monomer-template clusters based on similar hydrophobicity; as cluster formation accelerates, the colour of the polymerisation mixture changes from the characteristic rust colour of quercetin in solution, to a lighter yellow colour, as the quercetin molecules become encapsulated in an outer layer of monomer. One may postulate that the optimum 1:8 template/ monomer is thus most likely due to this clustering effect, based on LC and NMR findings. The excess concentration of monomer provides a protective hydrophobic shell wherein monomer-template complexes can survive polymerisation. To ensure that the exceptional retention observed with this MIP is not simply a surface effect, the surface area of a series of MIPs with various template-monomer ratios was also investigated via the Brunauer-Emmet-Teller adsorption isotherm method, which has been employed in the past to evaluate surface areas[13]. The results are displayed in Figure 3.23. As is evident, the surface area of the MIPs (compared with corresponding control polymers) showed no correlation. The optimum 1:8 ratio displays the greatest difference in surface area between MIP and control, although the control polymer had the higher surface area. This result precludes the possibility of highest retention simply being a consequence of a higher overall surface area. The formation of a pre-polymerisation complex can affect the progression of a polymerisation, leading to differences in the surface morphology compared to the corresponding blank polymer. The cause of retention phenomena on such polymer surfaces may thus be ambiguous – work by Lübke *et al.*[14] demonstrated the impressive

affinity of a polymer based on a stoichiometric interaction between monomer and template, up to $3.3x10^3$ M^{-1} for the template molecule. However, the surface area of the imprinted polymer was 338 m^2/g, compared with just 55 m^2/g for the corresponding blank polymer. Although such a high-performance material is undeniably useful for analytical application, the broad difference in surface areas raises questions as to polymerisation events within the imprinted mixture, and the validity of comparing retention on imprinted material with retention on blank material.

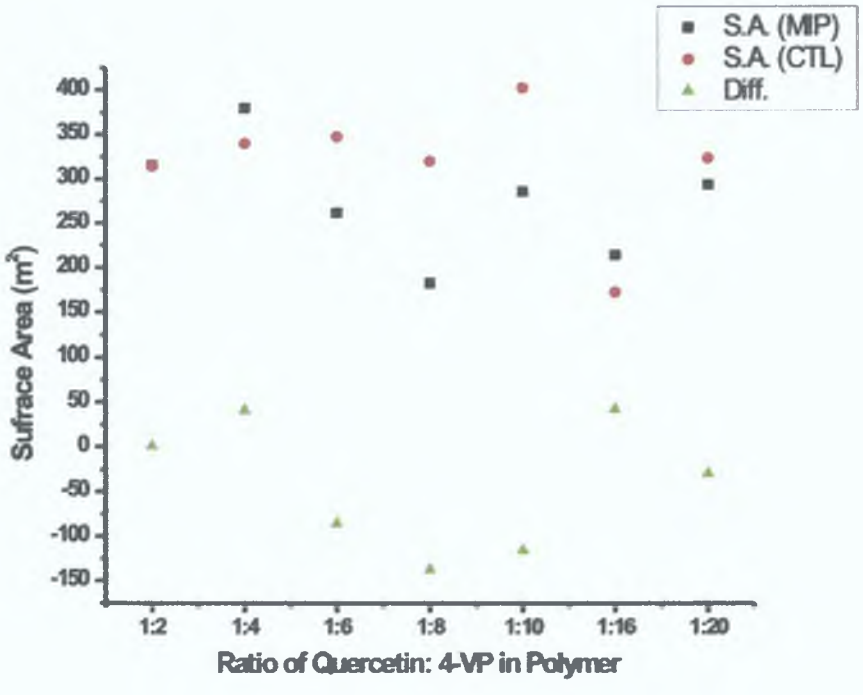

Fig. 3.23 - Comparison between surface areas of imprinted and non-imprinted polymers at various template: monomer ratios via BET adsorption isotherm method. For control polymers, identical polymerisation mixture is used, but with the exclusion of template.

3.6 Conclusion

The creation of strong imprints, for various applications, has been, and continues to be, the subject of much intensive research. However, a specific set of criteria for the design of high-performance MIPs for any given analyte has yet to be deduced. This work shows that in all probability, the number of variables affecting the outcome of an imprinting procedure precludes the possibility of developing such a generalised protocol. For the highly effective MIP examined here, the high degree of selectivity results from a careful choice of monomer, quantity of monomer, and solvent, which cooperatively interact with the template to create 'pockets' or clusters of highly specific binding sites during the polymerisation process. This raises the question of the importance of phase partition effects in typical imprinting processes, which will be further discussed in Chapter 4. One of the more significant outcomes of this research is the apparent utility of T_1 (spin-lattice) relaxation measurements for determining the mobility of monomer/ template complexes in solution. The most mobile pre-polymerisation complex monomer: template ratio also corresponded to the ratio with highest chromatographic performance. This result merits attention since most ^{1}H-NMR titration studies cited in the literature focus on the observable interactions, and determine stoichiometries and association constants based on these. With T_1 time studies, the measurements reflect the overall effect of complexation/ partition events on a molecule. Further investigation is merited to determine the effectiveness of using complex tumbling rates to predict chromatographic

performance of the polymer. Overall, the technique holds much promise for elucidating information on pre-polymerisation complexes, which can be the key factor in predicting the recognition properties of the final MIP formed. The observation of physical phenomena, such as the aggregation of complexes seen here, can be a significant aid in interpretation of polymer behaviour also, while measurement of surface area of the MIP is an essential step in eliminating the possibility of chromatographic behaviour being ascribed to a mere difference in surface area caused by the template molecule impeding or affecting the development of the polymer network in some way. Thus, this quercetin MIP performs exceptionally well apparently due to the preservation of pre-polymerisation complexes during the polymerisation process, as a result of complex aggregation due to a polymerisation phase partition. This is further supported by the use of a polar solvent acetone. This brings to mind the 'biomimetic' quality of MIPs, their behaviour being described as analogous to that of biological entities. This requirement, of needing to 'tune' polarity to optimise the MIP performance, further strengthens this analogy. Enzyme activity enables fast rates of reaction, frequently by virtue of performing reactions in an 'organic' environment, albeit with a hydrophilic exterior which permits solubility in aqueous environments. Monomer modification to adjust solubility of the final PPC, and create protective shells wherein PPCs are effectively conserved, should thus prove a useful technique in effective MIP design in the future.

Bibliography

[1] A. Molinelli, R. Weiss & B. Mizaikoff, *J. Agric. Food Chem.*, 50 (2002), 1804.

[2] J. Xie, L. Zhu, H. Luo, L. Zhou, C. Li & X. Xu, *J. Chrom. A*, 934 (2001), 1.

[3] G. Lancelot, *J. Am. Chem. Soc.*, 99 (1977), 7037.

[4] J. Hawley, N. Bampos, N. Aboitiz, J. Jiminez-Barbero, M. Lopez de la Paz, J.K.M. Sanders, P. Carmona & C. Vicent, *Eur. J. Org. Chem.*, (2002), 1925.

[5] I. Idziak, A. Benrebouh & F. Deschamps, *Anal. Chim. Acta*, 435 (2001), 137.

[6] H.S. Andersson & I.A. Nicholls, *Bioorg. Chem.*, 25 (1997), 203.

[7] E. Kiehlmann, K. Biradha, K. V. Domasevitch & M. J. Zaworotko, *Can. J. Chem.*, 77 (1999), 1437.

[8] P.J. Hore, *Nuclear Magnetic Resonance*, (2002), Oxford University Press (Oxford), 48.

[9] D.S. Terekhov, K.J.M Nolan, C.R. McArthur & C.C. Leznoff, *J. Org. Chem.*, 61 (1996), 3034.

[10] P.L.Husykens, *J. Am. Chem. Soc.*, 99 (1977), 2578.

[11] H. Tsukube, H. Furuta, A. Odani, Y. Takeda, Y. Kudo, Y. Inoue, Y. Liu, H. Sakamoto & K. Kimura in Comprehensive Supramolecular Chemistry, 1st Ed. (1996), Pergamon (New York), vol. 8, 437.

[12] A. Katz & M.E. Davis, *Macromolecules*, 32 (1999), 4112.

[13] O. Brüggemann, *Biomolecular Engineering*, 18 (2001), 1.

[14] C. Lübke, M. Lübke, M.J. Whitcombe & E.N. Vulfson, *Macromolecules*, 33 (2000), 5098.

Chapter Four

The Rational Design of 2,4-D MIPs – Probing the Monomer-Template Complex and its Consequences for MIP Behaviour.

4.1 Abstract

The preparation of molecularly imprinted polymers (MIPs) based on non-covalent interactions has become a widely used technique for creating highly specific sorbent materials used in sensing applications and separation chemistry. A crucial factor in a successful imprinting protocol is the optimisation of the template/functional monomer interaction in the pre-polymerisation mixture, eventually leading to a maximum of high-affinity binding sites in the resulting polymer matrix. In order to develop more efficient preparation technologies for imprinted polymers, a pre-polymerisation system was examined using NMR spectroscopic techniques for identifying types of interactions occurring in the pre-polymerisation mixture, and their implications for the subsequently formed imprinted polymer. Hydrophobicity has been spectroscopically followed and its contribution to the imprinting effect has been examined. The anomalous 2,4-D imprint system (strong imprint achieved in highly polar solvent) is used as the basis for investigation of some fundamental aspects of MIP technology: specifically, what factors play a part in determining the success, or failure, of an imprinting protocol? How closely do pre-polymerisation phenomena correspond to final MIP properties?

4.2 Introduction

4.2.1 Elucidating the Mechanism of Recognition

The imprinted polymer matrix is created by the co-polymerisation of a functional monomer/template molecule complex with a crosslinking agent in the presence of a porogenic solvent. Although imprinting is frequently represented by an idealised schematic (such as in Fig. 1.1, Chapter 1), the implications of using the typical imprinting conditions necessary to achieve an imprinting effect mean that the reality of an imprinting procedure may in fact be more complicated. This is evident in the work of, for example, Shea and Sasaki[1] in examining the properties of mono- and diketone-imprinted MIPs via solid-phase spectroscopic techniques. When imprinting using a dialdehyde, a greater percentage of one-point binding was observed, which the authors attributed to poorly defined binding sites occurring in less accessible domains. The creation of binding sites of variable specificity/ affinity for the template molecule is frequently observed in MIP technology. Further evidence of binding site heterogeneity is presented by Umpleby and colleagues[2] in their work on mathematical models which describe the binding properties of MIPs. The Freundlich isotherm model is frequently used to accurately model the adsorption isotherms of non-covalently imprinted polymers. Having demonstrated the validity of applying this model (up to saturation levels of analyte), the authors note that an important implication of the Freundlich isotherm is that there is an exponential distribution of binding sites,

although this is usually simplified by classing binding sites into either 'low affinity' or 'high affinity'.

The origins of this deviation from the ideal MIP protocol (i.e. each template molecule results in the formation of a specific binding site) for non-covalent imprinting is most likely due to the necessity of using excess functional monomer to drive pre-polymerisation equilibrium in favour of complex formation. The simultaneous ordering of several solution-phase molecules which is required for successful complex formation is energetically demanding, due to the associated loss in entropy[3], necessitating excess monomer. However, too high a ratio of functional monomer to template will have the result of randomly distributed excess monomer groups in the final polymer network contributing to non-specific binding events.

Consequently, the formation of a sufficiently strong pre-polymerisation complex between the template molecule and the functional monomer species is critical to the subsequent recognition properties of the polymer. However, an optimum monomer-to-template ratio must be determined to avoid inducing high levels of non-specific binding. This complex can also be formed using covalent bonds, as described by Wulff[4]. However, this approach has the associated difficulties of finding a suitable monomer linking to the template molecule, and the necessity of using more aggressive extraction procedures to remove the template from the polymer matrix afterwards. Thus, the limited number of functional groups which

can reversibly undergo covalent bond formation and cleavage under mild conditions has inhibited development of this type of molecularly imprinted polymer, despite the inherent advantage of formation of well-defined binding sites.

Complexes formed by non-covalent interactions (hydrogen-bonding, electrostatic interactions, hydrophobic interactions, π–π aggregation) were first utilised for imprinting purposes by Mosbach[5], and have been exploited largely due to their greater versatility (refer to Chapter 1 for further discussion of applications of non-covalently imprinted MIPs). To improve the efficiency of non-covalently imprinted systems, a better understanding of the events governing the formation of the complexes at a molecular level is required. In this chapter, the utility of NMR spectroscopy as a suitable tool for probing the complexation process in the pre-polymerisation mixture is discussed. Promising results indicate that observing these molecular events at a fundamental level provides insight on the crucial first steps of non-covalent molecular imprinting and will lead to optimised synthetic conditions for the creation of non-covalently formed MIPs.

NMR spectroscopy has revealed much information on the mechanisms by which recognition occurs[6] and how an imprint is achieved, and has been used to characterise pre-polymerisation complexes based on hydrogen bonds or electrostatic interactions. Elegant studies by Quaglia and co-workers[7] have demonstrated the significance of hydrogen bonding in achieving imprinting

effects. Work by Whitcombe *et al.*[8] has also demonstrated how NMR studies of monomer-template dissociation constants can predict MIP binding capacity whereas UV spectroscopy has also proved invaluable in examining pre-polymerisation events[3]. In the study described here, a 2,4-dichlorophenoxyacetic acid (2,4-D)/4-vinylpyridine (4-VP) template-monomer system is examined in detail. The data obtained from NMR analysis of this system permits a more comprehensive view of the complexation events in the pre-polymerisation solution, and the subsequent impact on the recognition properties of the MIPs created from this system. In this study, the NMR experiments are used as a versatile tool in explaining the behaviour of MIPs successfully synthesised in earlier studies[9]. Of particular importance is the clear observation of a π–π stacking effect, imparting hydrophobic properties to the imprinted cavities of the subsequently formed polymer. The effects of temperature on the complexes are investigated with a view to determining how stable the complexes are with respect to the polymerisation process, where the free radical-rich environment poses a threat to complex integrity (and thus to the formation of high-affinity binding sites). However, since π–π stacking (also called *aggregation*) has not previously been observed via ^{1}H-NMR in a MIP system, it is necessary to first discuss the theoretical background.

4.2.2 Identifying Aggregation Effects

Aromatic proton shifts can be significantly affected by the contribution of the aromatic ring current[10] (*i* in Fig. 4.1). The circulation of electrons around the aromatic ring induces a small magnetic dipole (μ) that opposes the applied magnetic field of the spectrometer, B, along the plane perpendicular to the aromatic ring. Along the six-fold axis of the aromatic ring, the additional magnetic field produced by the current opposes the applied field, causing an upfield (from left to right on the spectrum ppm scale) shift which is noticeable in the signals of protons that lie either above or below the plane of the benzene ring. The protons of the benzene ring are shifted downfield as a result of the ring current. It is for this reason that aromatic protons are generally found at a lower-field shift (7-8ppm) than protons attached to vinylic carbons, despite the similar sp^2 hybridisation of the molecular orbitals in both cases.

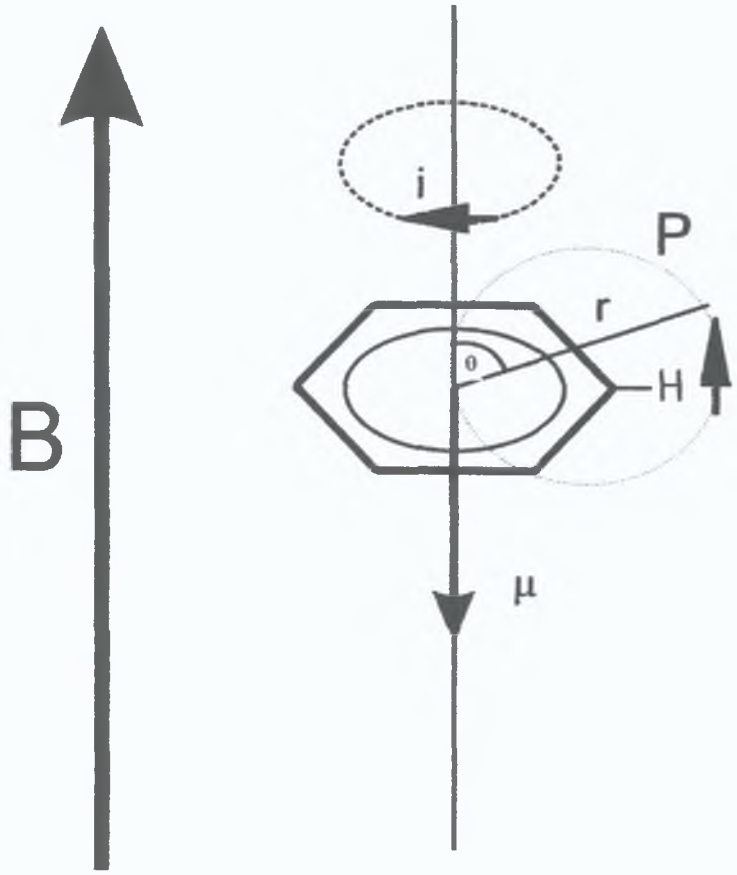

Figure 4.1 - The magnetic field effects experienced by an aromatic proton. From ref. 10.

This effect is noticeable in molecules that undergo π–π-stacking, and is evident in the below example of *[10]*-paracyclophane, where the chemical shift of the methylene protons reflects their positions with respect to the aromatic ring, those directly above the ring being affected the most (see Figure 4.2).

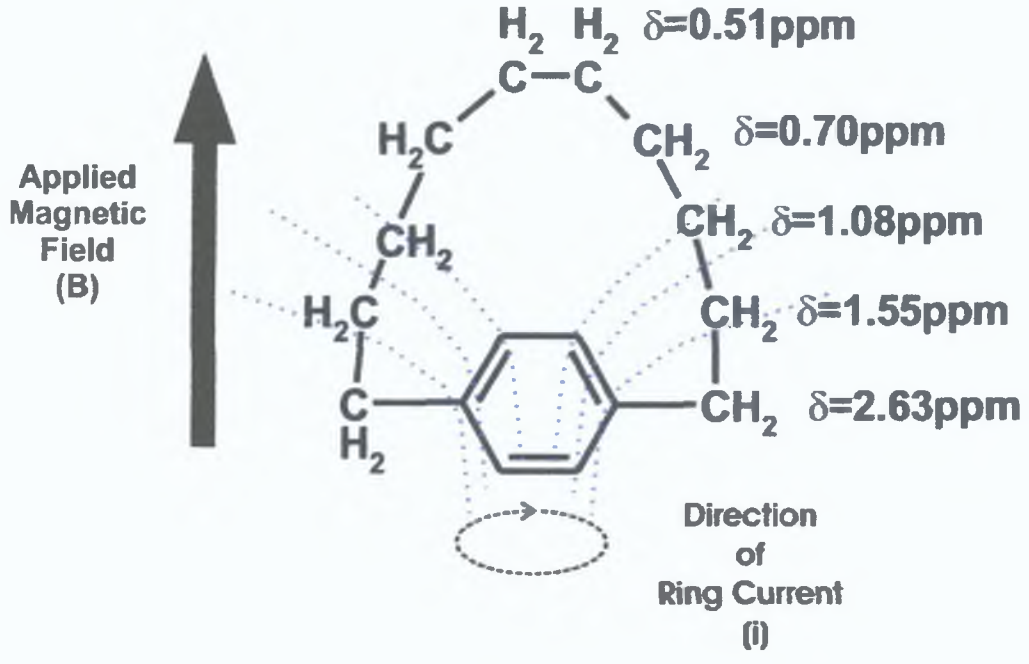

Figure 4.2 - Aromatic ring current effects on methylene protons in [10]-Paracyclophane (from reference 10). Magnetic field indicated by broken blue lines.

Thus, protons which have a close proximity to an aromatic system will experience the effects of the magnetic field with consequential changes in the observed chemical shifts. This phenomenon is common in supramolecular chemistry[11].

4.3 Materials

All chemicals were purchased from Sigma-Aldrich (Dublin, Ireland and Milwaukee, WI, USA). Solvents used (excluding deuterated solvents) were of HPLC grade and supplied by Labscan (Stillorgan, Dublin, Ireland). 4-Vinylpyridine, methacrylic acid and ethylene glycol dimethacrylate were vacuum distilled prior to use to remove inhibitors. Solvents used for NMR analysis were deuterium oxide, deuterated pyridine and deuterated chloroform (99.9%) and used as supplied. Solvents used for LC investigation were of HPLC grade and obtained from Burdick & Jackson (Muskegon, MI, USA).

4.4 Experimental

4.4.1 MIP Preparation

The MIPs used in this study were synthesised as described previously[9] and analysed as described in the following section. A template: monomer: crosslinker ratio of 1:4:20 was employed, as described in the literature. For each polymer synthesised, an identical blank (control) polymer was also made – of identical composition but excluding the template molecule. Thus, MIPs were synthesised using 5 cm^3 of solvent (4:1 MeOH/H_2O), 20 mmol of EGDMA as crosslinker (2.763 cm^3), 0.31 mmol of azobisisobutyronitrile as initiator (0.051 g) and 4 mmol of 4-vinylpyridine as monomer (0.429 cm^3). Both thermal and UV polymerisation was carried out; the nature of the MIPs described here are outlined in Table 4.1. Prior to polymerisation, MIP mixtures were placed in a glass tube and sonicated for 5 minutes to remove any dissolved oxygen. For thermal polymerisation, the polymerisation mixture was placed in a water bath at 45°C overnight. For UV polymerisation, an identical polymer composition was used. The UV lamp was set to a long wavelength (365 nm) and the set-up was placed in an aluminium foil-lined cardboard box.

Thermal polymerisation		**UV polymerisation**	
MIP	Blank	MIP	Blank
D1	D2	D5	D6

Table 4.1 – MIPs prepared for chromatographic characterisation.

The polymer monoliths produced by the process were then removed from the glass vials and broken up with a mortar and pestle. As described in Chapter 3, the fragments of polymer were then ground for 2-3 minutes in an electric grinder and wet-sieved to obtain particles of less than 25 μm in size. The particles were then sedimented 4-5 times in 250 cm^3 acetone, to remove fine particles of less than 5μm in size. The particles within the 5-25 μm size limit were then mechanically slurry packed into an empty 15 x 4.6 mm i.d. HPLC column for characterisation.

4.4.2 Characterisation of Molecularly Imprinted Polymers for 2,4-D

Literature studies referred to in this Chapter characterised MIPs for 2,4-dichlorophenoxyacetic acid using thin films coated onto the surface of attenuated total (ATR) reflection crystals and investigated via Fourier transform infrared (FT-IR) evanescent field spectroscopy. Also, radioligand binding assays were used to confirm selective retention of the imprint molecule[9]. For HPLC characterisation used in this study, the MIP (and blank polymer) columns were packed as described above. The UV/Vis bands used for identification were 232 nm and 283 nm (see Fig. 4.3). Columns were conditioned using methanol/ acetic acid (12%) until a stable baseline was achieved. The mobile phase used for characterisation was acetonitrile/ acetic acid (1%), at a flow rate of 1ml/min. For performance evaluation, the 2,4-D analogues shown in Fig.4.4 were used, all at a

concentration of 0.0025 g/l. Acetone was used as void marker. The properties of the MIP were evaluated as in Chapter 3.

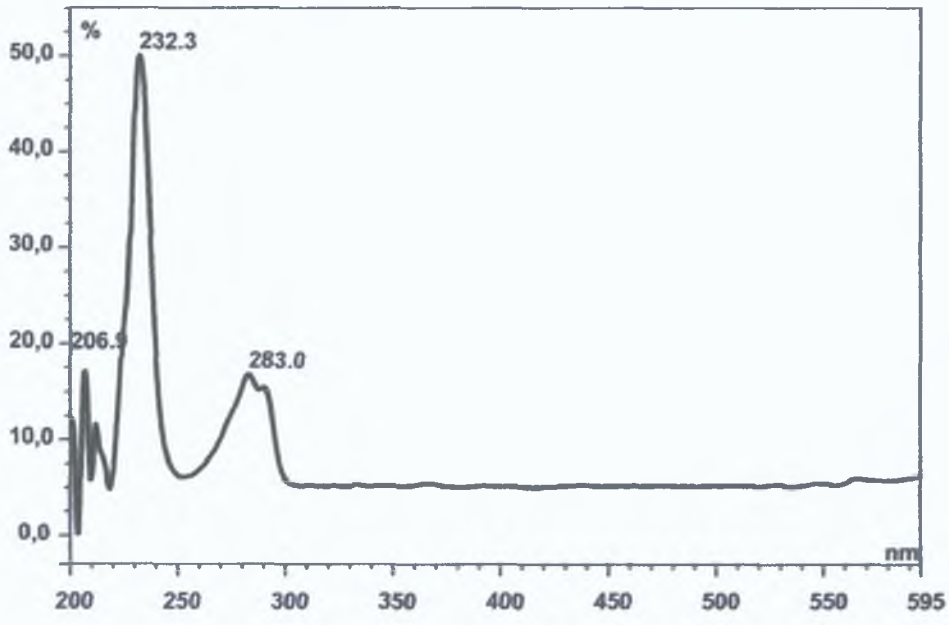

Fig. 4.3 – UV/Vis spectrum of 2,4-D, showing two main absorption bands suitable for use in chromatographic evaluation.

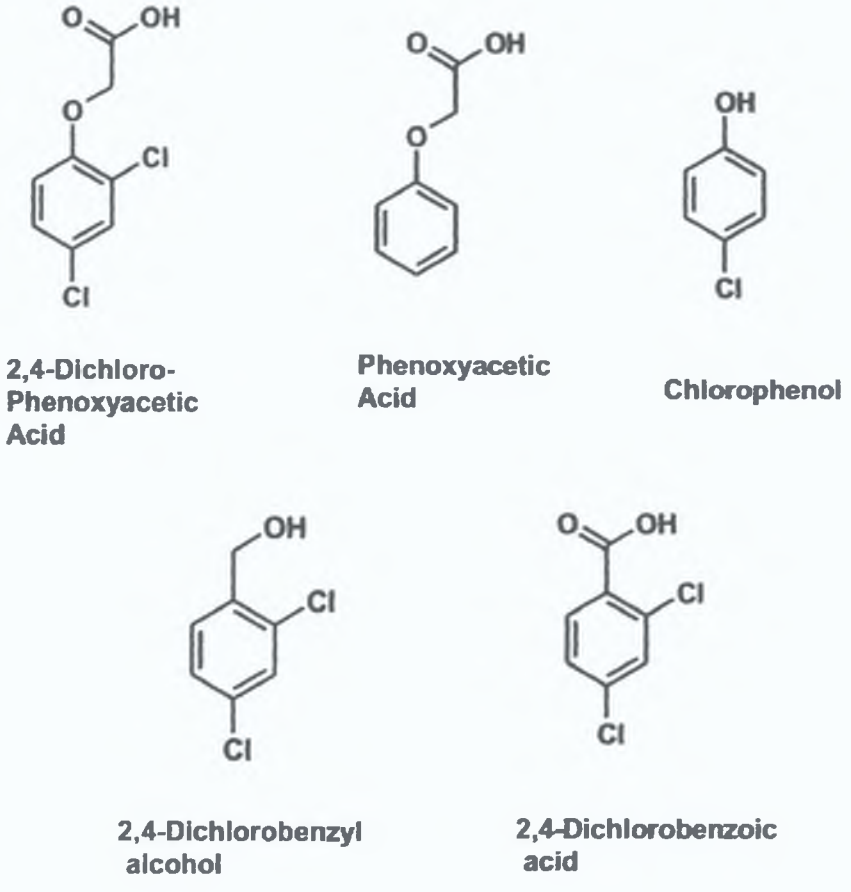

Fig. 4.4 – Compounds used in chromatographic characterisation.

4.4.3 NMR Analysis

NMR spectra for Section 4.5.1 were recorded on a Bruker AVANCE 400 MHz NMR spectrometer (Bruker Biospin UK) at 25°C. Chemical shifts are referenced to the solvent reference signal. Deuterated chloroform was analysed via NMR prior to use to ensure the absence of water. Complex stoichiometry was determined by Job's plot analysis, wherein the ratios of monomer and template are systematically varied (between 0:1 to 8:1) using equimolar solutions (0.04M), with a constant sample volume of 0.75 cm^3. Complex concentration was calculated as :

$$[complex] = [template]_{tot} \cdot (\delta_{obs} - \delta_{template}) / (\delta_{complex} - \delta_{template})$$

where $[template]_{tot}$ is the total template concentration, $\delta_{template}$ is the shift of the free template molecule, $\delta_{complex}$ is the chemical shift of the complex and δ_{obs} is the observed chemical shift. Association constants were determined differently, maintaining a constant amount of template and titrating increasing amounts of functional monomer, beginning with a 0.04 M concentration of template and titrating from 1 up to 20 equivalents of monomer. The association constants were then calculated using the mathematical model described by Atwood[12] to calculate association constants in weak complexes based on changes in observed NMR signal shifts, which in this case is:

$$\delta_{OBS} = \delta_{template} + \delta_{template}-\delta_{complex}/2[Monomer]_0\{[Monomer]_0 + [Template]_0 + 1/K - \sqrt{(([Monomer]_0+[Template]_0+1/K)^2 - 4\,[Monomer]_0\,[Template]_0)}$$

Additional variables are: $[Monomer]_0$ is the total monomer concentration, $[Template]_0$ is the total template concentration and K is the association constant. Dilution experiments were also performed to preclude self-association effects within the titrations. The dimerisation constant of butyric acid was determined to be 80 M^{-1} by Lancelot[13], suggesting that dimerisation of 2,4-D occurs at the concentrations used in these experiments and thus the association constant for the acid-base titration was in fact higher than measured. This has been neglected for consideration in this primarily qualitative study into the nature of the PPC. For the aromatic protons, an upfield shift of less than 0.003 ppm was observed upon increasing 2,4-D concentration from 0.0002 M to 0.02 M, suggesting self-stacking effects are negligible also.

NMR Spectra for Section 4.5.2 were performed on a Varian Gemini 300MHz spectrometer, at the temperatures described in Section 4.5.2. The spectrometer was allowed to equilibrate for 1 minute after each change in temperature prior to initiating the recording of spectra. 16 scans were taken for each sample, and deuterated chloroform and D_2O, as described above, were used as solvent. Measurement of association constants was performed via non-linear regression[16], using the software package OriginPro 7.0 (OriginLab Software, MA, USA). Samples for the ionic interaction measurements were performed as

described above for the Job's plot analysis (i.e. method of continuous variation, with an initial concentration of 0.04 M and a volume of 0.75 cm^3 for each sample). This was repeated for the hydrophobicity measurements; however, due to the nature of the shift, which is comparatively small, it was necessary to repeat it using the mole ratio method, with 11 samples measured (1:0 2,4-D/Pyr-d_5 up to 1:20), and increasing the initial concentration of analytes to 1 M to enhance the spectral signals. The determination of association constants for this interaction could not be performed using the equation described by Atwood for weak interactions (see above). This equation is sufficient only for determining association constants of self-associating systems or 1:1 interactions. For the evaluation of the higher order association constant in the π–π stacking interaction, a 2-site binding system is assumed and a Hill-type binding plot was used (GraphPad Software).

4.5 Results & Discussion

4.5.1. ^{1}H-NMR Analysis of Pre-polymerisation Mixture

Prompted by the intriguing results of the *quercetin* MIP investigation, this work began with an examination of the 2,4-D MIP pre-polymerisation mixture, to explore how interactions which could be observed at this stage have implications for the final polymer, and explain the recognition properties described above.

Given that the MIPs in this study were synthesised in a methanol/water mixture, the nature of the interactions at the binding sites was unlikely to be hydrogen bonding. A ^{1}H-NMR titration study of the system reveals that the primary interaction is based on electrostatic effects (Fig. 4.5), with the basic pyridine molecule and acidic 2,4-D molecule forming an ionic pair.

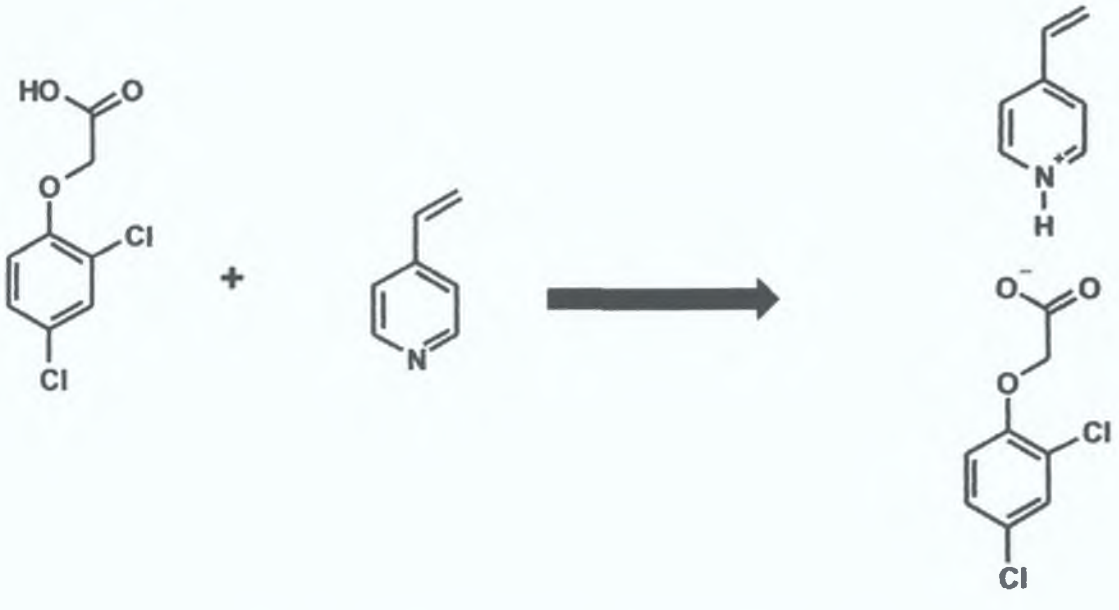

Fig.4.5 – Formation of the 2,4-D/4-VP ion pair.

Note that in these experiments, 4-VP was substituted with deuterated pyridine (pyr-d_5) to facilitate observation of aromatic proton shifts. The following study was performed in non-polar solvent (deuterated chloroform), since observations of such interactions in polar protic media such as methanol are difficult due to fast exchanges between labile protons of the analyte and solvent deuterium atoms[10]. The signal of the acidic proton of the carboxylic acid strongly migrates upfield as the titration progresses in favour of a higher 4-VP concentration as the 4-VP in solution increasingly becomes protonated (Fig. 4.6 and 4.7). The Job's plot of the interaction indicates the expected 1:1 template/monomer stoichiometry (see Fig.4.7), and the association constant was determined to be 172 M^{-1}.

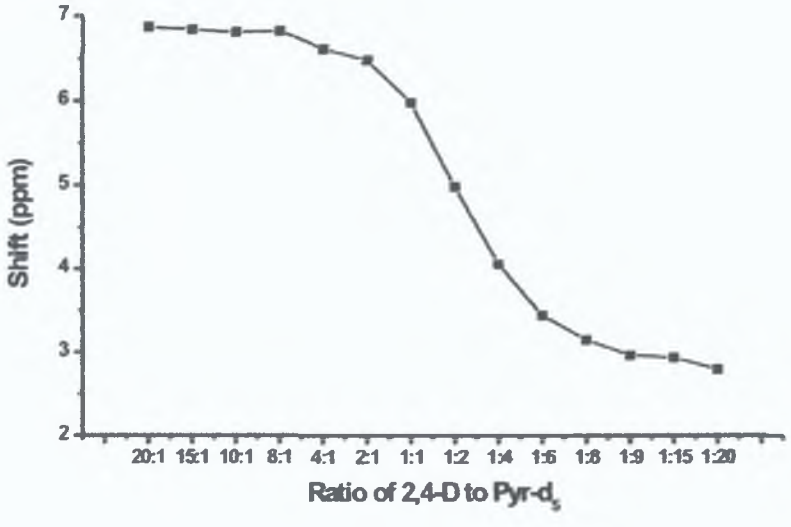

Fig.4.6 - Observed Shift of pyridinium proton in $CDCl_3$ (^{1}H-NMR at 25°C, 16 Scans). The curve is calculated for a K_a of 172 M^{-1}, and a $\delta_{complex}$ of 2.8ppm.

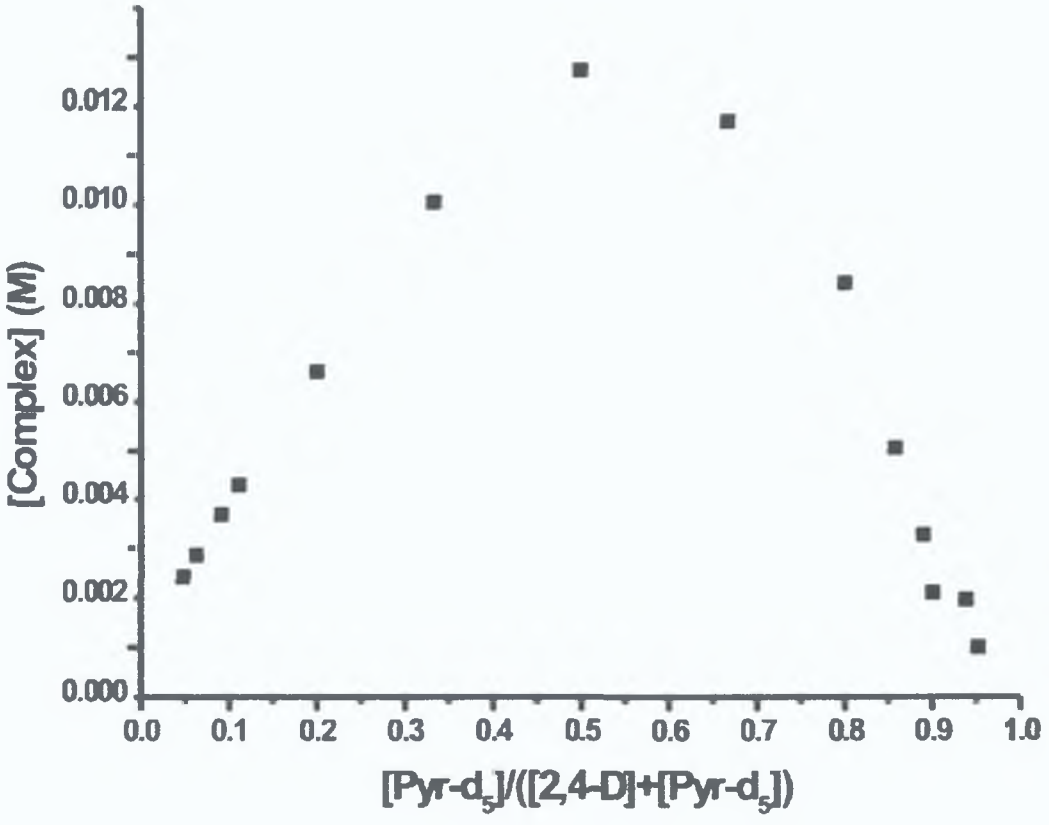

Fig. 4.7 - Job's Plot of 2,4-D/Pyridine-d_5 ionic interaction in $CDCl_3$

(^{1}H-NMR at 25°C, 16 Scans)

However, a simple one-point binding does not adequately explain the selectivity observed in this MIP, necessitating further investigation to identify other possible sources of selectivity, i.e. to determine the exact nature of the binding sites.

In the past, NMR studies have been used by the Mosbach group to investigate complex formation[6]. These studies entail the observation of peaks in the proton spectrum during a titration for any changes in peak width. As different complexes in the mixture reach equilibrium, a slow exchange of equivalent protons between the complexes causes *their* signal to broaden. A plot of peak width against molar ratio of one of the constituents of the titration mixture thus indicates complex stoichiometry. Applying this to the 2,4-D/4-VP system discussed here, the formation of three complexes is observed, described by three maxima, as indicated in Fig. 4.8 and 4.9.

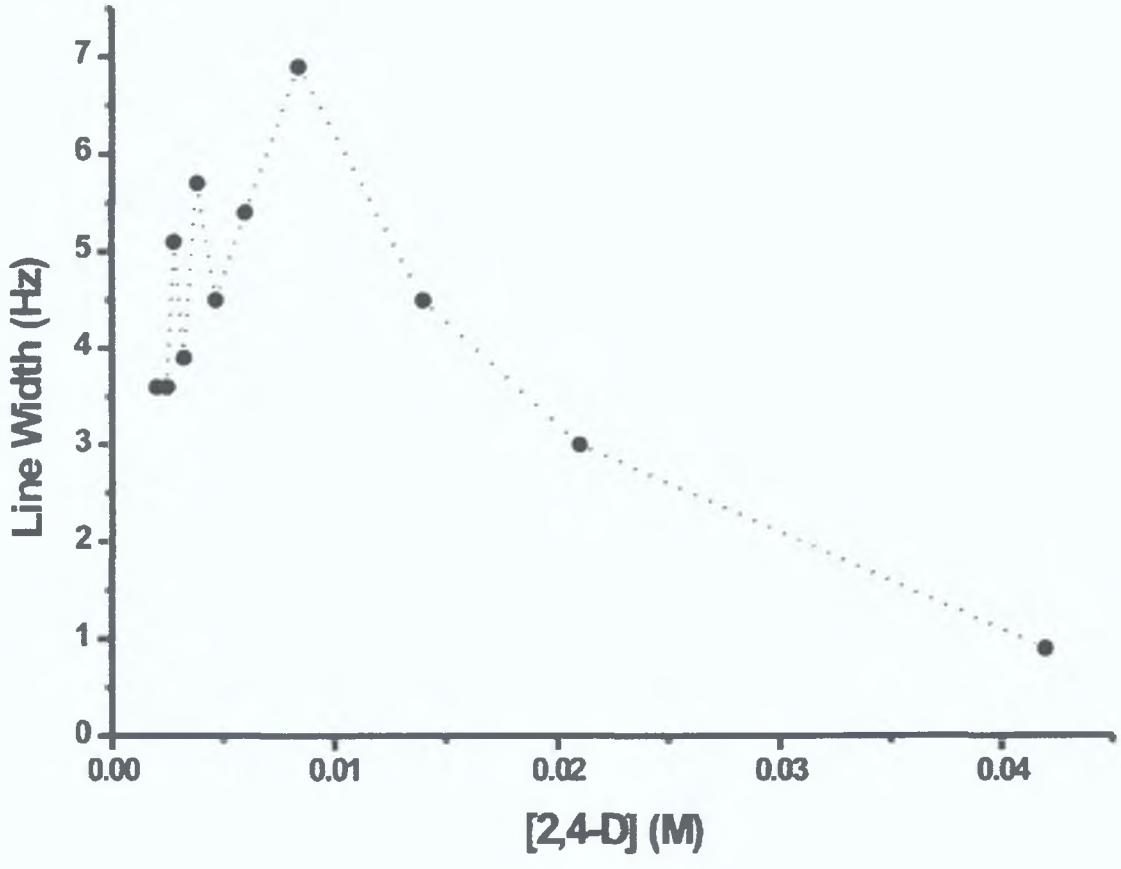

Fig. 4.8 - NMR line width experiment (2,4-D vs. 4-VP titration in $CDCl_3$): exchangeable acid proton (^{1}H-NMR at 25°C, 16 Scans).

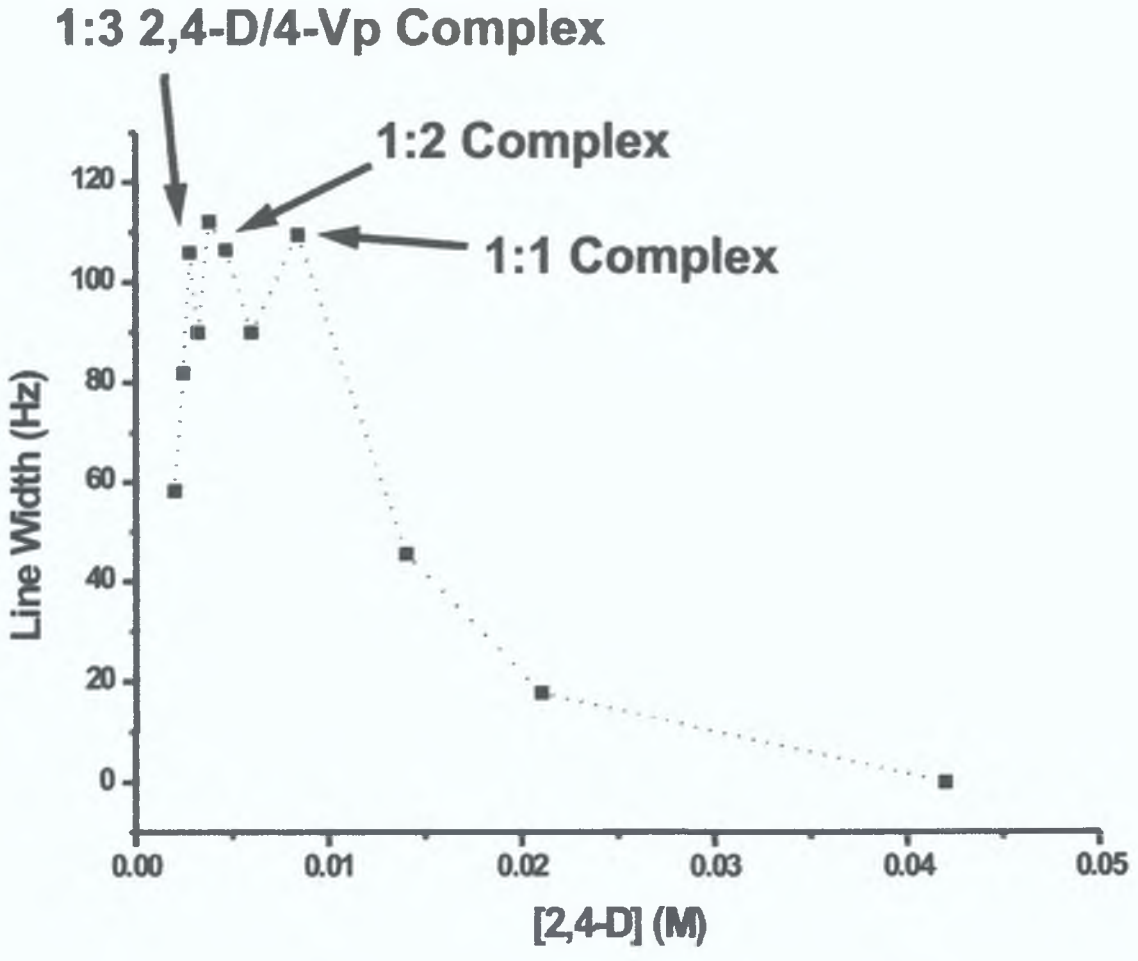

Fig. 4.9- NMR line width experiment (2,4-D vs. 4-VP titration in $CDCl_3$): vinyl methylene protons (^{1}H-NMR at 25°C, 16 Scans)

The three maxima are ascribed to the formation of the 1:1 complex ([2,4-D] ⇔ [(2,4-D/4-VP)]), the 1:2 complex ([(2,4-D/4-VP)] ⇔ [(2,4-D/$(4\text{-VP})_2$)]) and the 1:3 complex ([(2,4-D/$(4\text{-VP})_2$)] ⇔ [(2,4-D/$(4\text{-VP})_3$)]). It can be postulated that the interaction causing the formation of the latter two complexes may be a result a $\pi-\pi$ stacking effect. It may also be concluded that since both H-bonding and electrostatic interactions can be excluded in this instance, given that there are no

other possible points of electrostatic interaction and H-bonding available. Furthermore, the aromatic nature of both the template and functional monomer certainly offer the opportunity for such interactions.

Aromatic protons are usually found downfield of vinylic protons, due to the deshielding effect of the ring current of the aromatic ring, which contributes to the magnetic field experienced by protons located in the plane of the aromatic ring. However, above and below the ring, the extra magnetic field produced by the ring current opposes the applied magnetic field, causing protons interacting with this field to resonate further upfield[10]. Hence, when the aromatic protons of 2,4-D participate in a π–π stacking interaction, an upfield shift is observed as aggregated oligomers form in solution (see Fig. 4.10). A Job's plot of this interaction (see Fig. 4.11) shows a maximum at 0.75/0.8, suggesting a 1:3 (template: monomer) complex (and possibly a higher order complex) is being formed. As pyridine-d_5 is added in increasingly large quantities, the upfield shift continues, as the anisotropic disk effect becomes amplified by a "solvent changing" effect. The large excess of pyridine-d_5 means that the 2,4-D molecules are mostly solvated by pyridine-d_5, rather than D_2O. Thus, it is expected that beyond the scale indicated in Fig. 4.10, continued shift would be observed.

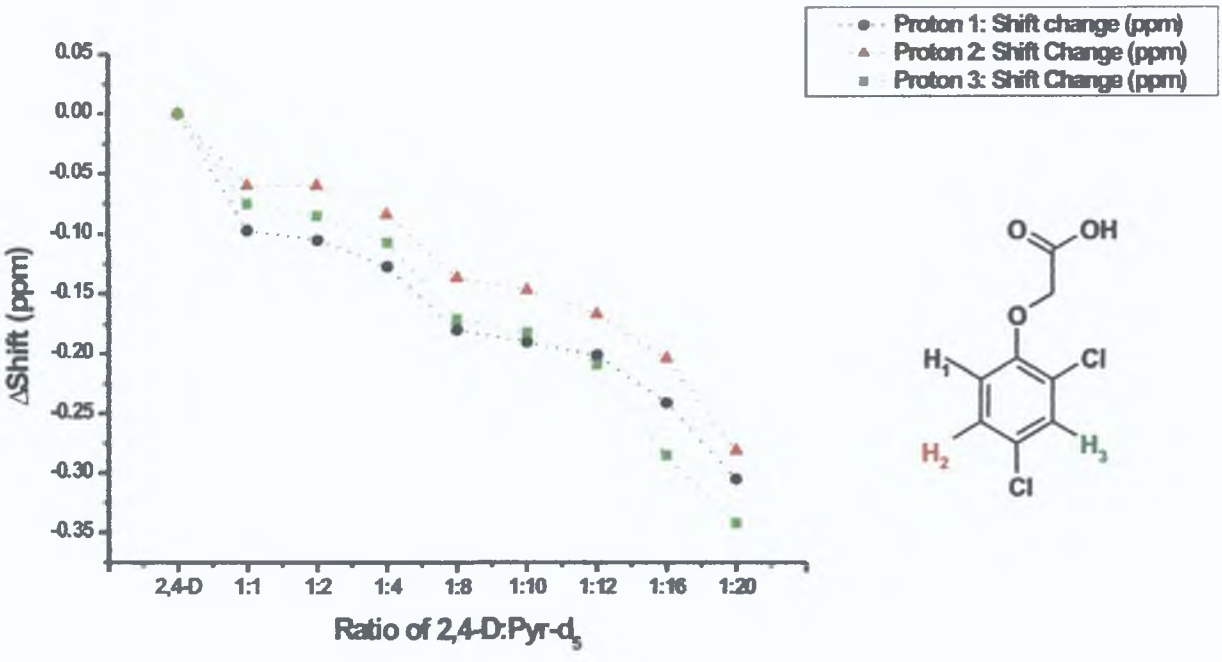

Fig. 4.10 - 2,4-D/Pyr-d_5 titration: shift of aromatic protons of 2,4-D in D_2O (^{1}H-NMR at 25°C, 16 Scans). The curve is calculated for a K_a of 22.86 M^{-1}, and a $\delta_{complex}$ of 6.58 ppm.

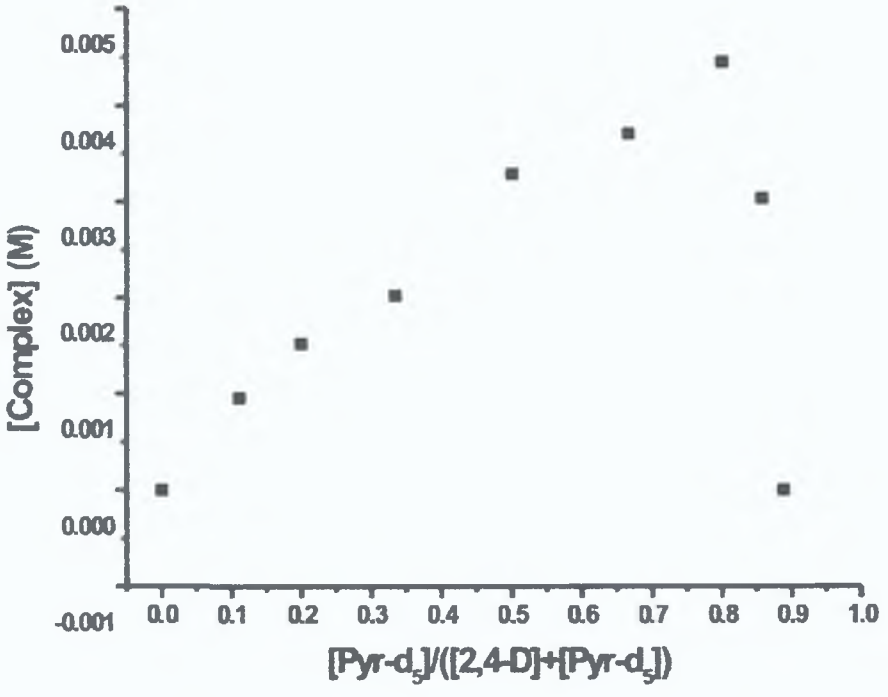

Fig. 4.11 - Job's Plot of 2,4-D/Pyridine-d_5 hydrophobic interaction (in D_2O).

(^{1}H-NMR at 25°C, 16 Scans).

This aggregation occurs as a result of hydrophobicity/ $\pi-\pi$ stacking. In order to reduce the total surface area of hydrocarbon exposed to aqueous media[14], the system 'stacks' the aromatic molecules, thereby decreasing this area. We conclude that this effect provides grounds for successful molecular imprinting in a polar methanol/water mixture. The additional stabilisation caused by stacking was determined to be K_a=22.86 M^{-1}. A control experiment was performed in a non-polar solvent (chloroform), and only slight changes in the aromatic proton shifts were observed (see Fig. 4.12). Without the hydrophobic phenomena induced by an aqueous environment, the added complex stability contributed by $\pi-\pi$ stacking is lost, and only an ionic interaction is observed - and as explained by Wulff[4], a simple one-point interaction is insufficient to create specific *binding* sites.

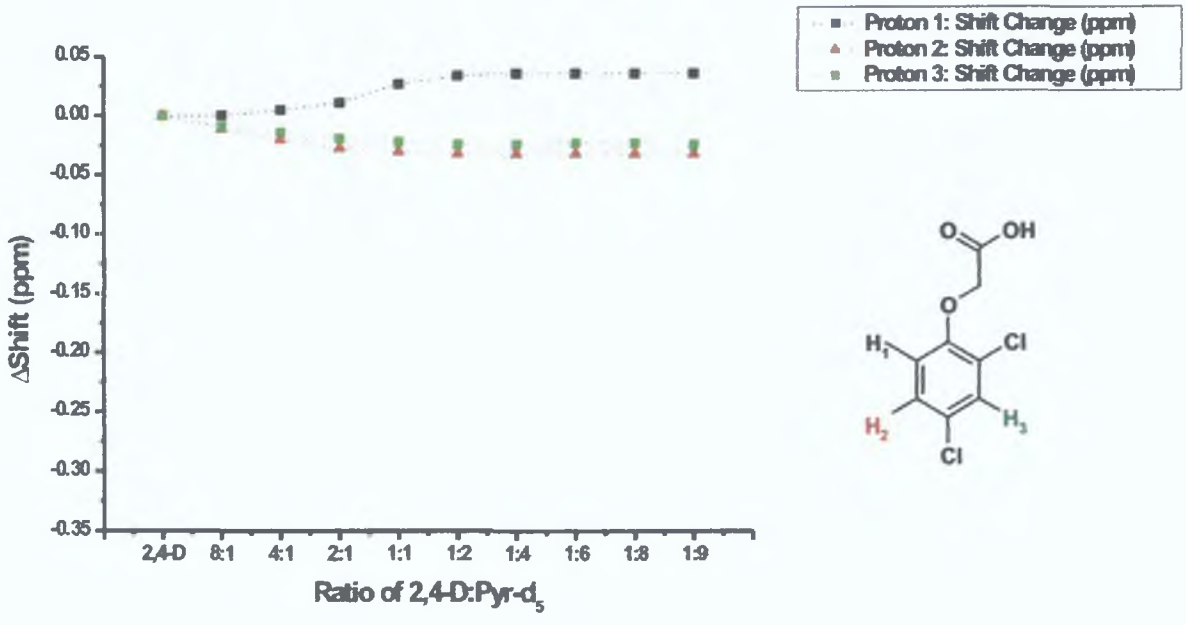

Fig.4.12 - 2,4-D/Pyr-d_5 titration: shift of aromatic protons of 2,4-D in $CDCl_3$ (^{1}H-NMR at 25°C, 16 Scans).

The NMR evidence suggests that the complex formed in solution is based primarily on electrostatic interactions, which are further stabilised by secondary aggregation of aromatic components. This permits us to propose a possible 3:1 4-VP/2,4-D complex existing in solution prior to polymerisation (see Fig. 4.13). However, as results from molecular modelling in Chapter 5 demonstrate, and has been reported in the literature[15], aromatic-aromatic interactions may adopt a number of orientations from offset face-to-face to edge-to face, and the model below represents but one of these possible configurations.

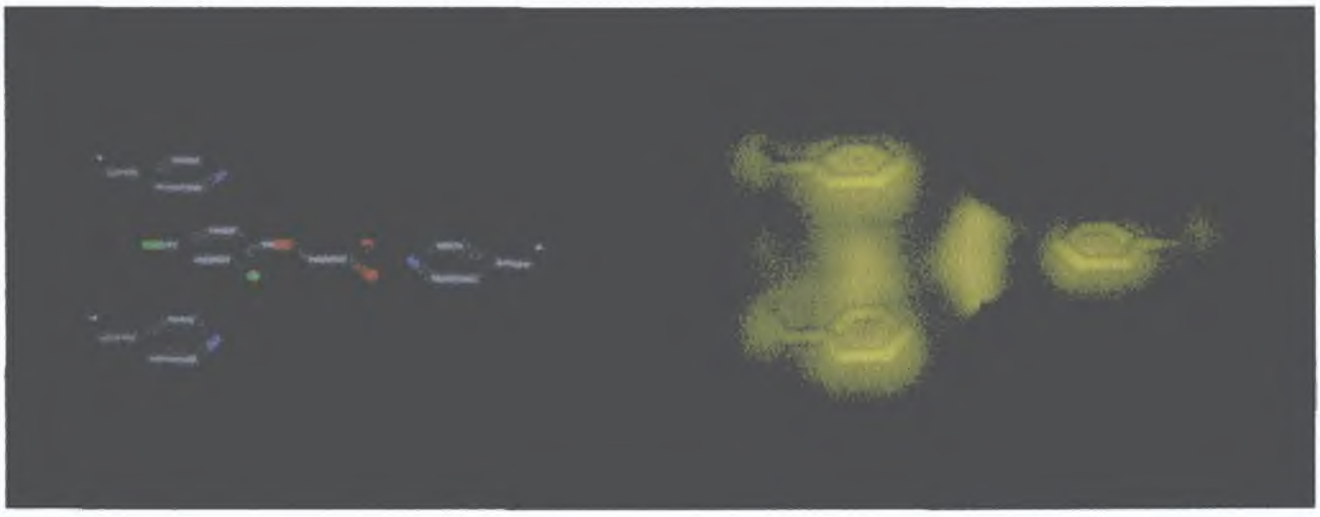

Fig. 4.13 - Proposed conformation of 3:1 4-VP:2,4-D complex formed, and of resultant cavity formed in the MIP (showing offset face-to-face orientation). Structures drawn in MDL ISIS/Draw 2.5; 3-D representations developed using Accelrys ViewerLite 4.2 and rendered using POV-Ray 3.5.

4.5.2 ^{1}H-NMR Thermal Study of Pre-Polymerisation Mixture

4.5.2.1. Investigation of Effect of Temperature on Ionic Interaction

Following earlier studies of the 2,4-D/ 4-VP pre-polymerisation complex which indicated ionic effects and hydrophobic interactions cooperatively stabilizing the complex, a temperature control study was performed on the system to examine the effects which a thermally-induced polymerization would have. With non-covalent complexes, such as the 2,4-D/4-VP complex being investigated here, the lower stability, relative to analogous complexes constructed with covalent bonds, mean that thermal effects may adversely affect complex integrity. Thus, establishing whether the complex is stable across the temperature range of polymerisation, typically up to 60°C, permits the researcher to choose between a typical thermally-initiated polymerisation, or a low-temperature UV-initiated protocol. The temperature range chosen was ambient (20°C) up to polymerization temperature (60°C), with ten-degree intervals.

The primary ionic interaction was examined first, using a non-polar solvent (chloroform) to avoid the possibility of proton exchange concealing the location of the 2,4-D acid proton signal which is indicative of this interaction. The titration was performed as before, across a range of monomer-template ratios (see Fig. 4.14). The main implication of this experiment is that during the polymerisation, ion-pair complex stability is not significantly compromised by thermal effects,

despite literature evidence of ionic interactions experiencing greater stability at lower temperatures[14].

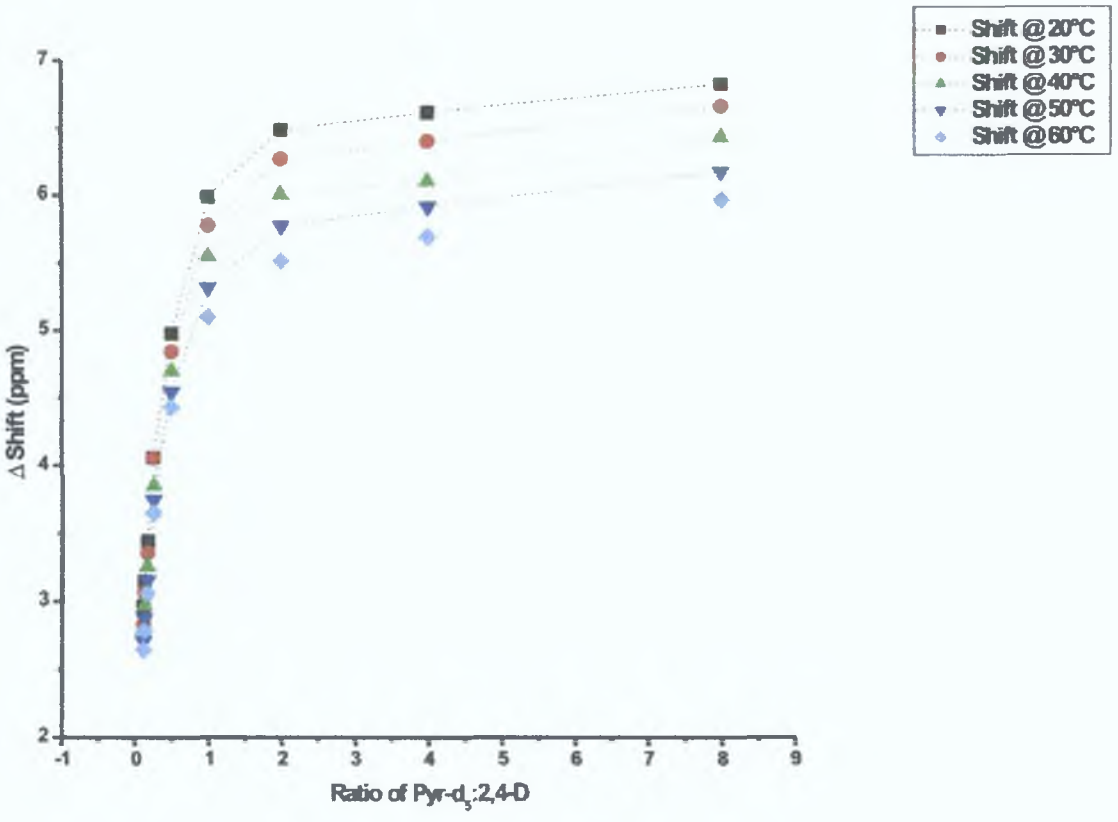

Fig. 4.14 – Temperature control 2,4-D/Pyr-d_5 titration: shift of acidic proton of 2,4-D in $CDCl_3$ (^{1}H-NMR, 16 Scans).

As demonstrated by the work of Snellink-Ruël *et al.*[16] on developing synthetic anion receptors, non-linear regression curve fitting can reveal the extent of complexation in terms of association constant. Job's plots have indicated that the expected 1:1 complex forms between the acid and base, and so a Hill-type binding plot can be utilised here, once stoichiometry has been established. The

individual temperature analyses, together with fitted curves, are displayed in Fig. 4.15, and Table 4.2 indicates the consequential change in association constant . Hill-type plots are primarily used in biochemistry to interpret the binding behaviour of proteins[17], with multiple-site binding models offering a versatile tool for the investigation of association constants. However, with a basic 1:1 interaction as is present here, the model is relatively simple. It is described by:

$$Y=B_{max}*(X/(X+K_D))$$

Y= Ratio of the total number of X molecules bound to the total number of binding sites, also called the average binding number.

B_{max}= Receptor density, in this case defined as a measure of the degree of accessibility of Pyr-d_5 for the ligand 2,4-D.

X= Concentration of ligand– in this study, we examine 2,4-D as ligand of interest.

K_D= Dissociation constant for complex. The final value of K_A is yielded from $1/K_D$.

As is evident from these figures, temperature does not adversely affect complex stability, as has been shown in previous studies[18]. This equilibrium is pushed in favour of complex formation by the increase in temperature, by approximately 9.78%. This again highlights that it is not possible to establish a set of generic rules in the development of MIPs, (such as ionic interaction-driven recognition mechanisms are enhanced by lower temperature conditions), but rather that it is imperative to evaluate each system individually to optimise interactions. However, the recognition mechanism in the 2,4-D MIP is a result of concerted hydrophobic and ionic interactions; thus the next step was to examine the effect of increased temperature on the hydrophobic interaction.

Temp (°C)	K_A (M^{-1})	R^2 Value
20	171.53	0.99315
30	174.22	0.99489
40	178.89	0.99385
50	182.48	0.99461
60	188.32	0.99489

Table 4.2 - Variation of 2,4-D/Pyr-d_5 ionic interaction association constant with increasing temperature, with R^2 value for fitted regression curve.

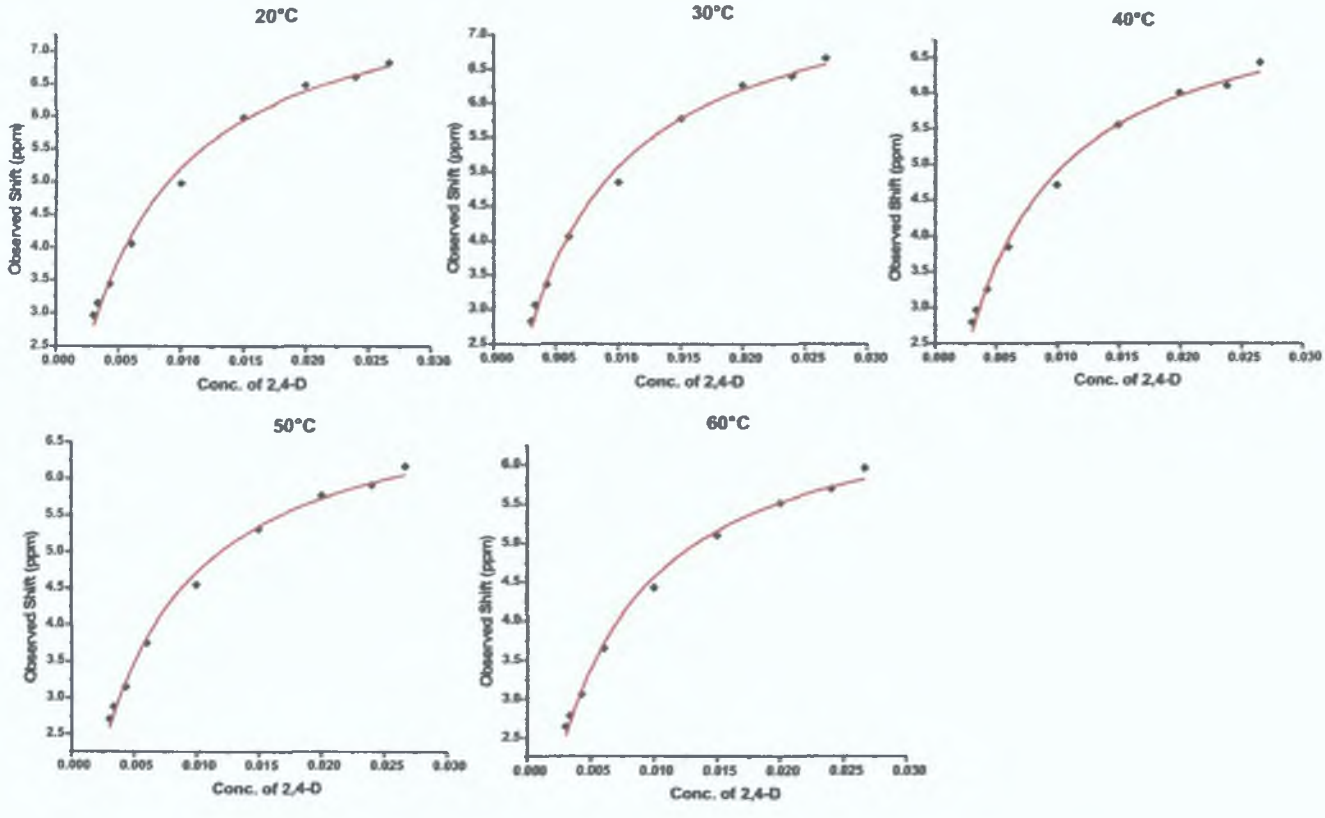

Fig. 4.15 – Relative shifts & fitted non-linear regression curves during variable-temperature titration study (2,4-D & Pyr-d_5 in $CDCl_3$).

4.5.2.2 Investigation of Effect of Temperature on Hydrophobic Interaction

The effects of temperature on hydrophobicity are another critical consideration for the creation of an effective imprinting effect – if changes in enthalpy impede hydrophobic effects, then the remaining ionic one-point interaction will result in poor selectivity. Hydrophobicity is entropically favourable at room temperature, as the energy penalty caused by the ordering of molecules to form complexes is compensated by the increase in entropy due to the release of ordered water molecules from hydrocarbon surfaces which are accessible before binding, but not afterwards[14]. However, due to the weak nature of such aggregation interactions (the contribution to stability given by π–π stacking is of the order of only 5-10KJ/mol)[19], they are typically sensitive to temperature. Indeed, the tendency of temperature to disrupt the type of weak non-covalent interactions found in biochemical systems is a significant factor in the observed temperature sensitivity of biological recognition systems. Bearing these considerations in mind, the π–π stacking observed in the 2,4-D/Pyr-d_5 in aqueous solvent system was examined to shed light on the effects of using thermal polymerisation on these PPCs. The results of this analysis are described in Table 4.3.

Temp (°C)	K_A (M^{-1})
20	45.717

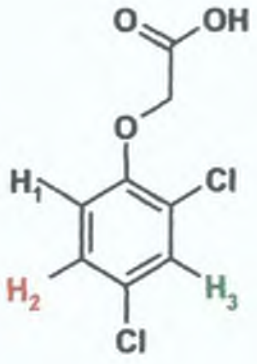

Table 4.3 – Effect of temperature on ^{1}H-NMR-observed hydrophobicity effect; aromatic proton 2 arbitrarily chosen for observation.

Applying the Hill-type 2-site binding plot for higher temperatures, a fitted curve could not be applied, suggesting a change in the complexes – most likely the effect of increased temperature disrupting the π–π stacking, though this cannot be conclusively determined here. Coupled with the increase in strength of the ionic interaction, one would thus expect to see a higher capacity, but lower specificity, in 2,4-D MIPs prepared thermally, compared to their UV-polymerised (i.e. low temperature) counterparts.

No direct conclusions about molecular-level events during polymerisation can be drawn on the basis of these experiments, as such NMR analyses are intended only as an aid to the researcher in designing a MIP and altering experimental variables. As a representation of the actual system during polymerisation, it is highly simplified. In an actual polymerisation mixture, both initiator and crosslinker are included. Although the crosslinker has not been observed to

disrupt monomer-template complexes significantly[3] via competition, because it is typically added in large excesses, it can contribute to macroscopic effects such as phase-partition phenomena, and so indirectly affect complex stability. This is pertinent in that while one can observe relative increases or decreases in complex stability via ^{1}H-NMR, these effects may not have the same relevance to the actual polymerisation mixture, where changes in the polarity caused by the crosslinker may exaggerate or negate them. The phenomenon of macroscopic phase separation in MIP preparations, as first described by Katz and Davis[20], is clearly evident in this system – see Figure 4.16. Thus, these experiments present direct evidence of the effects which dominate polymer recognition commencing in the pre-polymerisation mixture, but further experimentation would be required to quantify these effects with any degree of accuracy.

Figure 4.16 – Pre-polymerisation mixtures of 2,4-D MIPs in water/ methanol (i) and chloroform (ii). Greater 'clustering' of complexes is evident in mixture (i) – the photo on the right shows both mixtures after heating to 60°C in a water bath for 15 minutes.

Having thus examined the nature of the pre-polymerisation mixtures, the final step was to examine whether the effects of temperature on the PPCs evident in the ^{1}H-NMR studies, the final step was to explore whether similar behaviour could be observed in the final imprinted polymer material, via a chromatographic investigation.

4.5.3. 2,4-D MIP Properties – Chromatographic Evaluation

The composition of the imprinted polymers was derived from earlier work and the polymerisation, for both types of MIP, was performed as described in the experimental section, using both UV radiation and thermal energy to initiate the radical co-polymerisation, with the principal distinction being the temperature at which they were performed – ambient temperature (~21°C) for the UV MIPs and 45°C for the thermal MIPs. Chromatograms from the analyses are shown in Figure 4.17.

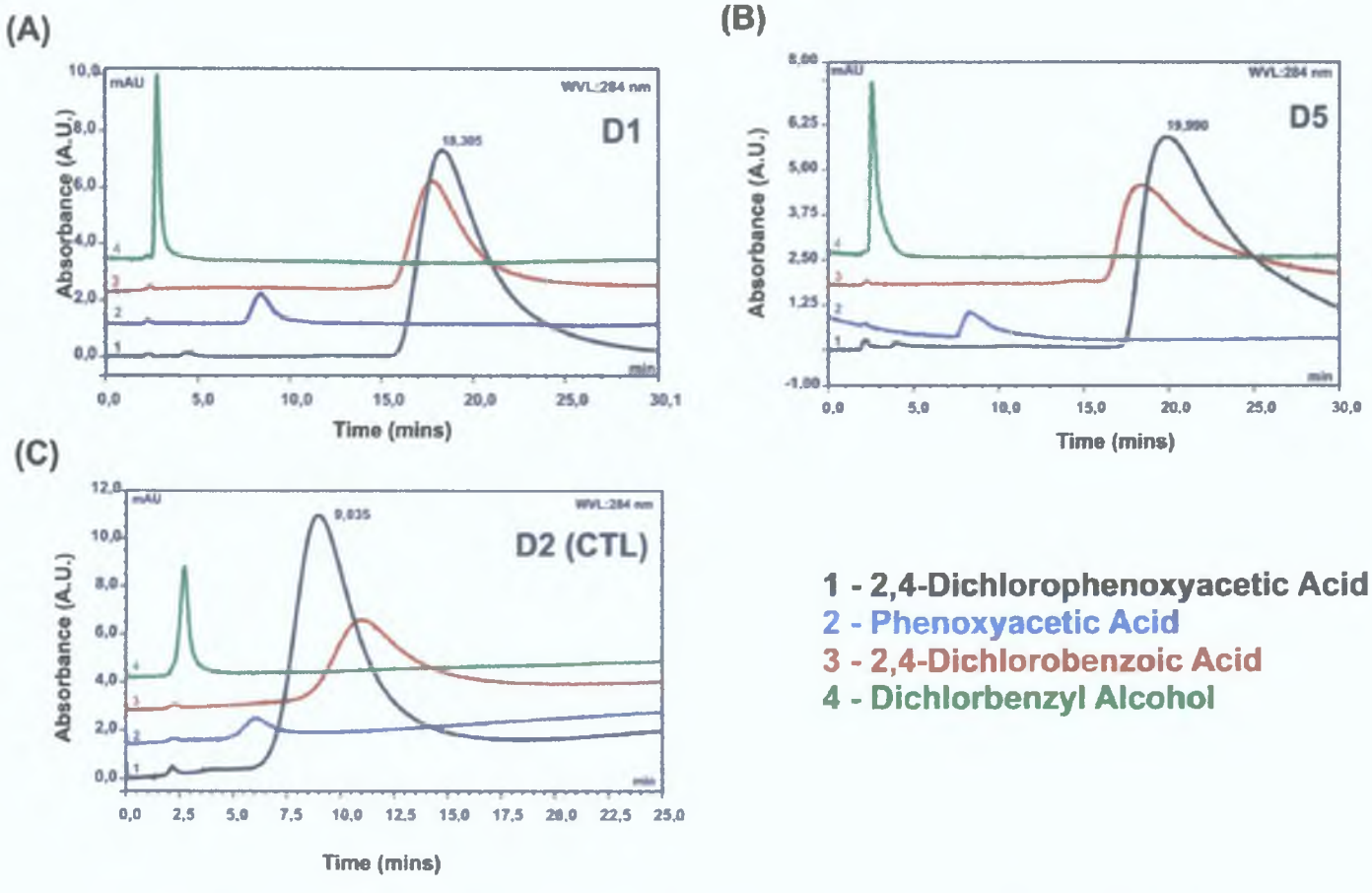

Fig. 4.17 – 2,4-D MIP chromatographic performance on (A) – Thermal imprinted D1, (B) Thermal Blank D2 and (C) UV imprinted D5. Mobile phase of acetonitrile/ acetic acid (1%) at 1ml/min.

The thermal control MIP was used in both cases as the UV control MIP proved unsuitable for packing due to the high back-pressure which resulted. This suggests that the polymerisation methods create MIPs with differing morphologies, something which indicates further investigation is required. However, for the purposes of this study, the point of contrast is chromatographic

performance. The retention times of the compounds are summarised in Table 4.4, and in Figure 4.18.

Analyte	t_{D1} [min]	t_{D2} [min]	t_{D5} [min]	t_{C18} [min]
Acetone	2.104	2.140	1.958	2.870
2,4-Dichlorophenoxyacetic acid	18.305	9.035	19.990	3.062
Phenoxyacetic acid	8.455	6.052	8.243	2.797
2,4-Dichlorobenzoic acid	17.801	10.954	18.398	3.351
2,4-Dichlorobenzyl alcohol	2.798	2.708	2.553	3.481
4-Chlorophenol	3.502	3.420	3.126	3.098

Table 4.4 – Retention times of compounds on imprinted & blank polymer columns. Retention on C18 column also included for comparison.

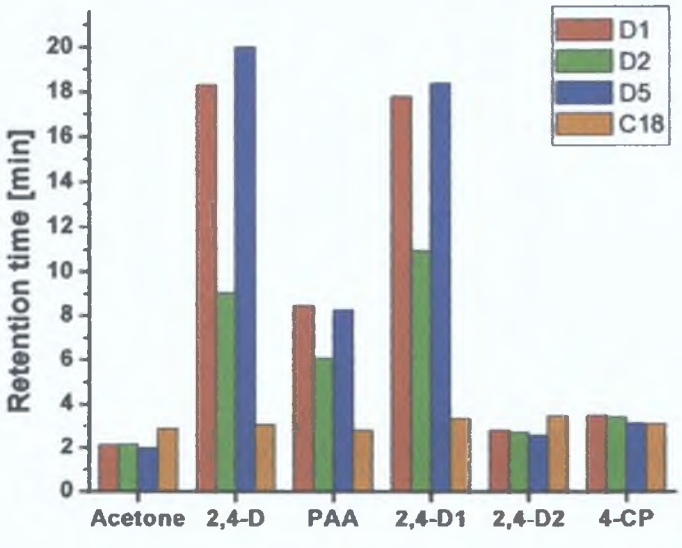

Fig. 4.18 – Relative retention times of compounds on MIP, blank & C18 columns. 2,4-D=2,4-Dichlorophenoxyacetic acid, PAA= Phenoxyacetic acid, 2,4-D1=2,4-Dichlorobenzoic acid, 2,4-D2= 2,4-Dichlorobenzyl alcohol, 4-CP= 4-chlorophenol (Chromatographic analysis performed by A. Molinelli).

Using the same parameters for evaluation as outlined in Chapter 3 – capacity factor (k'), separation factor (α) and retention index (RI), these results were further processed to facilitate easy comparison of MIP properties. Assuming that the retention properties of the thermally-prepared blank were analogous to those of the UV-prepared one, D2 was used as the reference polymer in both instances. These parameters are summarised in Table 4.5.

MIP vs. CTL (D2)	k'_{CTL} D2	k'_{MIP} D1	k'_{MIP} D5	α_{CTL} D2	α_{MIP} D1	α_{MIP} D5	RI (D1 /D2)	RI (D5 /D2)
Acetone	–	–	–	–	–	–	–	–
2,4-Dichlorophenoxyacetic acid	3.222	7.700	9.209	1	1	1	1	1
Phenoxyacetic acid	1.828	3.019	3.210	1.763	2.551	2.869	0.69	0.61
2,4-Dichlorobenzoic acid	4.119	7.461	8.396	0.782	1.032	1.097	0.76	0.71
2,4-Dichlorobenzyl alcohol	0.265	0.330	0.304	12.158	23.333	30.293	0.52	0.40
4-Chlorophenol	0.598	0.664	0.597	5.388	11.596	15.425	0.46	0.35

Table 4.5 – Summary of capacity factors, separation factors and retention indices from chromatographic study.

In synopsis of these figures, the imprinted polymers displayed greatest affinity for the template molecule, 2,4-D, which is evident in that all retention indices are less than one. However, the compounds 2,4-dichlorobenzoic acid and phenoxyacetic acid were also strongly retained compared to the control polymer. The polymer prepared at a lower temperature, D5, showed highest selectivity for the imprint molecule, using the closest structural analogue (2,4-dichlorobenzoic acid) for comparison (RI=0.76 for D1, but 0.71 for D5). This may suggest that the lower temperature favours preservation of the hydrophobic effects, which in turn

induces greater selectivity than the thermal preparation where electrostatic effects dominate. This appears to be corroborated by the findings of the NMR investigations, where the electrostatic interaction appears to strengthen with increasing temperature, and the hydrophobicity appears to be disrupted. However, further research is required to ensure that, given the morphological differences evident in the two kinds of MIP, this is not simply a physical effect.

4.6 Conclusion

MIP research has offered analytical chemistry a highly versatile, and effective, tool for separation applications (as well as others, such as catalysis and sensing); however, without an understanding of the fundamental processes that govern MIP properties, the advancement of the technology is limited. The work performed in this study explored an anomalous MIP system (2,4-D imprinted in a polar solvent system) and demonstrated that molecular-level events in the pre-polymerisation mixture mirror the properties of the final MIP, suggesting that the recognition behaviour can be controlled by carefully controlling the pre-polymerisation mixture to optimise the interactions therein. Interestingly, a thermodynamic study of binding to a MIP imprinted with 2,4-D (using 4-Vinylpydridine as functional monomer) performed by Chen et al.[19] concluded that $\pi-\pi$ stacking contributed strongly to the recognition properties of the MIP, concurring with what is observed in the pre-polymerization mixture. The importance of a secondary interaction in inducing selectivity cannot be underestimated – indeed, it would appear advisable to MIP researchers to deduce what these secondary interactions are for any given MIP system, and to promote the formation of these interactions. The preservation of these secondary effects (hydrophobicity-induced $\pi-\pi$ stacking) in the 2,4-D system is hypothesised to be the reason for greater selectivity being observed in a MIP prepared at lower temperature. As well as providing a means of further improving the recognition properties of this system, this underlines the principle tenet of

rational design in MIP technology – that it is necessary to carefully examine each MIP system in detail to create an efficient imprint – following typical literature recipes will not serve to advance the technology or current understanding of how it works.

Bibliography

[1] K.J. Shea & D.Y. Sasaki, *J. Am. Chem. Soc.*, 113 (1991), 4109.

[2] R.J. Umpleby, S.C. Baxter, M. Bode, J.K. Berch, R. N. Shah & K.D. Shimizu, *Anal. Chim. Acta*, 435 (2001), 35.

[3] H.S. Andersson & I.A. Nicholls, *Bioorg. Chem.*, 25 (1997), 203.

[4] G. Wulff, *Angew. Chem. Int. Ed. Engl.*, 34 (1995), 1812.

[5] L.I. Andersson, B. Sellergren & K. Mosbach, *Tetrahedron Lett.*, 25 (1984), 5211.

[6] B. Sellegren, M.Lepisto & K. Mosbach, *J. Am. Chem. Soc.*, 10 (1988), 5853.

[7] M. Quaglia, K. Chenon, A.J. Hall, E. De Lorenzi & B. Sellergren, *J. Am. Chem. Soc.*, 123 (2001), 2146.

[8] M.J. Whitcombe, L. Martin & E.N. Vulfson, *Chromatographia*, 47 (1998), 457.

[9] (a) K. Haupt, A. Dzgoev & K. Mosbach, *Anal. Chem.*, 70 (1998), 628.

(b) M. Jakusch, M. Janotta, B. Mizaikoff, K. Mosbach, & K. Haupt, *Anal. Chem.*, 71 (1999), 4786.

[10] R.J. Abrahams, J. Fisher & P. Loftus, *Introduction to NMR Spectroscopy*, Wiley (New York), 1988, 19.

[11] D.S. Terekhov, K.J.M. Nolan, C.R. McArthur, C.C. Leznoff, *J. Org. Chem.*, 61 (1996), 3034.

[12] J.L. Atwood, *Comprehensive Supramolecular Chemistry*, 1st Ed. (1996), Pergamon (New York), vol. 8, 431.

[13] G. Lancelot, *J. Am. Chem. Soc.*, 99 (1977), 7037.

[14] D.H. Williams, J.P.L. Cox, A.J. Doig, M. Gardner, U. Gerhard, P.T. Kaye, A.R. Lal, I.A. Nicholls, C.J. Salter & R.C. Mitchell, *J. Am. Chem. Soc.*, 113 (1991), 7020.

[15] A.V. Muehldorf, D.V. Engen, J.C. Warner & A.D. Hamilton, *J. Am. Chem. Soc.*, 110 (1988), 6561.

[16] B.H.M. Snellink-Ruël, M.M.G. Antonisse, J.F.J. Engbersen, P. Timmerman & D.N. Reinhoudt, *Eur. J. Org. Chem.*, (2000), 165.

[17] G.L. Zubay, *Biochemistry*, 3rd Ed. (1993), Wm. C. Brown Publishers (Dubuque, Iowa), 110.

[18] J. Svenson, H.S. Andersson, S.A. Piletsky & I.A. Nicholls, *J. Mol. Recog.*, 11 (1998), 83.

[19] W.Y. Chen, C.S. Chen & F.Y. Lin, *J. Chromatogr. A*, 923 (2001), 1.

[20] A. Katz & M.E. Davis, *Macromolecules*, 32 (1999), 4113.

Chapter Five

Investigating the Applicability of Molecular Modelling to the Elucidation of the Structure and Nature of Pre-polymerisation Complexes in MIP Research.

5.1 Abstract

The previous two chapters on the mechanisms governing the creation of a successful imprint have described the numerous effects which can inhibit or promote the formation of high-affinity binding sites in a polymeric synthetic receptor. The broad range of factors which play a role points to the need to develop a strategy for the integration of information garnered from such rational-design experiments to create optimised MIPs. The possibility of using a molecular modelling approach to create optimised models of pre-polymerisation complexes, with restrictions on possible conformations imposed by data from spectroscopic PPC investigations, is examined in this chapter. Some of the more important findings indicate that for the 2,4-D/ 4-VP system examined, the probability of an acid-base ion-ion pair surviving in solution is high, but less so is the probability of a π-stacked complex due to the weaker nature of the bonds involved. This work should provide a useful framework for the future development of this approach. The work also indicates the suitability of other types of NMR experiments to developing refined models of PPCs.

5.2 Introduction

5.2.1 Molecular Modelling Approaches in Molecular Imprinting Technology.

In current literature on the subject of computational methods as a tool in the design of optimised molecularly imprinted polymers, the work of Sergey Piletsky *et al.* at Cranfield University (Cranfield, UK) offers excellent examples of how such an integrated approach to MIP design can drastically improve the efficiency of creating a MIP for a given analyte. In a technique they describe as 'MIP dialling'[1], the design, synthesis and testing of a MIP targeting the antibiotic tylosin was achieved in an impressive 21 days. Of particular interest here were the recognition properties of the MIP in aqueous media as well as in organic solvent – the ability of a MIP to perform in aqueous media portends to be an important consideration in future MIP design, in order to extend the biomimetic aspect of molecular imprinting. This work is an extension of earlier research by the group[2] which laid the foundations for the development of their methodical approach to MIP optimisation. The computational aspect of this work involved the creation of a library of 20 commonly-used functional monomers, and models of all template molecules being examined, which then underwent energy minimisation. The team subsequently used a LEAPFROG processing algorithm to screen the functional monomers in the library for potential interactions with the template. The functional monomers displaying the greatest affinity for the ephedrine template were then used to create MIPs, which were then examined to see whether the predicted behaviour (from the modelling studies) correlated to the

observed behaviour in these MIPs. It was observed that the monomers with highest binding energy scores in the modelling study (in this case, itaconic acid and methacrylic acid) produced the polymers with highest affinity for template in HPLC analysis. However, one notable exception was the performance of hydroxyethyl methacrylate (HEM), which had a significantly lower binding strength than calculated. The authors speculate that this may be attributed to the hydrophobic nature of HEM, resulting in trapping of the monomer in hydrophobic portions of the polymer network and thus lower accessibility for template interaction during rebinding. This explanation does not seem to concur with the findings of Chapters 3 and 4, whereby the hydrophobic effect appeared to accentuate the imprinting effect, by virtue of preservation of the PPCs within a hydrophobic shell, suggesting that perhaps the chosen polymerisation conditions here negatively affect PPC integrity, which will not be predicted by the modelling data. This draws attention to the inherent limitations with modelling PPCs – partition effects, polymer chain growth, changes in PPC equilibria due to temperature changes and other factors associated with the actual polymerisation step, which may fundamentally influence the quality of an imprinting procedure, cannot be accounted for. Despite this, the achievements of the Piletsky group in this and other[3, 4] modelling strategies for MIPs are impressive and remain some of the most important reference works for any MIP/modelling protocol.

As well as being extremely effective, the approach described by Wu *et al.*[5] is perhaps the most accessible modelling for MIPs technique yet described in the literature. The monomer-template interaction simulations were run on a standard workstation (previous work had required an expensive SGI workstation setup) – using a commercial distribution of Linux, (Redhat 7.3), 512Mb RAM and a Pentium 4 2.2GHz processor; these specifications are currently offered on workstations available for ~€500. The computational work was also performed using two different modelling methods – a semi-empirical quantum method (PM3) and an *ab initio* method (Hartree-Fock method with 6-31G basis set). Both semi-empirical quantum methods and *ab initio* methods offer means of elucidating the energy of a system based on quantum mechanical descriptions of molecular systems, but with some simplifications to avoid the arduous calculations implied by energy derivations using Schrödinger's wave function equation. Hartree-Fock methods involve the creation of several wave functions, with the assumption that the better the calculated wave function approximates the true wave function, the lower the energy of this wave function – the best approximation being when energy reaches a minimum. Approximate molecular orbital theories (semi-empirical quantum methods) are less demanding computationally and can yield results of similar accuracy. This is achieved by broader simplifications – e.g. approximation, rather than explicit calculation, of integrals, which are typically the most computational-intensive aspect of *ab initio* methods. Also, only valence electrons are considered for calculation, assuming that the inner-shell electrons form part of an inner atomic core which does not affect interatomic interaction[6] .

Both methods offer superior means of simulating atomic behaviour compared to more typical molecular mechanics force fields, where relatively simple models are used to describe processes such as bond stretching, rotation and bond angle opening or closing in energy terms. Such simplified approaches, although potentially useful in describing systems with larger numbers of atoms, cannot describe properties ascribed to electron distribution in molecules. This may be of significance in describing pre-polymerisation complexes, where secondary, more subtle interactions (such as the π-stacked complexes observed in Chapter 4), which may be inherently linked to electron distribution, are responsible for inducing a strong imprinting effect in the polymer formed. Returning to the work published by Wu and colleagues, the benefits of such an approach may be mirrored in the impressive results this work yielded – the hierarchy of interaction energies between monomer and template was found to correspond to the order of the capacity factors of the HPLC columns packed with MIPs of the same monomer: template composition. The inherent drawback of the *ab initio* and the semi-empirical method used, though, is that models are created in vacuum, neglecting solvent influence. This flaw is not inconsiderable, given the role of solvent in affecting PPC equilibria. This study also contains a brief examination of polyclonality in the final MIP produced, attributing the range of affinities observed to the polymerisation of different types of PPC.

Finally, the exceptional utility of molecular modelling as a means of optimising MIPs, and it's inherent limitations associated with the inability to predict macroscopic effects such as phase separation or polymer chain growth effects, are perhaps best exemplified by the work of Sellergren, Lepistö and Mosbach[7, 8], and follow-up analysis performed by Katz and Davis[9] on the same amino acid-imprinted MIP system (using L-Phenylalanine anilide and L-phenylalanine-N-methylanilide). Sellergren and colleagues determined that the explanation for the difference between observed MIP chromatographic behaviour and NMR-observed PPC formation was a self-association mechanism. However, the formation of a dominant 2:1 monomer: template PPC was proposed to explain the observed selectivity of the MIP – a primary ionic interaction stabilised by a secondary hydrogen bond. The further research performed by Lepistö and Sellergren[8] determined that different conformations of the imprint molecule (due to the presence of the methyl substituent of L-phenylalanine-N-methylanilide) were sufficient to induce selectivity towards whichever conformation was used as template. Nuclear Overhauser enhancement NMR allowed accurate models of the individual conformations to be created (see Fig. 5.1). The authors surmise that the binding site shape is a direct consequence of the template molecule conformation in the pre-polymerisation mixture. This would appear to underline the findings of Spivak on the importance of template molecule shape and size to the outcome of an imprint[10].

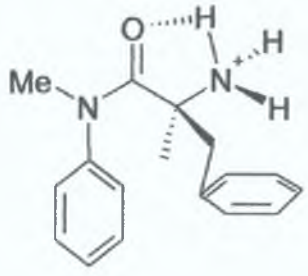

L-Phenylalanine -N-methylanilide

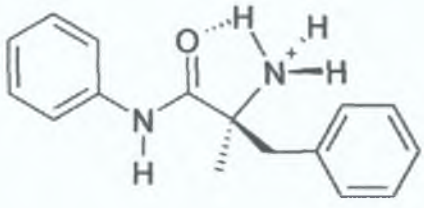

L-Phenylalanine anilide

Fig. 5.1 – Conformations of L-Phenylalanine-N-methylanilide and L-Phenylalanine anilide as proposed by Lepistö & Sellergren (ref.8).

Molecular modelling in this case allows the researchers to hypothesise on the nature of the binding sites of molecularly imprinted polymers. The work of Katz and Davis disputes the nature of the recognition mechanism in this system proposed by these researchers, however. They found that no multiple-point interactions between monomer and template were observable in ^{1}H-NMR, and that a mixture of monomer and template separates out from the remainder of the cross-linked network. These results suggested that several template molecules were self-associating, becoming integrated into the polymer, and then acting as a site for rebinding of the template. This interpretation permits explanation of binding site heterogeneity as is commonly observed with MIPs[11]. Also, the authors calculate that for specific-cavity mechanism to be the dominant means of retention, the extraction of template molecule from the polymer matrix needs to be of the order 99.9%; with such a highly cross-linked chemical entity, such quantitative extraction of template seems unlikely. This underlines the need to

conduct PPC modelling optimisation experiments in tandem with careful analysis of polymerisation events to ensure preservation of the PPCs. Modelling should thus facilitate MIP design, but does not offer a means of avoiding MIP testing to gauge chromatographic performance – and so perhaps a 'functional monomer library' approach could result in the exclusion of monomers which, although not resulting the highest binding score, will aid in the preservation of PPCs during polymerisation to the greatest extent possible.

5.2.2 Typical Procedure for Modelling a PPC System

Modelling of a pre-polymerisation complex system involves several discrete steps. To summarise these stages, firstly any molecules involved in the system are modelled (monomers and templates only). Crosslinker molecules are excluded from the simulation, assuming they do not disrupt complex formation. Work by Andersson and Nicholls has already shown this to be a valid assumption[12] – they found a decrease in PPC stability of only ~4.5% upon addition of crosslinker to their monomer/ template mixture. Solvent molecules will be already contained in a reference library in commercial modelling programs, and if a continuum solvent model is used, discrete solvent molecules will not be included in the simulation. Subsequently, these molecule models are subjected to an energy minimisation step to find their individual lowest energy conformations. These models are then placed in a hypothetical 'box' of fixed dimensions, which is then filled with solvent molecules (assuming solvent is being modelled discretely). The PPC molecules are then held fixed, while the solvent molecules are energy-minimised around them to allow any repulsive/ attractive solvent-PPC interactions to equilibrate. The entire system is then relaxed, and then a molecular dynamics simulation is run to simulate the behaviour of the molecules. Thus it can be deduced whether interactions between monomer and template are viable, and if so, how many can exist and survive in solution. This is the strategy typically employed in molecular modelling

in MIP applications[4], and it is the method by which modelling is employed in this preliminary investigation of the utility of modelling in rational design strategies.

5.3 Materials - Hardware/ Software

The work was performed on a dual processor machine with 1GHz Pentium III CPUs and 2GB of RAM; the front-end node also used a 1GHz Pentium III processor, with 512MB of RAM. The main software package used was *AMBER7* (Scripps' Institute, California, USA). This comprises of many different programs, and where appropriate, the programs used throughout the experiments will be identified. Other software used was ISIS^{TM}/Draw 2.5(MDL Information Systems Inc.), for drawing of chemical structures; ViewerLite 4.2 (Accelrys Inc.), for 3-D viewing of molecules, generation of initial .pdb files and creation of .pov files; POV-RAY^{TM} for Windows 3.5 (POV Development Team^{TM}) for generation of bitmap images of molecules; VMD[13] for WIN32 v.1.8.2 (University of Illinois) for visualisation of molecular dynamics; Videomach 2.72 (© Gromada.com) for compilation of molecular dynamics videos; and WinaXe Plus 7.4 (Lab-NC Ltd.) as X-server for Windows and ftp program.

5.4 Experimental - Protocol for Molecular Modelling of PPCs.

This section contains the sequence of steps required for running a comprehensive MD (molecular dynamics) analysis on a system, making specific reference to examples from the system examined in this research, i.e. 2,4-D and 4-VP complexing in chloroform. Section 5.6 gives specific program content at each stage to demonstrate the command structure necessary to perform each step. A comprehensive description of the capabilities of each of the programs in the *AMBER7* suite, as well as definitions of each of the commands, can be found in the *AMBER7* manual, which is available online[14].

5.4.1 Generation of Basic Structure Files

A molecular modelling approach for this type of work begins with the creation of the basic structure files which contain essential information about the molecules being simulated, i.e. atom type, atom charge, atom connectivity, starting Cartesian coordinates. These files are known as **topology** files and are generally created in Brookhaven Protein DataBank format (more commonly known as PDB format, which is also the extension associated with these file types - *.pdb). X-ray crystallographic data and NMR spectroscopic data are typically used to determine these parameters. PDB files for larger proteins and other molecules of biochemical interest may be obtained from online academic resources such as the aforementioned Brookhaven database[15] or the Cambridge Crystallographic

Data Centre[16]. For the purposes of examining smaller organic molecules, as is the case with this study, it is sufficient to create the molecule using a commercial chemical drawing package such as MDL's ISIS™/Draw application. This may then be exported as a molfile (*.mol) and imported into a molecular viewing package (e.g. Accelrys' ViewerLite) and from there converted in a .pdb file (see Fig. 5.2). A common problem when working with *AMBER7* software is the fact that PDB files can have slight differences, depending on their origin, and thus may require some slight modification before being accepted by the programs for further processing. Labelling issues appear to be the most common source of incompatibility in this regard.

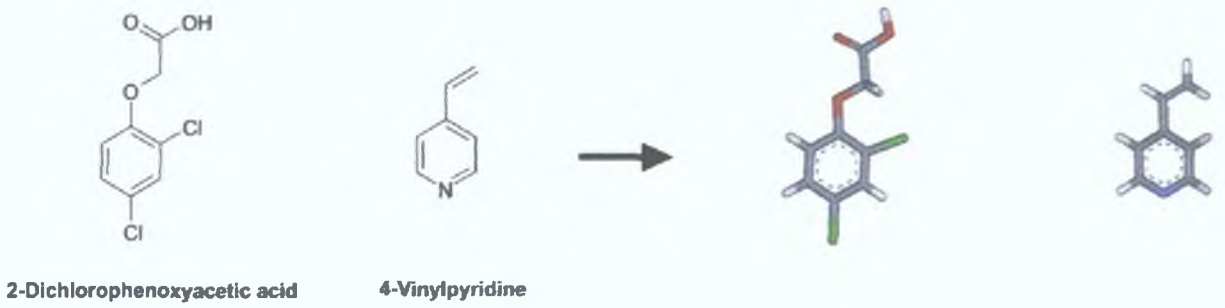

Fig. 5.2 – Conversion of basic ISIS™/ *Draw* structures to PDB format

5.4.2 Preparation of Structure Files for use in LEaP: Antechamber and *Parmchk.*

The flexibility of the *AMBER* package permits the user to alter atom types and connectivity (from within the confines of the *LEaP* program), but it is simpler to begin working with a thus-imported PDB file. The program is supplied with topology files for many common biomolecules – amino acids, DNA, RNA – but not for the type of organic molecule generally used in the monomer-template type interaction of interest in this research. To this end, *AMBER7* is supplied with applications (*Antechamber* and *Parmchk*) designed to modify and rectify flaws in imported structural files. The first step in the generation of a new system for a molecular dynamics simulation is then to prepare the input file in a suitable format. It is important to note here that the versatility of *Antechamber* permits the use of other file formats other than PDB (such as Hyperchem *.hin* format or MDL *.mdl* formats), but in the scope of this investigation, PDB format proved the most compatible. Having created the 'prepin' input file required by *LEaP* for energy minimisation (see 2,4-D.prepin in Section 5.6), the program *Parmchk* is the next step, to investigate whether the prepin file violates the requirements for application of the force field at the next stage. For this type of application, the *AMBER7* documentation recommends application of the 'gaff' (general Amber force field) force field. The *Parmchk* program identifies missing parameters in the prepin file and also creates any necessary force field modifications in an frcmod file (see 24Dfrcmod in Section 5.6). In this case, the two molecules (2,4-D and 4-

VP) were assembled with sufficient proximity of the pyridine ring N atom and the acidic proton for a hydrogen bonding interaction (see Fig 5.3).

Fig. 5.3 – Interaction between acid proton and pyridinyl N atom.

5.4.3 Preparation of Structural Files for use in Sander: xLEaP and tLEaP.

Following an initial (unsuccessful) minimisation run wherein the two molecules were not tethered together by any kind of distance restraints, the analysis was recommenced, this time beginning with both molecules existing in one PDB file (with the PDB file carefully examined to ensure appropriate labelling). The structures were prepared via *Antechamber* and *Parmchk* and introduced into *LEaP* for visualisation. At this point, any remaining structural flaws can be rectified manually using the graphical *LeaP* interface, *xLEaP*. It is also possible to apply all *LeaP* commands from a text-only interface via the program *tLEaP*. Once the complex PDB and Prepin files have been loaded into *LeaP*, the complex can

then be solvated. Here, the work focused on the behaviour of these complexes in a non-polar environment and so chloroform was chosen (Fig. 5.4 shows this – the above complex solvated in a $10Å^3$ chloroform box). The *LeaP* program is also necessary to generate the two types of file required for the actual minimisation run – a list of Cartesian coordinates of all atoms in the file (a prmcrd file) and a topology file (a prmtop file). These two files are the only format accepted by *SANDER*, the *AMBER7* program employed in molecular dynamics, simulated annealing and energy minimisation analyses.

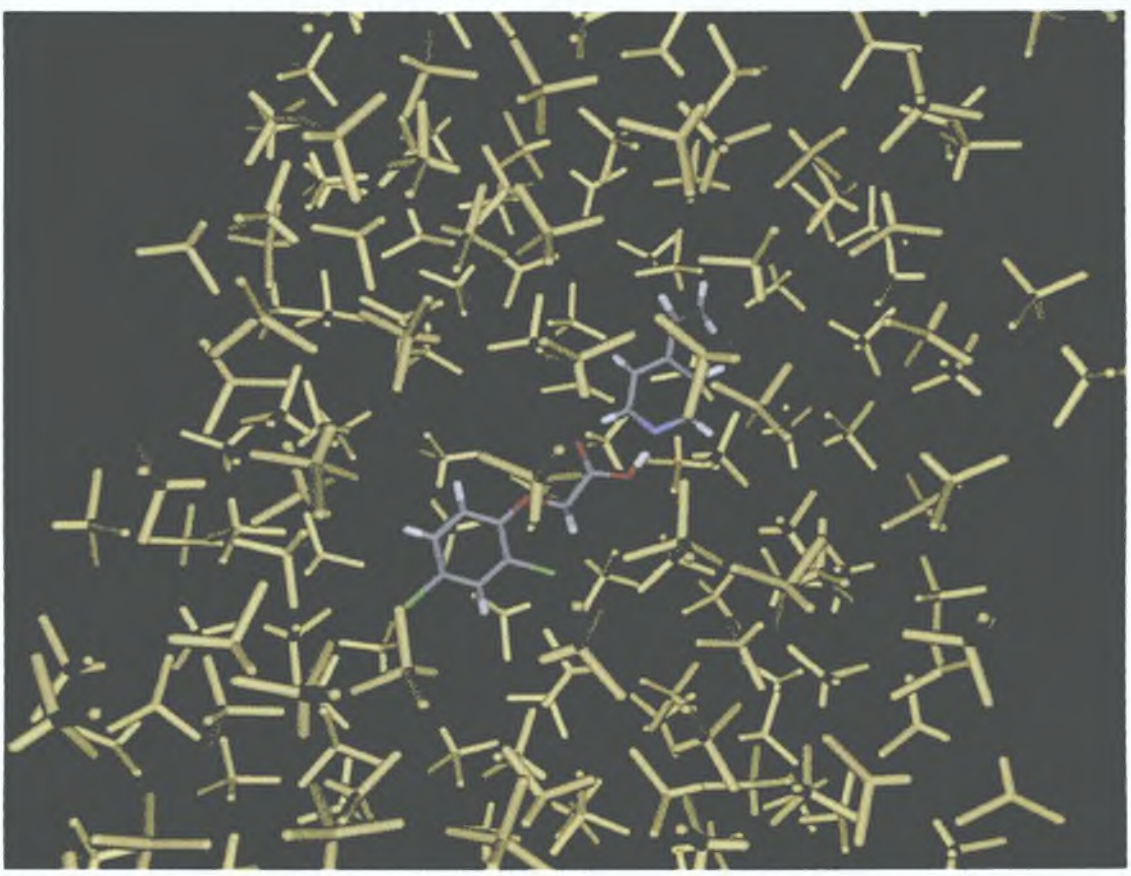

Fig. 5.4 – 2,4-D/4-VP Complex solvated in $10Å^3$ chloroform (in yellow) box.

5.4.4 Energy Minimisation: Using *SANDER*.

After this somewhat lengthy start, the system is now ready to undergo energy minimisation. This is where the user may designate restraints to be imposed during the energy minimisation run as well as the number of energy minimisation steps to put the system through. This is written into one text input file (see min.in in Section 5.6), from where *SANDER* will read all commands and apply them to the system. *SANDER* also reports on the energy state of the system at regular intervals (the frequency of which is determined by the user) by writing an mdinfo file, which tells the user the energy state of the system at the last step recorded. The coordinates of the atoms at each step recorded are output to a coordinate file (mdcrd), permitting the user to later examine the movements of the complex during minimisation using molecular dynamics visualization programs (such as the University of Illinois's *VMD* package). The final coordinates of the system at the end of the run are written to a file called a restart file. However, of greatest interest to the user will be the mdout file created by *SANDER* which documents energy changes for the duration of the minimisation run. For the purposes of the 2,4-D/4-VP complex of interest here, a distance restraint of 3 angstroms was placed between the hydrogen bond donor (the nitrogen atom of the pyridine ring) and the acceptor (the acidic proton of the 2,4-D molecule). This restraint was imposed to prevent the molecules drifting too far apart at the energy minimisation stage. Energy minimisation itself involves the following steps before the user may

begin the next stage, (equilibration of the system prior to molecular dynamics runs):

- Application of distance restraints
- Minimisation of the system, holding solute molecules fixed.
- Minimisation of the entire system, without fixing any molecules

After these three steps, the user may proceed to the actual molecular dynamics stage. This approach to minimisation permits the system to find it's low optimum energy configuration first as an isolated complex, and then as a complex relative to the surroundings.

5.4.5 Molecular Dynamics Equilibration and Runs Using *SANDER.*

Molecular dynamics permits the user to observe the molecule(s) of interest interacting with its environment during a pre-determined timestep – usually in the order of nanoseconds. It is necessary to first allow the system to achieve thermodynamic equilibrium by applying various pressure and temperature restraints to the system and varying these parameters until the markers of thermodynamic stability (such as system density, pressure, potential energy, temperature and the root mean square deviation of atom coordinates) achieve a stationary state. Thus, the system is put through a molecular dynamics run first with the condition of constant volume. The periodic boundary condition of constant volume is imposed on the system using the 'ntb' command. Equilibration runs are typically short – in the case of the 2,4-D/4-VP system

examined here, 5 picoseconds was more than adequate for temperature to be raised to the desired 300k and achieve equilibrium, as is evident in Fig.5.5.

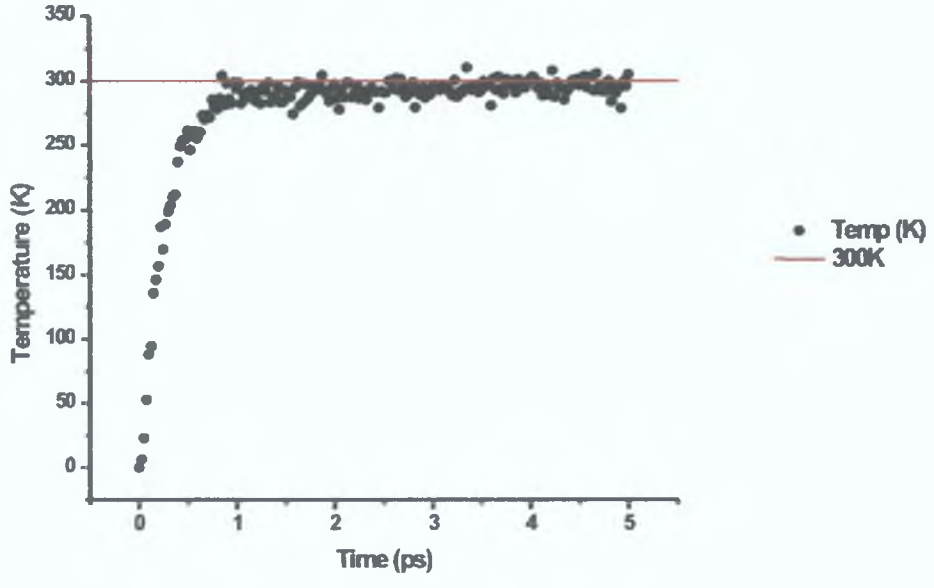

Fig. 5.5 – Equilibration data for 2,4-D/ 4-VP complex in chloroform, temperature vs. time, 5 picoseconds duration at *constant* volume. System is monitored to ensure desired temperature of 300K is attained.

The equilibration is then extended to applying a constant pressure restraint. To achieve this, the volume of the unit cell is adjusted gradually to make the computed pressure approach the target pressure, *pres0* (default is 1 bar). The objective of these equilibration steps is to attain a constant-energy system. Equilibration is monitored by observing parameters such as density – the experimental value of the solvent used (chloroform, ρ=1.49 g/cm^3) may be used as a reference for what the approximate equilibration value should be, although the effects of the partial molar volumes of the solute molecules in the cell will

affect the overall density, and so calculated density may deviate from the experimental density of the solvent (as in Fig. 5.6). At this point, it should be noted that attaining equilibrium required slightly longer – approximately 50 picoseconds in the given example. With any equilibration step, the process is allowed to continue until the observed thermodynamic properties (here, the system density and the root means square value of coordinate deviation) achieve stability.

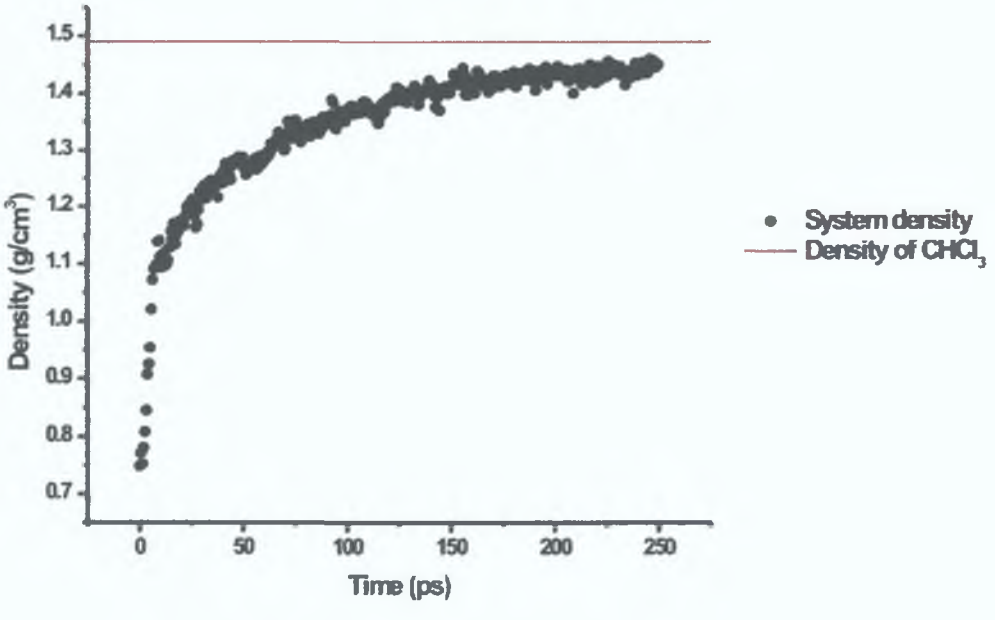

Fig. 5.6 – Equilibration data for 2,4-D/4-VP complex in chloroform, density vs. time, 250 picoseconds at constant volume and pressure.

Observing the root mean square deviation of the coordinates of the selected atoms (in the case of the 2,4-D/4-VP system, just these molecules and not the solvent molecules) is another effective means of gauging the stability of the

system. Figure 5.7 is data from the same equilibration run, looking at how these two molecules' coordinates deviate for the 250 picosecond duration.

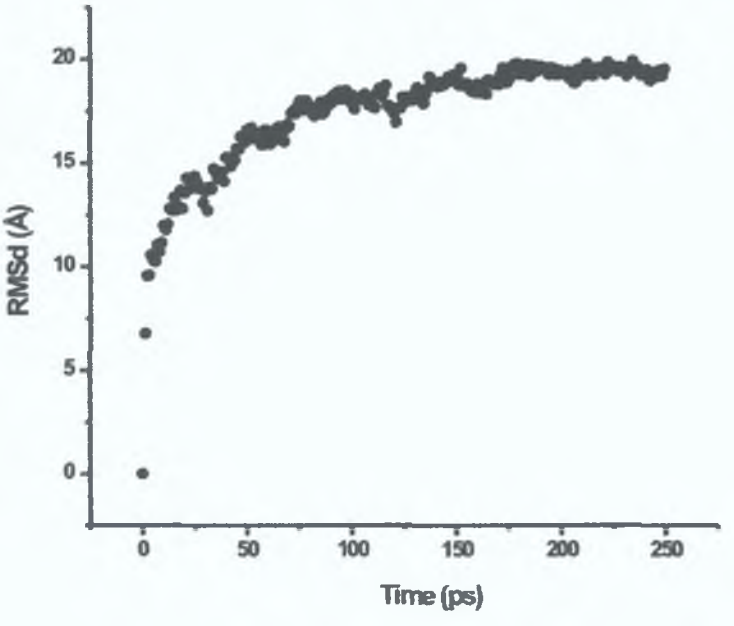

Fig. 5.7 – Equilibration data for 2,4-D/4-VP Complex in chloroform, RMSd vs. time, 250 picoseconds at constant volume and pressure.

It is necessary to note here that calculation of RMSd values is performed using the *Ptraj* program in the *AMBER7* suite, and not *SANDER*.

Equilibration terminates with a gradual increase of the pressure relaxation time (controlled by the *taup* command written into the md.in file).Having thus equilibrated the system, it is now possible to run a system at constant energy and examine the 'true' trajectory of the complex across a 1-nanosecond timescale, without any artificial restraints imposed. Molecular dynamics runs use the NVE (or microcanonical) ensemble, i.e. constant number of particles, constant volume

and constant energy. A 1-nanosecond run requires much processing time and so the preceding steps in equilibration tend to be limited to up to 250 picoseconds. The actual MD run is known as a production run and it is from this simulation that important conclusions and statistics on the entire analysis are drawn. Statistical analysis of final trajectories may be performed using both the *Ptraj* and *Carnal* applications. In the case of the complex being looked at here, the use of *Ptraj* enabled the observation of changes in the distance of the H-bond donor-acceptor pair. Figure 5.8 shows how this interaction varied for the duration of the run (NB: After equilibration has been completed, the molecular dynamics simulation is a continuation of the run, rather than a restart, thus the timescale beginning at 1000ps).

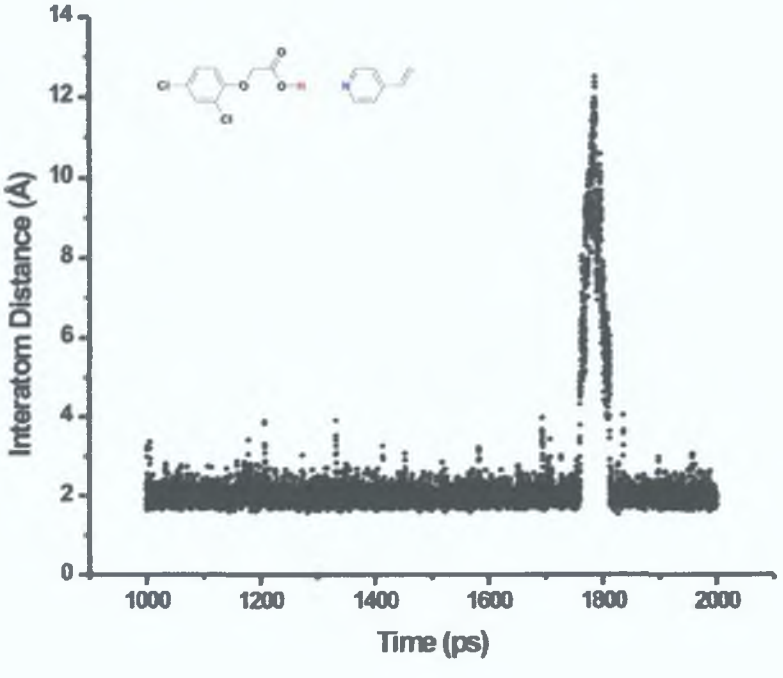

Fig. 5.8 – The variation of interatom distance during MD run, pyridinyl nitrogen atom and acidic proton.

It is of significance here that the interaction does not remain intact for the entirety of the run; however, the *ptraj* report, printed when the program has terminated its analyses, can report on the integrity of this interaction. In this case, the interaction is intact for a total of 98.56% of the MD run – the integrity of the interaction is visible in the last frame of the trajectory (as shown in Fig.5.9). The large interatomic distance after ~1800ps (and subsequent return to values lower than 4Å) may be due to one of the molecules drifting out of the boundaries of the box, with its image subsequently entering on the opposite side and reforming the H-bond.

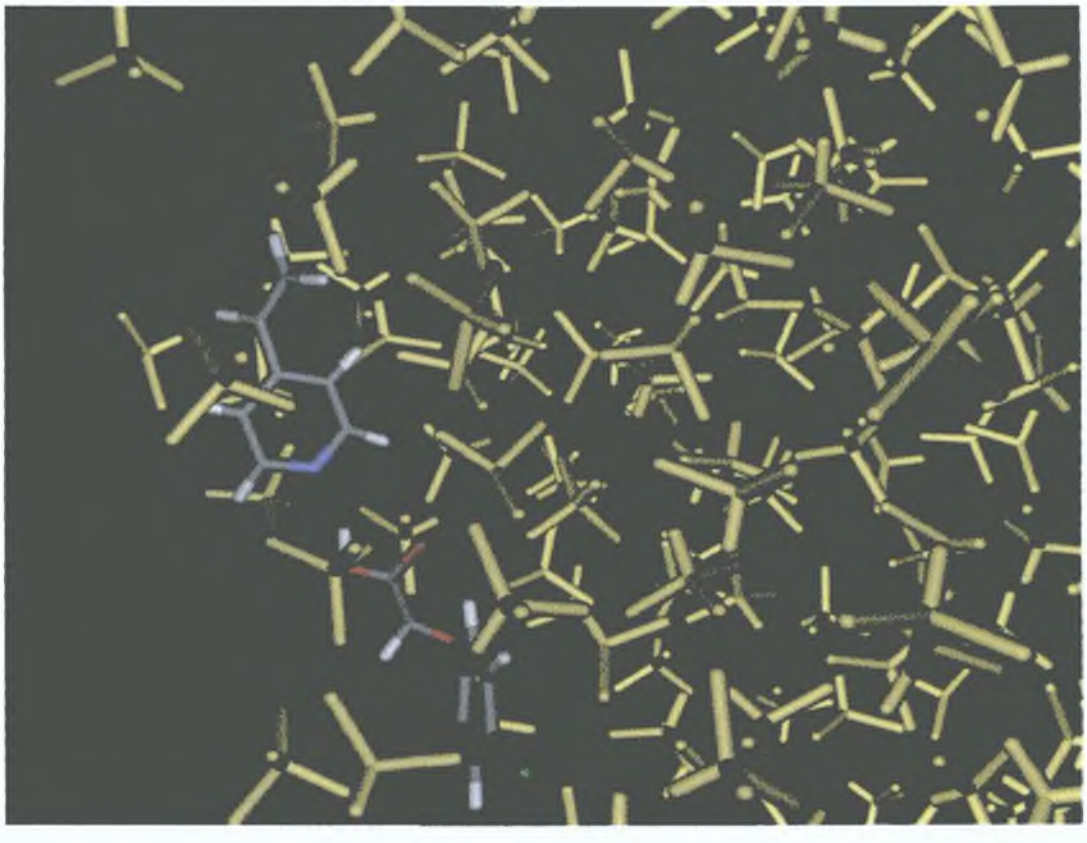

Fig. 5.9 – Final frame of NVE MD run, with interaction still intact (hydrogen bonds indicated with broken green line).

A further method used frequently in molecular modelling strategies is that of simulated annealing, which involves heating the system to high temperatures and cooling it slowly. Annealing itself is the process whereby a molten substance is cooled gradually until the substance crystallizes to give a very large single crystal – in simulation, this perfect crystal corresponds to the global minimum of the free energy (although to achieve the simulated equivalent of a perfect crystal, an infinitely long cooling step would be required, which is impractical). This approach offers the benefit of permitting the system to overcome energy barriers and rapidly find optimum low-energy configurations. The temperature profile for a typical MD run resembles that shown in Figure 5.10.

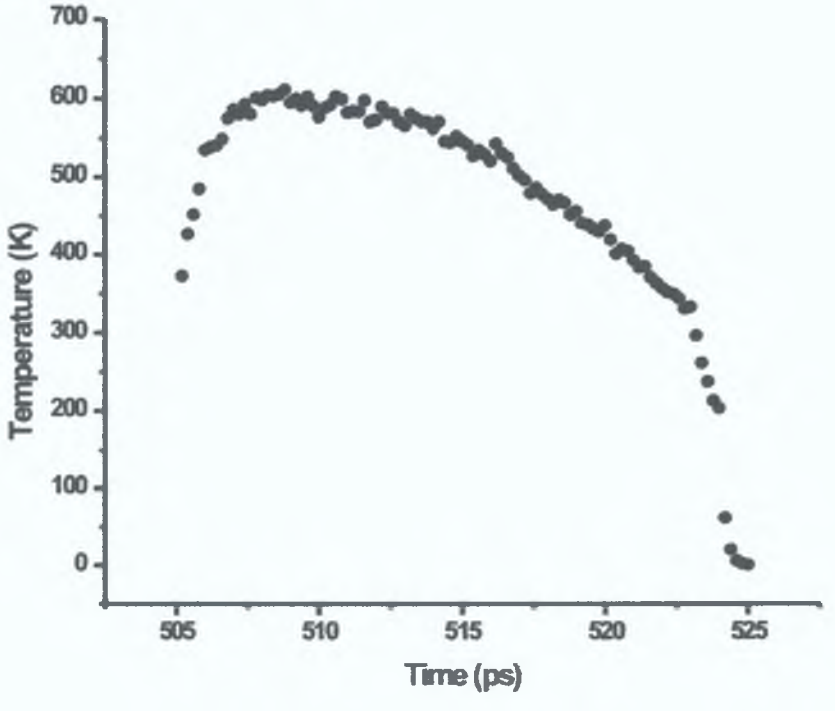

Fig. 5.10 – Temperature profile for simulated annealing MD run.

This particular run involved heating the system from a starting temperature of 300K up to a maximum of 600K, before gradually cooling it; the final phase of the run is a rapid cooling to 0K.

5.5 Results & Discussion

Equilibration of the system begins with a 5-picosecond run at constant volume, bringing temperature up to 300K, as shown in Figure 5.5. The next equilibration step is applying a constant pressure constraint to the system; as demonstrated in Figure 5.11, the temperature and potential energy of the system is monitored at each step to ensure thermodynamic stability.

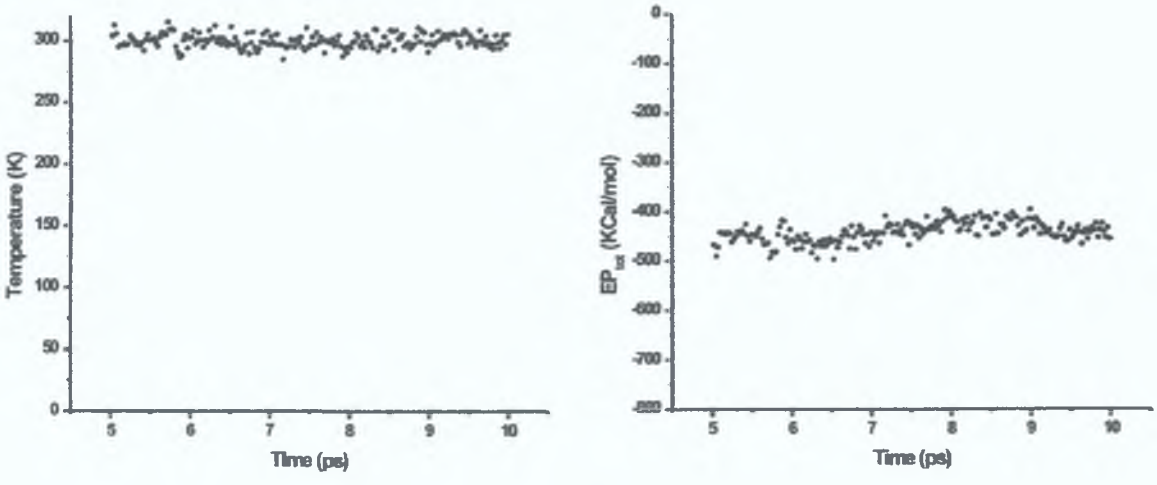

Fig. 5.11 – Analysing temperature and potential energy during constant pressure MD equilibration step.

As described in Section 5.4.5, the system's density was also monitored to observe whether it approximated the experimental value of 1.49 g/cm^3; Figure 5.12 shows variations in system density as the constant pressure system is allowed to *equilibrate*.

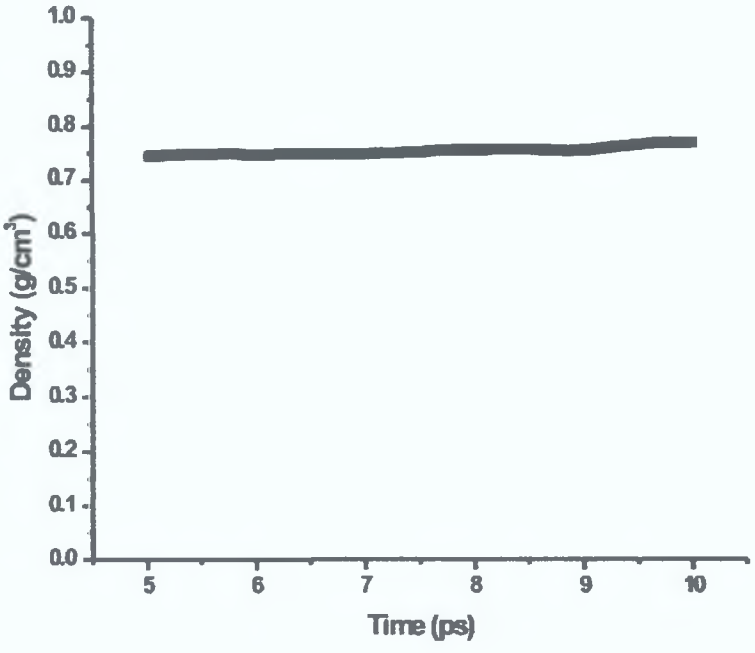

Fig. 5.12 – Density of system during constant pressure stage of equilibration.

It becomes evident here that the density has not yet reached equilibration, given the disparity between the observed value and the experimental value; a longer equilibration was performed to examine whether further stabilisation would occur. Extending the equilibration to 250 picoseconds, as in Figure 5.6, shows a more reasonable value for density can be obtained this way. It is also possible to observe that the coordinate deviations (for the two molecules of interest here, the 2,4-D and 4-VP) have stabilised by the end of this time period (see Figure 5.7), suggesting that the system has achieved equilibrium. This concluded the equilibration stage. The production run results can then be examined for indications that the complex remained stable, once distance restraints have been

removed, and so a 1ns production run was performed. The first parameters analysed, as before, are temperature and potential energy of the system, can be used to ensure stability of the system during the run. These values are graphed in Figure 5.13.

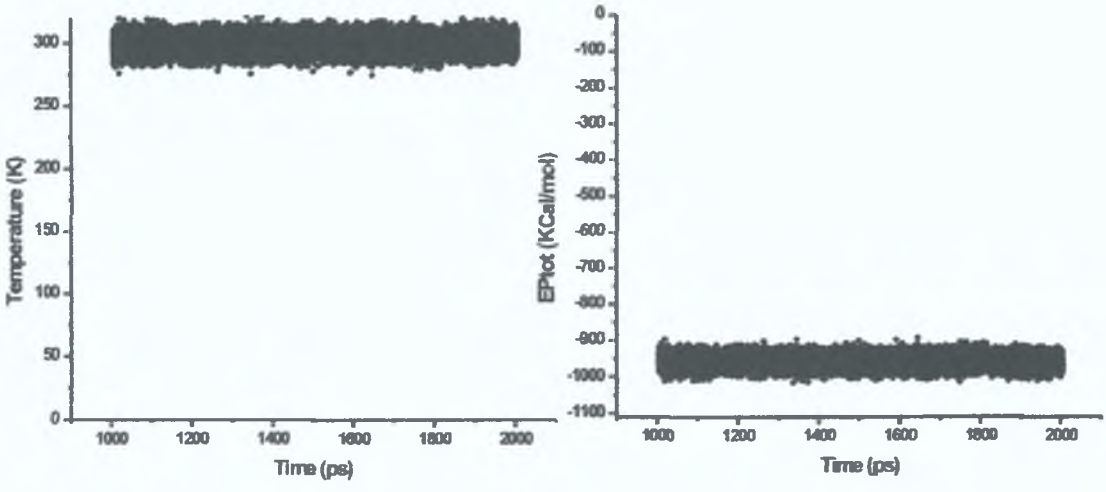

Fig. 5.13 – *Temperature and potential energy profiles during production run.*

Of greater influence, however, is data relating to complex integrity during the run. As specified in Section 5.4.5, the distance between two atoms during a run may be monitored using the *Ptraj* program. This permits us to track changes in the distance between the hydrogen bond donor and acceptor (i.e. the nitrogen atom of the pyridine ring and acidic proton of the 2,4-D), as is displayed in Figure 5.8. The report produced by the *Ptraj* module reveals that the bond is intact 98.6% of the duration of the run. Essentially, the complex is intact for the vast majority of the time (Fig.5.14), but briefly separates (Fig.5.15).

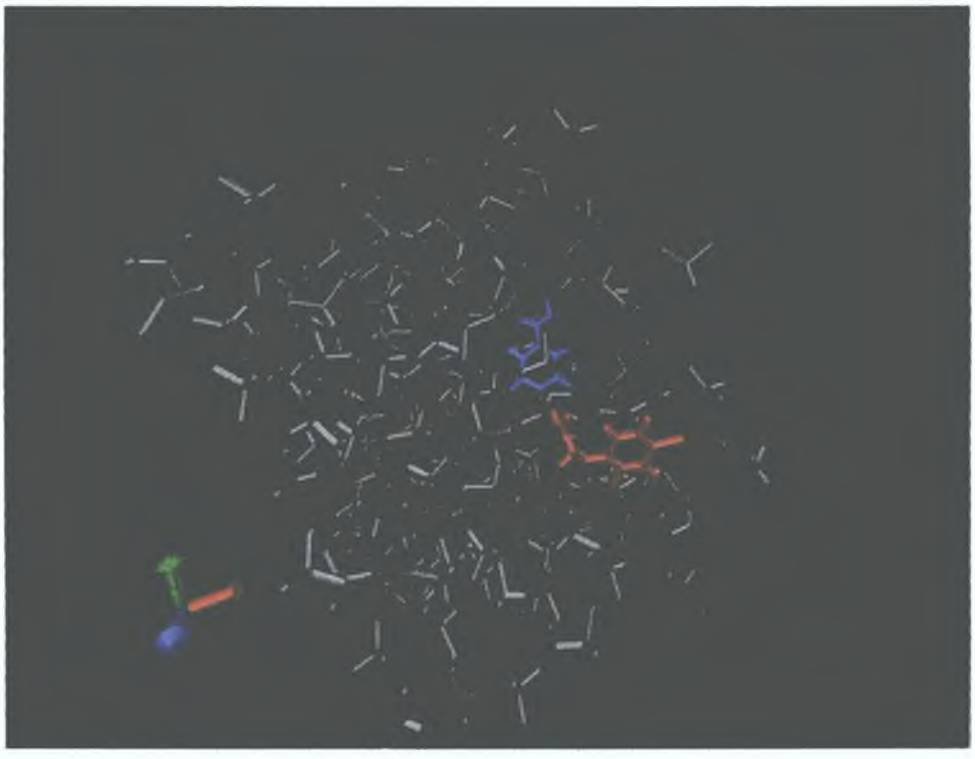

Fig. 5.14 – The 2,4-D/4-VP complex during NVE MD run, while intact.

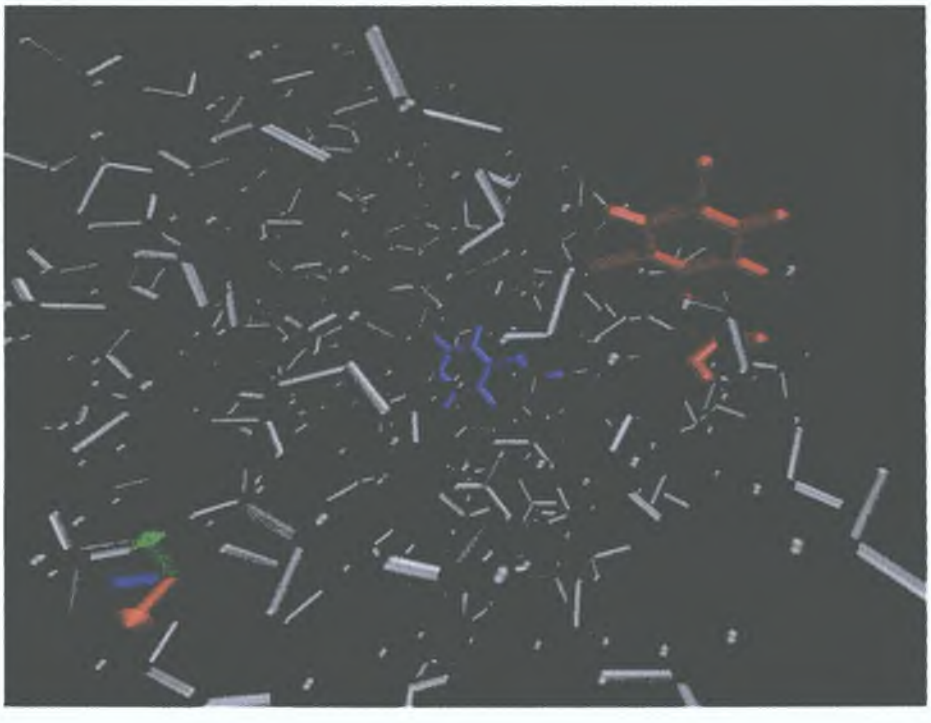

Fig. 5.15 – The molecules drift apart during the run, as evident in this frame from the NVE MD run.

Similarly, a simulated annealing run was also performed before performing an identical 1-nanosecond NVE MD production run, using the temperature profile specified in Figure 5.10. During the actual simulated annealing, the hydrogen bond experiences variations in it's length/ integrity (Fig. 5.16). A snapshot of the system at the end of the annealing run shows that the complex remaining intact is in fact an energetically-preferred configuration for the system, with the H-bond still existing after the run (Fig.5.17).

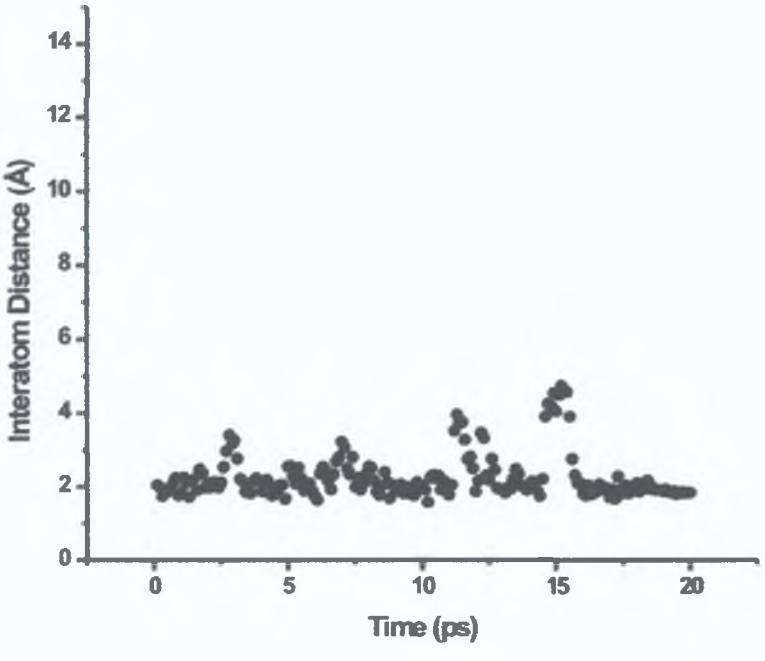

Fig. 5.16 – Hydrogen-bond distance during 20ps simulated annealing.

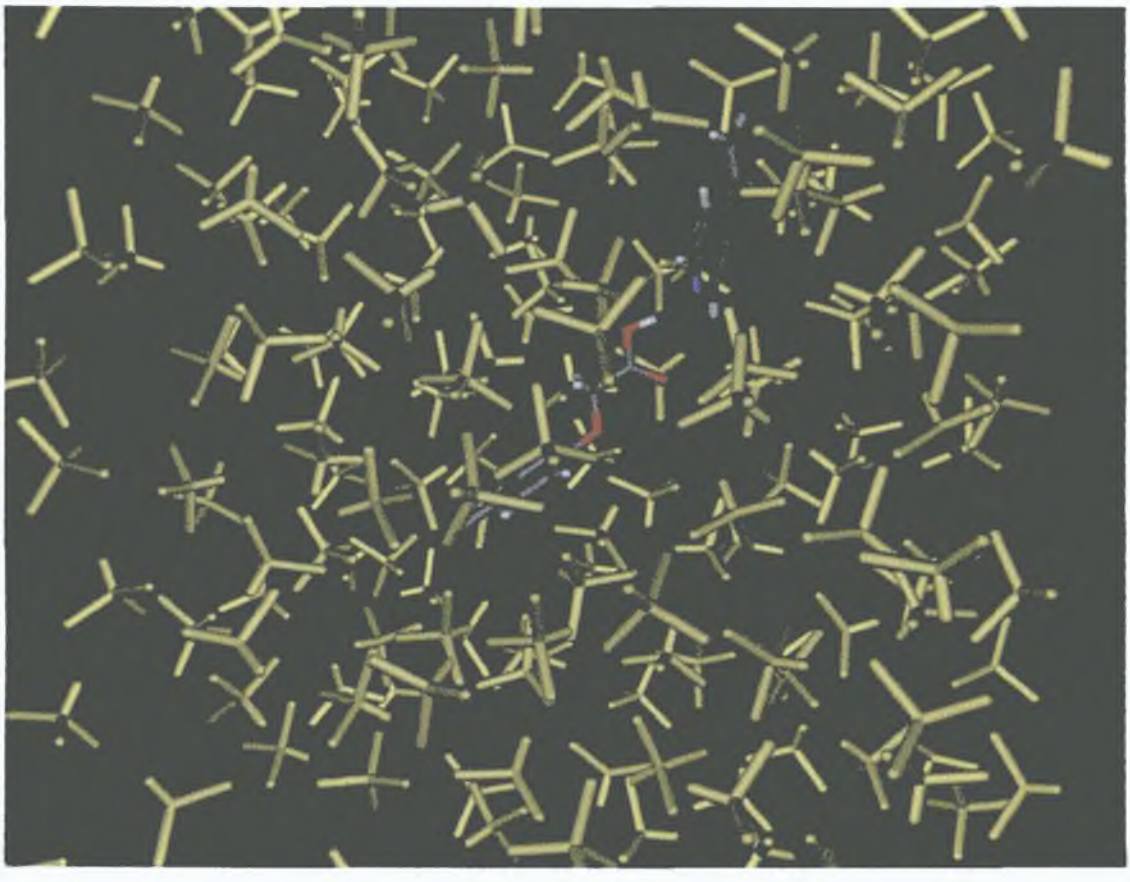

Fig. 5.17 – Complex at the end of the simulated annealing run (chloroform in yellow).

After this quick, 20-ps annealing, the system was put through a 1ns simulated annealing run to examine the stability of the complex afterwards. An interesting effect of the annealing is that the complex seems to have achieved it's most stable configuration, without any break-up of the hydrogen bond during this run (Fig.5.18).

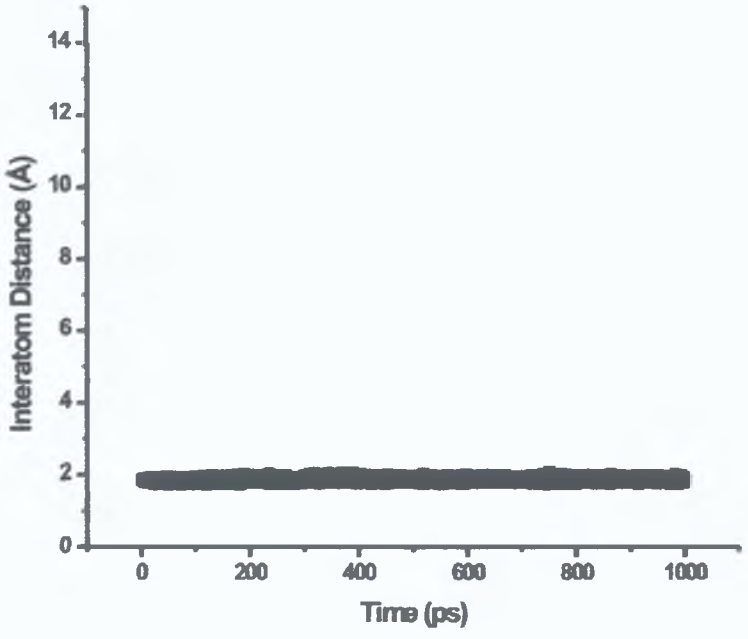

Fig. 5.18 – Distance between pyridinyl N-atom and 2,4-D acidic proton during NVE MD run.

5.6 Annex: Input Files Required

(i) PDB files in the following format:

```
REMARK   Accelrys ViewerPro PDB file
REMARK   Created:  Mon Jan 26 09:20:07 W. Europe Standard Time 2004

ATOM      1 C18  24D     1       2.568  -1.315  -1.108  1.00  0.00
ATOM      2  C1  24D     1       0.864  -1.096  -1.033  1.00  0.00
ATOM      3  C2  24D     1       0.017  -2.075  -1.530  1.00  0.00
ATOM      4  H14 24D     1       0.396  -2.909  -1.931  1.00  0.00
ATOM      5  C4  24D     1      -1.355  -1.897  -1.469  1.00  0.00
ATOM      6 C17  24D     1      -2.407  -3.111  -2.086  1.00  0.00
ATOM      7  C6  24D     1      -1.879  -0.742  -0.911  1.00  0.00
ATOM      8  H16 24D     1      -2.871  -0.614  -0.867  1.00  0.00
ATOM      9  C5  24D     1      -1.031   0.236  -0.416  1.00  0.00
ATOM     10  H15 24D     1      -1.412   1.070  -0.015  1.00  0.00
ATOM     11  C3  24D     1       0.343   0.061  -0.476  1.00  0.00
ATOM     12  O9  24D     1       1.169   1.033   0.014  1.00  0.00
ATOM     13  C10 24D     1       2.586   0.944  -0.090  1.00  0.00
ATOM     14  H17 24D     1       2.825   0.932  -1.061  1.00  0.00
ATOM     15  H18 24D     1       2.875   0.087   0.336  1.00  0.00
ATOM     16  C11 24D     1       3.235   2.122   0.597  1.00  0.00
ATOM     17  O13 24D     1       4.592   2.204   0.658  1.00  0.00
ATOM     18  H19 24D     1       5.025   2.990   1.101  1.00  0.00
ATOM     19  O12 24D     1       2.552   2.996   1.080  1.00  0.00
TER
ATOM      1  C1  4VP     1       6.681   6.107   1.002  1.00  0.00
ATOM      2  H9  4VP     1       7.424   6.513   1.537  1.00  0.00
ATOM      3  C2  4VP     1       6.618   4.735   0.832  1.00  0.00
ATOM      4  H10 4VP     1       7.315   4.147   1.243  1.00  0.00
ATOM      5  N4  4VP     1       5.588   4.186   0.090  1.00  0.00
ATOM      6  C6  4VP     1       4.618   4.991  -0.484  1.00  0.00
ATOM      7  H12 4VP     1       3.878   4.585  -1.018  1.00  0.00
ATOM      8  C5  4VP     1       4.681   6.361  -0.313  1.00  0.00
ATOM      9  H11 4VP     1       3.985   6.951  -0.724  1.00  0.00
ATOM     10  C3  4VP     1       5.712   6.913   0.429  1.00  0.00
ATOM     11  C7  4VP     1       5.776   8.373   0.609  1.00  0.00
ATOM     12  H13 4VP     1       5.080   8.918   1.078  1.00  0.00
ATOM     13  C8  4VP     1       6.815   9.069   0.129  1.00  0.00
ATOM     14  H14 4VP     1       6.853  10.062   0.254  1.00  0.00
ATOM     15  H15 4VP     1       7.553   8.598  -0.354  1.00  0.00
TER
```

(ii) PREPIN file for use in *LEaP* and *Parmchk*:

```
molecule.res
4VP    XYZ  0
CORRECT     OMIT DU   BEG
  0.0000
   1  DUMM  DU    M    0  -1  -2     0.000      .0        .0
.00000
   2  DUMM  DU    M    1   0  -1     1.449      .0        .0
.00000
   3  DUMM  DU    M    2   1   0     1.522   111.1        .0
.00000
   4  C1    ca    M    3   2   1     1.540   111.208   180.000    -
0.239
   5  H9    ha    E    4   3   2     1.000   151.783  -159.572
0.144
   6  C2    ca    M    4   3   2     1.383    87.306     7.027
0.393
   7  H10   h4    E    6   4   3     1.000   120.190  -172.742
0.021
   8  N4    nb    M    6   4   3     1.384   119.537     7.237    -
0.664
   9  C6    ca    M    8   6   4     1.384   120.861     0.048
0.392
  10  H12   h4    E    9   8   6     1.000   120.291   179.970
0.022
  11  C5    ca    M    9   8   6     1.383   119.561    -0.042    -
0.239
  12  H11   ha    E   11   9   8     1.000   120.071  -179.958
0.143
  13  C3    ca    M   11   9   8     1.384   119.710     0.005    -
0.018
  14  C7    cd    M   13  11   9     1.473   119.545  -179.974    -
0.126
  15  H13   ha    E   14  13  11     1.000   124.414    62.812
0.129
  16  C8    c2    M   14  13  11     1.340   120.449  -117.216    -
0.192
  17  H14   ha    E   16  14  13     1.000   120.052  -179.992
0.118
  18  H15   ha    E   16  14  13     1.001   119.965    -0.002
0.116
LOOP
   C3   C1

IMPROPER
   C3   C2   C1   H9
   C1  H10   C2   N4
   C5  H12   C6   N4
   C3   C6   C5  H11
   C5   C1   C3   C7
   C8   C3   C7  H13
   C7  H14   C8  H15

DONE
STOP
```

(iii) Frcmod file – modifications for force field in *LEaP*:

```
MASS

BOND
c2-ha  354.50   1.080        same as c2-hc

ANGLE

DIHE
ca-ca-cd-ha    1    1.000        180.000           2.000      same as X -
c2-cd-X
ca-ca-cd-c2    1    1.000        180.000           2.000      same as X -
c2-cd-X

IMPROPER
ca-ca-ca-ha          1.1          180.0         2.0          Using
default value
ca-h4-ca-nb          1.1          180.0         2.0          Using
default value
ca-ca-ca-cd          1.1          180.0         2.0          Using
default value
c2-ca-cd-ha          1.1          180.0         2.0          Using
default value
cd-ha-c2-ha          1.1          180.0         2.0          Using
default value

NONBON
```

(iv) Distance Restraint file for energy minimisation/ MD equilibration:

```
#
#   1  24D H19       2  4VP N4            3.0
 &rst
  ixpk= 0, nxpk= 0, iat=  18,  24, r1= 1.30, r2= 1.80, r3= 3.00, r4=
3.50,
      rk2=20.0, rk3=20.0, ir6=1, ialtd=0,
 &end
```

(v) mdin for energy minimisation, with restraint imposed (no molecules fixed):

```
Minimization run
&cntrl
imin=1,
ntb=1,
ntc=1,
maxcyc=500, ntpr=25
&end
DISANG=RST.dist
```

(vi) mdin for energy minimisation, with restraint imposed (chloroform held fixed):

```
Minimization run
&cntrl
imin=1,
ntb=1,
ntc=1,
maxcyc=500, ntpr=25
&end
1.0
CL3 3 172
end
end
DISANG=RST.dist
```

(vii) Equilibration of system pre-MD run, constant volume:

```
MD
&cntrl
imin=0,
nmropt=1,
ntx=1,
iwrap=1,
irest=0,
tempi=0,
temp0=300,
tautp=0.2,
ntt=1,
ntb=1,
ntp=0,
nstlim=5000,
ntwe=100,
ntwx=100,
ntpr=25
&end
&wt
  type='REST',
  istep1=1,
  istep2=5000,
  value1=1,
  value2=1
&end
&wt type='END'  &end
LISTIN=POUT
LISTOUT=POUT
DISANG=RST.dist
```

(viii) Equilibration of system pre-MD run, constant pressure:

```
MD
&cntrl
imin=0,
nmropt=1,
ntx=7,
iwrap=1,
irest=1,
temp0=300,
tautp=0.2,
ntt=1,
ntb=2,
ntp=1, taup=0.05,
ntc=2, ntf=2,
nstlim=250000,
ntwe=100,
ntwx=100,
ntpr=25
&end
&wt
  type='REST',
  istep1=1,
  istep2=5000,
  value1=1,
  value2=1
&end
```

(ix) Input file for 1-nanosecond MD run :

```
MD
&cntrl
imin=0,
ntx=7,
iwrap=1,
irest=1,
temp0=300,
tautp=0.2,
ntt=0,
ntb=1,
ntp=0, taup=1,
ntc=2, ntf=2,
nstlim=1000000,
ntwe=100,
ntwx=100,
ntpr=25
&end
&wt
```

(x) Input file for simulated annealing MD run:

```
simulated annealing protocol, 20 ps

 &cntrl
    imin=0, irest=1, ntx=7,
    nstlim=20000, pencut=0.1,
    nmropt=1, ntb=1, tautp=2.0,
    ntpr=25, ntt=1, ntwx=100,
    iwrap=1, scee=1.2, ntc=2,
    vlimit=10,
 &end
#
#Simple simulated annealing algorithm:
#
#from steps 0 to 5000: heat the system to 600K
#from steps 5001-18000: re-cool to low temperatures with long tautp
#from steps 18001-20000: final cooling with short tautp
#
 &wt type='TEMP0', istep1=0,istep2=5000,value1=600.,
            value2=600.,    &end
 &wt type='TEMP0', istep1=5001, istep2=18000, value1=600.0,
            value2=100.0,     &end
 &wt type='TEMP0', istep1=18001, istep2=20000, value1=0.0,
            value2=0.0,     &end

 &wt type='TAUTP', istep1=0,istep2=5000,value1=0.4,
            value2=0.4,     &end
 &wt type='TAUTP', istep1=5001,istep2=18000,value1=4.0,
            value2=4.0,     &end
 &wt type='TAUTP', istep1=18001,istep2=19000,value1=1.0,
            value2=1.0,     &end
 &wt type='TAUTP', istep1=19001,istep2=20000,value1=0.1,
            value2=0.05,    &end

 &wt type='END'  &end
LISTOUT=POUT
```

5.7 Conclusion

It has been demonstrated that over the 1ns of simulated molecular dynamics presented here, the acid-base complex remains intact in non-polar solvent. This concurs with NMR evidence from the previous chapter – although an ion pair is the more likely physical form of this complex, a hydrogen-bonded complex was modelled here to simplify calculations by excluding charged entities. The polar nature of the acidic and basic components of (respectively) 2,4-D and 4-vinylpyridine provided a sufficiently strong interaction to remain intact following removal of imposed restraints.

The modelling results described here represent an effective means of integrating molecular modelling into a multi-step rational design approach to MIP creation. Molecular modelling has been used extensively as a tool in organic chemistry, in determining probable conformations of molecules, protein structure or biological receptor structure. However, the somewhat complex nature of the work has meant that to date, it has not been used as part of an integrated approach to MIP design, but rather as an independent method to developing MIPs. The work described within this chapter shows that by using spectroscopic data as a basis for molecular modelling work, the validity of results of molecular modelling analysis can be checked to ensure that the method being employed results in realistic PPC conformations being created, as well as allowing imposition of restraints to cut down on modelling time. Use of two-dimensional NMR

techniques like COSY and ROESY, as is commonly applied in protein structure determinations, represents one possible avenue of research in this area, to contribute to the starting-point knowledge of the structure of PPC components. The aforementioned work of Katz and Davis, who successfully isolated PPCs and determined via X-ray crystallography the structure thereof, demonstrates another important means of obtaining structural information for refining molecular modelling data.

The work described here showed that the 2,4-D/ 4-VP ion-paired complex would most probably remain intact in a non-polar medium. Tandem work performed by a research partner[17] in which the same system in water was modelled, showed that in a polar medium, ionic interactions become less important and hydrophobicity becomes the governing mechanism in maintaining PPC integrity, with a $\pi-\pi$ stacked configuration which appeared to oscillate between face-to-face and edge-on conformation. These results would appear to corroborate the findings of HPLC analysis, whereby a non-polar medium resulted in a MIP with poor recognition properties, compared to an imprint obtained using a polar water/ methanol mixture[18]. This method may thus be used to investigate which kinds of interaction may influence formation of the PPCs, although crucially, the validity of the structure of the PPC in terms of explaining subsequent MIP binding site structure must be investigated by careful examination of the polymerisation processes for effects which may negatively affect PPC integrity. An extended study, carefully correlating properties of a pre-polymerisation mixture as identified

by NMR and chromatography with events observed in simulation, should provide a wealth of information on the true relationship between pre-polymerisation events and the recognition properties of the MIP system.

Bibliography

[1] S.Piletsky, E. Piletska, K. Karim, G. Foster, C. Legge & A. Turner, *Anal. Chim. Acta*, 504 (2004), 123.

[2] S.A. Piletsky, K. Karim, E.V. Piletska, C.J. Day, K.W. Freebairn, C. Legge & A.P.F Turner, *Analyst*, 126 (2001), 1826.

[3] S. Subrahmanyam, S.A. Piletsky, E.V. Piletska, B. Chen, K. Karim & A.P.F. Turner, *Biosensors & Bioelectronics*, 16 (2001), 631.

[4] E. Piletska, S. Piletska, K. Karim, E. Terpetsching & A. Turner, *Anal. Chim. Acta*, 504 (2004), 179.

[5] L. Wu, B. Sun, Y. Li & W. Chang, *Analyst*, 128 (2003), 944.

[6] A.R. Leach, *Molecular Modeling: Principles & Applications*, (2001), 2nd Ed., Pearson (Harlow, England), 26-88.

[7] B. Sellergren, M. Lepistö & K. Mosbach, *J. Am. Chem. Soc.*, 110 (1988), 5853.

[8] M. Lepistö & B. Sellergren, *J. Org. Chem.*, 54 (1989), 6010.

[9] A. Katz & M.E. Davis, *Macromolecules*, 32 (1999), 4113.

[10] D. Spivak, R. Simon & J. Campbell, *Anal. Chim. Acta*, 504 (2004), 23.

[11] R.J. Umpleby, S.C. Baxter, M. Bode, J.K. Berch, R. N. Shah & K.D. Shimizu, *Anal. Chim. Acta,* 435 (2001), 35.

[12] H.S. Andersson & I.A. Nicholls, *Bioorg. Chem.*, 25 (1997), 203.

[13] W.Humphrey, A. Dalke & K. Schulten, *J. Molec. Graphics*, 14 (1996), 33.

[14] http://amber.scripps.edu

[15] www.rscb.prg/pdb/

[16] www.ccdc.cam.ac.uk

[17] A. Molinelli (Georgia Institute of Technology), *PhD. Thesis*, (2004), *in preparation.*

[18] K. Haupt, A. Dzgoev & K. Mosbach, *Anal. Chem.*, 70 (1998), 628.

Chapter Six

Conclusions and Future Work.

6.1 Conclusions

The proper development and application of molecular imprinting technology is evidently a multi-discipline research task. Chapter 2 demonstrates that although the technology is effective – such as in a sample clean-up procedure – the performance can be poor, suggesting that the usual schematic employed (see Fig. 1.1) is far too simplistic to adequately represent the myriad processes which act in concert to produce the kind of molecular specificity associated with these materials. Although Chapter 2 shows that a MIP can be developed using the typical methods cited in the literature – using methacrylic acid or 4-vinylpyridine as functional monomer to prepare a bulk polymer, using the ground material as an SPE stationary phase – the researcher faces the dilemma of having only a trial-and-error approach as a means of refining and improving the MIP product. This problem was the foundation of the research in Chapters 3-5.

In Chapter 3, the problem of creating a high-performance MIP material is approached from a different perspective. Using a highly specific imprinted polymer for quercetin (which was developed via a trial-and-error approach), is it possible to identify specific properties of this particular polymer which imbue it with this high degree of specificity? This line of investigation yielded some of the more significant findings of the project overall. A direct correlation between the optimum ratio of monomer: template in the imprinted polymer composition, as measured in terms of chromatographic performance, and the most mobile pre-

polymerisation complexes (within their own microenvironment), as determined by ^{1}H-NMR T_1 relaxation studies, was established. This is one of the few examples, of a quantitative correlation between a PPC physical property and polymer performance, and opens up the avenue of further research to predict polymer performance using this method. However, despite the establishment of this correlation, the overall view of the polymerisation process garnered from this body of work is one of great complexity, with participation of macroscopic phase partition effects in the preservation of PPCs as a likely factor in the high performance of these MIPs. Measuring surface area of the MIPs indicated that the high retention capability was not simply due to a greater surface area in the imprinted polymer relative to the blank. However, at very low monomer: template ratios (lower that 6:1), the imprinted polymer produced a matrix too dense to be processed according to the typical procedure, although the blank polymers did not display this quality. This is another indication of the template molecule affecting the actual polymerisation process, and future research into the effect of template molecule on polymer chain formation, polymerisation rate and final polymer density should prove invaluable in explaining how imprinting works.

Chapter four continued this line of research, with a view to broadening the understanding of how an effective imprint can be achieved. This time, the pesticide 2,4-dichlorophenoxyacetic acid was used as the template of choice. This imprinting system has been explored at length in the literature, most notably by Karsten Haupt. Aside from high performance, one characteristic of this system

which merited investigation was the fact that the polymerisation was achieved in a mixture of methanol and water. This contrasts with the usual criterion of using a non-polar porogen to avoid disrupting the subtle non-covalent interactions which are crucial to creating a successful imprint. Exhaustive ^{1}H-NMR investigation of the pre-polymerisation system again yielded detailed information on the molecular-level processes which dictate the success of the imprint. Previous papers on the system had speculated on the participation of hydrophobicity, given that the template is composed of an ionisable acid end-chain and a non-polar aromatic portion. Careful ^{1}H-NMR observation of the aromatic protons in both polar and non-polar solvents showed a definite tendency to form stacked complexes in polar conditions – a hydrophobic effect. This kind of experiment is essential in removing the speculation from molecular imprinting technology – such techniques permit researchers to prove the existence of a subtle non-covalent interaction, rather than simply proposing it as a possible source of selectivity. Also, this finding concurs with a published study on the nature of rebinding events with this MIP system as determined via microcalorimetry (see Section 4.6 for discussion of this), lending further weight to the proposed theory of hydrophobic forces acting in concert with ionic interactions as the origin of this MIP's high performance. An awareness of which kinds of interaction are taking place in the pre-polymerisation mixture can also permit the researcher to carefully choose the polymerisation conditions – with this system, a lower-temperature UV polymerisation led to greater preservation of PPCs and a higher observed selectivity in the final MIP.

Chapter five extends the scope of the research performed in Chapters 4 and 5. Molecular modelling has been used in the past for developing molecularly imprinted systems. This chapter explores the possibility of incorporating spectroscopic data on PPCs into optimised models of PPCs, with a view to refining current modelling approaches and creating more selective MIPs. The work this entails is extensive, with the research contained in Chapter 5 offering a framework for the development of a molecular modelling approach integrating spectroscopic data, but is by no means complete. To develop a comprehensive modelling method for MIP technology, other aspects of the technique would need to be considered – such as changes in polarity of the system as polymerisation progresses, the growth of polymer chains resulting in lower molecular mobility, PPC degradation by free radicals and other variables. Despite this, the molecular modelling work performed to date has resulted in modelled systems which appear to coincide with the PPC systems found spectroscopically in Chapter 4 – the preservation of an ion-paired complex in non-polar media, and the preservation of a hydrophobicity-induced π-stacked complex in polar media (whose behaviour would appear to simulate real π-stacked complexes, oscillating between a edge-to-face configuration and a face-to-face configuration). These results are promising and offer much potential for future development of this technique – showing that this first coupling of PPC spectroscopic studies with molecular modelling may yet prove to be an essential means of accurately modelling PPCs and thus predicting optimum polymer composition.

6.2 Future Work

Future developments in MIP technology, further integration into analytical and sensing applications and commercial exploitation of the technique may all depend heavily on the outcome of current 'rational design' approaches described in the literature, which should result not just in MIPs of higher performance, but also in a greater understanding of the variables which affect MIP recognition properties to the greatest extent. Chapter two shows how MIPs can be successfully employed in a sample-clean-up application, and as MIP technology is highly transferable, it could potentially be used against a range of analytes of pharmaceutical or environmental interest.

Chapter 3 demonstrated that with tandem pre-polymerisation characterisation (^{1}H-NMR T_1 relaxation studies) and post-polymerisation characterisation (HPLC), MIP performance may be understood in greater detail than the depth of information offered by a typical trial-and-error variable-recipe approach, as in Chapter 2. The high performance MIP material produced was tested in a real analytical application – isolating a structural analogue of quercetin (luteolin – a potential lead compound for cancer treatment) from a herbal tea preparation (see Fig. 6.1).

SPE Clean-up of "Essiac" Tea using Quercetin-imprinted Polymer

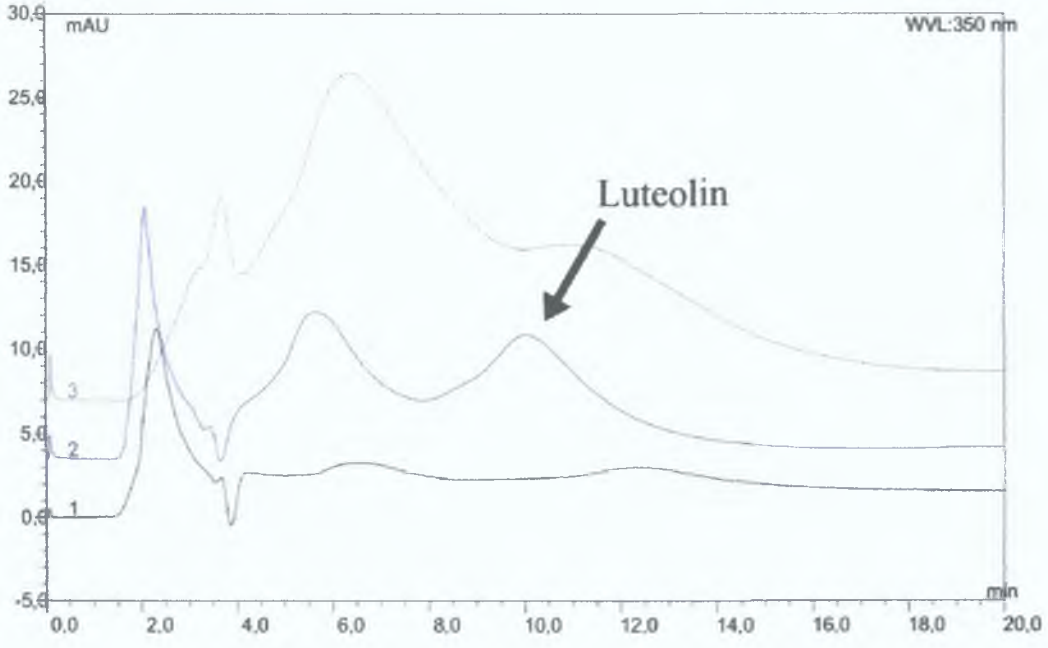

1-SPE Elution fraction from non-imprinted polymer
2-SPE Elution fraction from imprinted polymer
3-Direct Injection of "Essiac" Tea

Fig. 6.1 – Clean-up of herbal tea sample using Quercetin-imprinted polymer. Mobile phase: Acetonitrile/ H2O/ acetic Acid (80:10:10) @ 1ml/min.

This demonstrates the utility of an optimised MIP system – although quercetin is a relatively cheap compound to purchase, luteolin (a potential anti-cancer agent) is not, and thus this type of analogue imprinting offers a cheap method of obtaining compounds of high commercial or pharmaceutical value. Quercetin is an ideal template in this case, differing from quercetin by only one hydroxyl group (see Fig. 6.2).

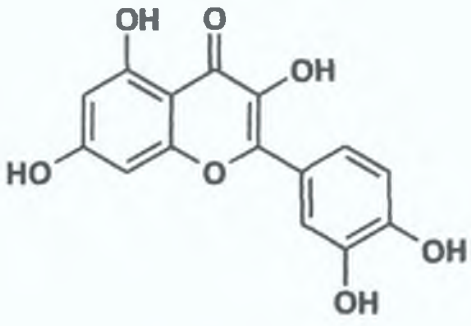

Quercetin

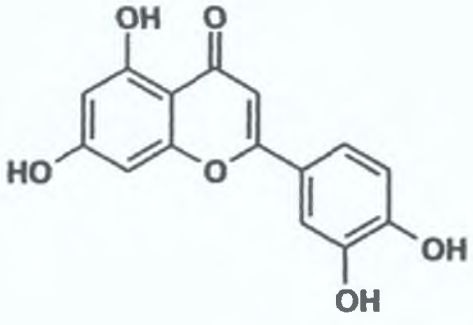

Luteolin

Fig. 6.2 – Structures of quercetin and luteolin.

Chapters 2 and 3 thus demonstrate the potential of imprinting both for analytical research purposes and commercial exploitation; the subsequent two chapters describe means of improving MIP performance. Chapter 4's examination of the role of hydrophobic effect in creating an imprinting effect point to the possibility of tailoring monomers to suit template molecules, via addition of aromatic or aliphatic substituents to impart hydrophobic properties to the monomer. Carefully-controlled exploitation of macroscopic phase partition effects this way may result in higher performance MIP materials. In addition to tandem IR spectroscopy on the system performed by a collaborative research partner, detailed NMR studies have shown that effects such as the temperature dependence of PPC stability, along with self-association phenomena as measured by IR, can be accounted for prior to the actual polymerisation, and polymerisation conditions (temperature, concentration) may be adjusted accordingly to produce MIPs with a greater number of high-fidelity binding sites.

Finally, Chapter 5 represents an evolution of the research from Chapters 3 and 4 and holds perhaps the greatest potential for future development. As the simulation of the PPC system is refined and improved, it is expected that further spectroscopic data from IR spectroscopy, UV spectroscopy, microcalorimetry, studies on the rates of polymerisation and two- and three-dimensional NMR studies will eventually result in a comprehensive protocol that will enable both prediction of MIP performance and design of optimised MIP systems.

List of Publications:

1. J. O'Mahony, A. Molinelli, K. Nolan, M.R. Smyth, B. Mizaikoff, "Anatomy of a Successful Imprint: Analysing the Recognition Mechanisms of a Molecularly Imprinted Polymer", Macromolecules, *submitted*, 2004

2. A. Molinelli, J. O'Mahony, K. Nolan, M.R. Smyth, B. Mizaikoff, "Probing the Nature of Molecular Imprinting Mechanisms with NMR and IR Spectroscopy", Nature Materials, *in preparation*, 2004

3. J.O'Mahony, A. Molinelli, K. Nolan, M.R. Smyth, B. Mizaikoff, "Towards the Rational Development of Molecularly Imprinted Polymers: ^{1}H-NMR Studies on Hydrophobicity and Ion-Pair Interactions as Driving Forces in Selectivity", Biosensors & Bioelectronics, *accepted*, 2004

4. J.O'Mahony, K. Nolan, M.R. Smyth, B. Mizaikoff, "Molecularly Imprinted Polymers – Potential And Challenges in Analytical Chemistry", Analytica Chimica Acta, *accepted*, 2004